

# Recursion Relations in $p$ -adic Mellin Space

Christian Baadsgaard Jepsen<sup>1\*</sup> & Sarthak Parikh<sup>2†</sup>

<sup>1</sup>*Joseph Henry Laboratories, Princeton University, Princeton, NJ 08544, USA*

<sup>2</sup>*Division of Physics, Mathematics and Astronomy,  
California Institute of Technology, Pasadena, CA 91125, USA*

## Abstract

In this work, we formulate a set of rules for writing down  $p$ -adic Mellin amplitudes at tree-level. The rules lead to closed-form expressions for Mellin amplitudes for arbitrary scalar bulk diagrams. The prescription is recursive in nature, with two different physical interpretations: one as a recursion on the number of internal lines in the diagram, and the other as reminiscent of on-shell BCFW recursion for flat-space amplitudes, especially when viewed in auxiliary momentum space. The prescriptions are proven in full generality, and their close connection with Feynman rules for real Mellin amplitudes is explained. We also show that the integrands in the Mellin-Barnes representation of both real and  $p$ -adic Mellin amplitudes, the so-called pre-amplitudes, can be constructed according to virtually identical rules, and that these pre-amplitudes themselves may be re-expressed as products of particular Mellin amplitudes with complexified conformal dimensions.

May 27, 2022

---

\*cjepsen@princeton.edu

†sparikh@caltech.edu

# Contents

<b>1</b>	<b>Introduction and Summary</b>	<b>2</b>
<b>2</b>	<b>Mellin Amplitudes and Pre-Amplitudes</b>	<b>5</b>
<b>3</b>	<b>Construction of Mellin Amplitudes</b>	<b>11</b>
3.1	Recursive prescription for $p$ -adic Mellin amplitudes . . . . .	11
3.2	Feynman rules for real Mellin amplitudes . . . . .	19
<b>4</b>	<b>Construction of Pre-Amplitudes</b>	<b>21</b>
4.1	Obtaining pre-amplitudes from Mellin amplitudes . . . . .	22
4.2	Pre-amplitude examples . . . . .	27
4.3	Integrating the pre-amplitude to obtain the amplitude . . . . .	30
<b>5</b>	<b>On-Shell Recursion for Mellin Amplitudes</b>	<b>33</b>
5.1	Factorization property of undressed diagrams . . . . .	33
5.2	$p$ -adic on-shell recursion relation and proof . . . . .	38
<b>6</b>	<b>Outlook</b>	<b>43</b>
<b>A</b>	<b>Useful Formulae and Conventions</b>	<b>45</b>
<b>B</b>	<b>Inductive Proof of Prescription III for Pre-Amplitudes</b>	<b>46</b>
B.1	Outline of the proof . . . . .	46
B.2	Details of the proof . . . . .	48
<b>C</b>	<b>Inductive Proof of Prescription I for Mellin Amplitudes</b>	<b>61</b>
C.1	The “leg adding” operation . . . . .	63
C.2	Integrating pre-amplitudes using “leg addition” . . . . .	64
C.3	Proof of the general “leg adding” operation . . . . .	69
<b>D</b>	<b>BCFW-Shifts of Auxiliary Momenta</b>	<b>76</b>
D.1	Four-point exchange diagram . . . . .	76
D.2	Five-point diagram with two internal lines . . . . .	83

# 1 Introduction and Summary

Mellin amplitudes share many properties with flat space scattering amplitudes and have been especially useful in studying holographic CFTs [1]. Until very recently, this story has remained restricted to the study of amplitudes in field theories defined over real-valued spacetimes. In this paper, we continue the holographic investigation of Mellin amplitudes in the context of  $p$ -adic AdS/CFT [2, 3] initiated in Ref. [4]. These so-called  $p$ -adic Mellin amplitudes were shown to have analytic properties similar to those of traditional real Mellin amplitudes for several classes of bulk diagrams [4]. At the same time,  $p$ -adic Mellin amplitudes were found to be significantly simpler than their real counterparts owing to the absence of descendants [5] in the corresponding  $p$ -adic CFTs, thus providing a new technically simpler arena for studying generic features of Mellin amplitudes. In this paper, we establish systematically the analytic similarities between the real and  $p$ -adic amplitudes for *all* tree-level bulk diagrams involving scalars. The main questions we answer are: What is the  $p$ -adic Mellin amplitude of an arbitrary tree-level diagram, and what recursion relations do the amplitudes obey? We establish three prescriptions for writing down arbitrary Mellin amplitudes, two of which are recursive, and proceed to establish the precise connections with analogous prescriptions satisfied by corresponding real Mellin amplitudes.

For real Mellin amplitudes, the final expressions, obtained via the Feynman rules for Mellin amplitudes, are usually written in terms of unevaluated infinite sums over terms corresponding to the exchange of descendant fields in the intermediate channels. For scalar operators, the amplitudes for tree-level bulk diagrams take the following schematic form, which we refer to as the series representation of the Mellin amplitudes [6, 7, 8],

$$\mathcal{M} \sim \sum_{m_{i_1}, \dots, m_{i_K}=0}^{\infty} \left( \prod_{i \in I} \frac{1}{s_i - \Delta_i - 2m_i} \right) \left( \prod_{\text{vertices}} V(\{m_I\}) \right) \quad I = \{i_1, \dots, i_K\}, \quad (1.1)$$

where the set  $I$  labels the internal lines of the diagram, each admitting the exchange of a single trace operator of conformal dimension  $\Delta_i$  for  $i \in I$  (with non-zero  $m_i$  corresponding to the exchange of descendants from its conformal family), and each contact vertex in the diagram has an associated factor  $V$  which depends on the conformal dimensions of the external operator insertions incident at that vertex, as well as the dimensions  $\Delta_i$  and the associated integers  $m_i$  of operators running along internal lines incident on the same vertex. For each internal line  $i \in I$  there is a “propagator factor”, which depends on a particular Mandelstam-like variable  $s_i$ , which itself depends on the Mellin variables. To obtain the full

Mellin amplitude, one must sum over all integers  $m_i$  for  $i \in I$ ; typically these sums are hard to evaluate analytically. This series representation makes the pole structure of the Mellin amplitude manifest — the Mandelstam variables pick up poles in the infinite sum (1.1) when fields propagating along the internal lines go on-shell, signaling the exchange of single-trace operators and their descendants in the intermediate channels, and the residue at each pole factorizes into a product of left and right sub-amplitudes [6, 7, 9].

Alternatively, real (and  $p$ -adic) Mellin amplitudes also admit a contour representation, which we will refer to as the Mellin-Barnes integral representation. Schematically, it takes the form

$$\mathcal{M} \sim \left( \prod_{i \in I} \int_{-i\infty}^{i\infty} \frac{dc_i}{2\pi i} f_{\Delta_i}(c_i) \right) \widetilde{\mathcal{M}}(\{c_I\}, \{\gamma_{ij}\}) \quad I = \{i_1, \dots, i_K\}. \quad (1.2)$$

where the weight  $f_{\Delta_i}(c_i)$  depends on the dimension  $\Delta_i$  of the internal operator exchanged along the internal line  $i \in I$  as well as the spacetime dimension, and takes as argument a complex parameter  $c_i$ , while  $\widetilde{\mathcal{M}}$ , which following Refs. [10, 11] we refer to as the “pre-amplitude”, is a function that is significantly simpler in form than the full, integrated amplitude  $\mathcal{M}$  and depends on the Mellin variables  $\gamma_{ij}$ , the complex parameters  $c_I$ , and the dimensions solely of external operators.

While in principle the series and Mellin-Barnes representations solve the problem of obtaining real tree-level scalar correlators, they do not yield a closed-form expression for the amplitudes (except in a few simple cases such as the three- and four-point functions). And while Mellin amplitudes for special kinds of one-loop diagrams were already available in the early days of the Mellin program [1], and recent progress has been made in studying bulk diagrams at one-loop, both in position space [12, 13] and Mellin space [10, 11], the current technology at loop-level leaves more to be desired when compared with the state-of-the-art for flat-space amplitudes. The flat-space amplitudes program has benefited from many extremely powerful tools and techniques which go beyond summing Feynman diagrams, such as BCFW recursion [14], but these have so far remained elusive in Mellin space and serve as one of the motivations for this work.<sup>1</sup>

---

<sup>1</sup>It should be mentioned, though, that methods based on general consistency and symmetry have been successful in a variety of settings, e.g. conformal bootstrap for higher dimensional CFTs in position space [15, 16, 17, 18, 19, 20, 21] and Mellin space [22], use of crossing symmetry to constrain 1-loop Mellin amplitudes [23, 24, 25], as well as techniques utilizing superconformal Ward identities to obtain total on-shell amplitudes without resorting to summing individual bulk diagrams in e.g. type IIB supergravity in both position and Mellin space [26, 27], to name a few. See also Refs. [28, 29] for work on BCFW recursion relations for bulk diagrams in *momentum space*.

Turning to  $p$ -adic Mellin amplitudes (see Ref. [4] for a detailed introduction and section 2 for a quick overview, definitions and conventions), explicit computations of the amplitudes for tree-diagrams with up to three internal lines [4] hint at the existence of recursion relations obeyed by the  $p$ -adic Mellin amplitudes of arbitrary tree-level bulk diagrams. In section 3, we present such a relation which is recursive in the number of internal lines in the diagram, with a proof in appendix C. The prescription consists of assigning factors to each vertex and internal line of a given bulk diagram and then writing down the Mellin amplitude by taking a product over all these factors, but also subtracting off all possible diagrams obtained by collapsing in the original diagram every possible subset of internal lines. The expressions for the diagrams to be subtracted off are obtained by a recursive application of this procedure. In the end the entire Mellin amplitude is expressible in closed-form in terms of the factors associated with contact interaction vertices and internal lines. Explicit examples are also provided, and in section 3.2 we present the Feynman rules for real Mellin amplitudes for comparison.

As pointed out above, real and  $p$ -adic Mellin amplitudes admit a Mellin-Barnes representation in terms of multi-contour integrals. The reason such a representation exists is that by applying the split representation to all the bulk-to-bulk propagators of the diagram, a Mellin amplitude can be written as a multi-dimensional contour integral over what is referred to as the *pre-amplitude*. In section 4 we formulate a set of rules for constructing any tree-level pre-amplitude. Curiously, this prescription applies universally to *both*  $p$ -adic and real Mellin amplitudes.

In the same section we also describe an interesting connection between pre-amplitudes and Mellin amplitudes, which holds true for both  $p$ -adic and real Mellin amplitudes: We show that pre-amplitudes may be obtained by taking products of diagrams which appear in the recursive prescription for Mellin amplitudes,<sup>2</sup> except with the dimensions in the diagrams assigned specific complex values that depend on the complex variables of the contour integrals. This prescription is proven in section B via an inductive argument, and explicit examples are provided in section 4.2.

We emphasize that the claim of the previous paragraph essentially is that the *integrand* in the Mellin-Barnes integral representation of the Mellin amplitude secretly takes the same functional form as the *integral*, i.e. the full Mellin amplitude. Thus the pre-amplitude is given simply by a product of a particular set of full Mellin amplitudes with the dimensions

---

<sup>2</sup>In section 3 we refer to these diagrams as “undressed diagrams”, and they are essentially the same as Mellin amplitudes up to simple overall factors associated with each vertex. These diagrams can be obtained via the prescriptions of sections 3 and 5 over  $p$ -adics and the Feynman rules [6, 7, 8] over reals.

of certain operators set to special values. Although the series and Mellin-Barnes integral representations of the real Mellin amplitudes obfuscate this property, it holds true even over the reals as discussed in section 4.1.

In section 5 we move on to present a different type of recursion relation obeyed by  $p$ -adic Mellin amplitudes, which makes the factorization property of  $p$ -adic Mellin amplitudes manifest. This prescription allows for an arbitrary tree-level bulk diagram to be expressed in terms of lower-point bulk diagrams with shifted Mandelstam-like invariants, constructed out of the same interaction vertices as the original diagram. We prove in section 5 that this prescription follows from the recursive prescription from section 3. We also argue that an adaptation of this prescription applies to real Mellin amplitudes and in fact gives back the Feynman rules prescription. In appendix D we illustrate with the help of explicit examples, how this prescription originates from an application of Cauchy’s residue theorem to complex deformed Mellin amplitudes obtained via complex shifting (auxiliary) momenta, *à la* on-shell BCFW recursion relations in flat space [14]. Thus this prescription is closer in form to on-shell recursive relations in flat space since it provides a decomposition of Mellin amplitudes into products of lower-point sub-amplitudes with all external legs “on-shell”, joined together by “propagator” factors, reminiscent of BCFW recursion. We stress, however, that the recursive relation applies at the level of *individual* diagrams, and not at the level of full amplitudes. We close with final comments and future directions in section 6.

## 2 Mellin Amplitudes and Pre-Amplitudes

In this section we recall some basic facts and results for  $p$ -adic holography and Mellin amplitudes and provide relevant definitions and normalizations which will be used throughout.<sup>3</sup> More details can be found in Ref. [4] (see also Refs. [2, 30]). Many results in  $p$ -adic AdS/CFT closely resemble their real counterparts, not just in physical interpretation but also in their mathematical formulation. To facilitate comparison and emphasize the striking similarities, we will often present a  $p$ -adic result or definition along with its real counterpart from conventional continuum AdS/CFT. In such cases, we will label the equations with a “ $\mathbb{Q}_p^n$ ” or an “ $\mathbb{R}^n$ ” depending on whether they hold in  $p$ -adic AdS/CFT or real Euclidean AdS <sub>$n+1$</sub> /CFT <sub>$n$</sub> .

In the  $p$ -adic setup, the bulk geometry is given by the Bruhat–Tits tree  $\mathcal{T}_p^n$ , which is an infinite  $(p^n + 1)$ -regular graph without cycles, and the bulk scalar degrees of freedom live on the vertices of the tree. The boundary of the tree,  $\partial\mathcal{T}_p^n$ , is the projective line over the

---

<sup>3</sup>For recent developments in  $p$ -adic holography, see Refs. [2, 3, 4, 30, 31, 32, 33, 34, 35, 36, 37, 38, 39, 40, 41, 42].

degree  $n$  unramified extension of the  $p$ -adic numbers, denoted  $\mathbb{P}^1(\mathbb{Q}_{p^n})$ .  $\mathbb{Q}_{p^n}$  may also be thought of as an  $n$ -dimensional vector-space over the base field  $\mathbb{Q}_p$ , thus we will refer to  $n$  as the dimension of the boundary field theory. The vertices of the tree can be labelled by bulk coordinates  $(z_0, z)$  where  $z_0$ , the bulk depth coordinate, is an integral power of  $p$  and  $z \in \mathbb{Q}_{p^n}$  represents the boundary direction. The vertices are not labelled uniquely by this coordinate representation: two coordinate pairs  $(z_0, z)$  and  $(z'_0, z')$  label the same vertex iff  $z_0 = z'_0$  and  $z' - z \in z_0 \mathbb{Z}_{p^n}$ , where  $\mathbb{Z}_{p^n} = \{x \in \mathbb{Q}_{p^n} \mid |x|_p \leq 1\}$ .  $|\cdot|_p$  denotes the ultrametric  $p$ -adic norm,  $|\cdot|_p : \mathbb{Q}_{p^n} \rightarrow \mathbb{R}^{\geq 0}$ . On the real side, the bulk geometry is  $(n+1)$ -dimensional Euclidean anti-de Sitter space. In the two formalisms, the free bulk actions are given by

$$\mathbb{Q}_{p^n}) \quad S_{\text{kin}} = \sum_{\langle (z_0, z), (w_0, w) \rangle} \frac{1}{2} (\phi_{i(z_0, z)} - \phi_{i(w_0, w)})^2 + \sum_{(z_0, z) \in \mathcal{T}_{p^n}} \frac{1}{2} m_{\Delta_i}^2 \phi_{i(z_0, z)}^2, \quad (2.1)$$

$$\mathbb{R}^n) \quad S_{\text{kin}} = \int_{\text{AdS}_{n+1}} dZ \left[ \frac{1}{2} (\nabla \phi_i(Z))^2 + \frac{1}{2} m_{\Delta_i}^2 \phi_i^2(Z) \right],$$

where we have expressed the real action in embedding space coordinates such that the bulk coordinate  $Z$  lives in an  $(n+2)$ -dimensional Minkowski space satisfying  $Z^2 \equiv Z \cdot Z = -1$ . The bulk scalar fields  $\phi_i$  have masses  $m_{\Delta_i}^2$  and scaling dimensions  $\Delta_i$ , related to each other via

$$\mathbb{Q}_{p^n}) \quad m_{\Delta}^2 = \frac{-1}{\zeta_p(-\Delta) \zeta_p(\Delta - n)}, \quad \mathbb{R}^n) \quad m_{\Delta}^2 = \Delta(\Delta - n), \quad (2.2)$$

where  $\zeta_v : \mathbb{C} \rightarrow \mathbb{C}$ , which will be called the local zeta function, is a meromorphic function defined for  $v = p$  and  $v = \infty$  by

$$\zeta_p(z) = \frac{1}{1 - p^{-z}}, \quad \zeta_{\infty}(z) = \pi^{-\frac{z}{2}} \Gamma\left(\frac{z}{2}\right). \quad (2.3)$$

The bulk-to-boundary propagators for a bulk scalar of dimension  $\Delta$  are given by

$$\mathbb{Q}_{p^n}) \quad K_{\Delta}(z_0, z; x) = \zeta_p(2\Delta) \frac{|z_0|_p^{\Delta}}{|z_0, z - x|_s^{2\Delta}}, \quad (2.4)$$

$$\mathbb{R}^n) \quad K_{\Delta}(Z, P) = \frac{\zeta_{\infty}(2\Delta)}{(-2P \cdot Z)^{\Delta}},$$

where  $|\cdot, \cdot|_s$  denotes the supremum norm,

$$|x, y|_s \equiv \sup\{|x|_p, |y|_p\}, \quad (2.5)$$

and the real bulk-to-boundary propagator is expressed in the embedding space formalism, with the boundary coordinate satisfying  $P^2 = 0$ .

The  $p$ -adic and real bulk-to-bulk propagators, each of which admits a *split representation* in terms of integrals over bulk-to-boundary propagators, are given by

$$\begin{aligned} \mathbb{Q}_{p^n}) \quad G_\Delta(z_0, z; w_0, w) &= \zeta_p(2\Delta) p^{-\Delta d[z_0, z; w_0, w]} \\ &= \int_{-\frac{i\pi}{\log p}}^{\frac{i\pi}{\log p}} \frac{dc}{2\pi i} f_\Delta(c) \int_{\partial\mathcal{T}_{p^n}} dx K_{h-c}(z_0, z; x) K_{h+c}(w_0, w; x), \end{aligned} \quad (2.6)$$

$$\begin{aligned} \mathbb{R}^n) \quad G_\Delta(Z, W) &= \frac{\zeta_\infty(2\Delta)}{(Z-W)^{2\Delta}} {}_2F_1\left(\Delta, \Delta - h + \frac{1}{2}; 2\Delta - 2h + 1; -\frac{4}{(Z-W)^2}\right) \\ &= \frac{1}{2} \int_{-i\infty}^{i\infty} \frac{dc}{2\pi i} f_\Delta(c) \int_{\partial\text{AdS}} dP K_{h-c}(Z, P) K_{h+c}(W, P), \end{aligned}$$

where we have defined

$$h \equiv \frac{n}{2}, \quad (2.7)$$

with

$$\mathbb{Q}_{p^n}) \quad f_\Delta(c) \equiv \frac{\nu_\Delta}{m_\Delta^2 - m_{h-c}^2} \frac{\zeta_p(2\Delta - 2h)}{\zeta_p(2c)\zeta_p(-2c)} \log p, \quad (2.8)$$

$$\mathbb{R}^n) \quad f_\Delta(c) \equiv \frac{\nu_\Delta}{m_\Delta^2 - m_{h-c}^2} \frac{\zeta_\infty(2\Delta - 2h)}{\zeta_\infty(2c)\zeta_\infty(-2c)},$$

and

$$\mathbb{Q}_{p^n}) \quad 2\nu_\Delta \equiv p^{\Delta_+} - p^{\Delta_-} = \frac{p^\Delta}{\zeta_p(2\Delta - n)}, \quad \mathbb{R}^n) \quad 2\nu_\Delta \equiv \Delta_+ - \Delta_- = 2\Delta - n, \quad (2.9)$$

and  $d[z_0, z; w_0, w]$  denotes the graph distance between two nodes  $(z_0, z)$  and  $(w_0, w)$  on the Bruhat–Tits tree, while  $(Z - W)^2$  is related to the chordal distance in real continuum AdS.

We note that consistent with Ref. [4], we are using non-standard normalizations for the bulk-to-boundary and bulk-to-bulk propagators, so that the  $p$ -adic and real bulk-to-bulk

propagators satisfy the equations<sup>4</sup>

$$\begin{aligned} \mathbb{Q}_{p^n}) \quad & (\square_{z_0, z} + m_\Delta^2) G_\Delta(z_0, z; w_0, w) = 2\nu_\Delta \zeta_p(2\Delta - 2h) \delta(z_0, z; w_0, w), \\ \mathbb{R}^n) \quad & (-\nabla_Z^2 + m_\Delta^2) G_\Delta(Z, W) = 2\nu_\Delta \zeta_\infty(2\Delta - 2h) \delta(Z - W). \end{aligned} \quad (2.10)$$

We will consider bulk contact-interactions of the type

$$\mathbb{Q}_{p^n}) \quad \sum_{(z_0, z) \in \mathcal{T}_{p^n}} \prod_{i=1}^{\mathcal{N}} \phi_i(z_0, z), \quad \mathbb{R}^n) \quad \int_{\text{AdS}_{n+1}} dX \prod_{i=1}^{\mathcal{N}} \phi_i(X), \quad (2.11)$$

and study boundary correlators  $\langle \mathcal{O}_{\Delta_1}(x_1) \dots \mathcal{O}_{\Delta_{\mathcal{N}}}(x_{\mathcal{N}}) \rangle$ , which are functions of boundary insertion points  $x_i$ , and are built holographically from  $\mathcal{N}$ -point position space amplitudes  $\mathcal{A}(\{x_i\})$ . These amplitudes are given by products of bulk-to-boundary and bulk-to-bulk propagators with bulk vertices integrated over the entire bulk, and they depend on the boundary insertion points only via the  $\mathcal{N}(\mathcal{N} - 3)/2$  independent conformally invariant cross-ratios constructed out of the boundary points.<sup>5</sup>

*Mellin amplitudes* are defined via multi-dimensional inverse-Mellin transforms of the position space amplitudes,

$$\begin{aligned} \mathbb{Q}_{p^n}) \quad & \mathcal{A}(\{x_i\}) = \int [d\gamma] \mathcal{M}(\{\gamma_{ij}\}) \prod_{1 \leq i < j \leq \mathcal{N}} \frac{\zeta_p(2\gamma_{ij})}{|x_i - x_j|_p^{2\gamma_{ij}}}, \\ \mathbb{R}^n) \quad & \mathcal{A}(\{x_i\}) = \int [d\gamma] \mathcal{M}(\{\gamma_{ij}\}) \prod_{1 \leq i < j \leq \mathcal{N}} \frac{\zeta_\infty(2\gamma_{ij})}{|x_i - x_j|^{2\gamma_{ij}}}. \end{aligned} \quad (2.12)$$

The definition of Mellin amplitudes over the reals differs from the ones usually found in the literature only in the choice of normalization of  $\mathcal{M}$ . As will become clear shortly, this choice makes the parallels between real and  $p$ -adic results the crispest. The complex  $\gamma_{ij}$  variables above are the Mellin variables, which satisfy

$$\gamma_{ij} = \gamma_{ji}, \quad \sum_{j=1}^{\mathcal{N}} \gamma_{ij} = 0 \quad \text{and} \quad \gamma_{ii} = -\Delta_i \quad (\text{no sum over } i) \quad i = 1, \dots, \mathcal{N}, \quad (2.13)$$

<sup>4</sup>The relative sign mismatch in (2.10) is merely cosmetic, and an artifact of the sign convention used in defining the Laplacian operator  $\square$  on the Bruhat–Tits tree [2].

<sup>5</sup>To obtain this counting, we assume  $n + 1 \geq \mathcal{N}$ .

leading also to  $\mathcal{N}(\mathcal{N} - 3)/2$  independent components. The integration measure in (2.12) is over the independent Mellin variables,

$$\begin{aligned} \mathbb{Q}_{p^n}) \quad [d\gamma] &\equiv \left(\frac{2 \log p}{2\pi i}\right)^{\frac{\mathcal{N}(\mathcal{N}-3)}{2}} \left[ \prod_{1 \leq i < j \leq \mathcal{N}} d\gamma_{ij} \right] \left[ \prod_{i=1}^{\mathcal{N}} \delta\left(\sum_{j=1}^{\mathcal{N}} \gamma_{ij}\right) \right], \\ \mathbb{R}^n) \quad [d\gamma] &\equiv \left(\frac{1}{2\pi i}\right)^{\frac{\mathcal{N}(\mathcal{N}-3)}{2}} \left[ \prod_{1 \leq i < j \leq \mathcal{N}} d\gamma_{ij} \right] \left[ \prod_{i=1}^{\mathcal{N}} \delta\left(\sum_{j=1}^{\mathcal{N}} \gamma_{ij}\right) \right], \end{aligned} \tag{2.14}$$

and the precise contour prescription is similar in both cases, with the main distinction being that the Mellin variables in  $p$ -adic Mellin space live on a “complex cylinder”,  $\mathbb{R} \times S^1$  where the imaginary direction is periodically identified:  $\gamma_{ij} \sim \gamma_{ij} + \frac{i\pi}{\log p}$  [4]. This distinction arises for the following reason. Mellin variables may be identified as the conjugate of the dilatation parameter. However the dilatation group for  $p$ -adic coordinates is discrete, owing to the discreteness of the  $p$ -adic norm, and the Pontryagin dual of a discrete group is compact.<sup>6</sup>

The constraints in (2.13) can be solved in auxiliary momentum space, provided the fictitious momenta  $k_i$  satisfy the following constraints,

$$k_i \cdot k_j = \gamma_{ij}, \quad \sum_{i=1}^{\mathcal{N}} k_i = 0, \quad i, j \in \{1, \dots, \mathcal{N}\}, \tag{2.15}$$

and the on-shell condition,

$$k_i^2 = k_i \cdot k_i = -\Delta_i, \quad i \in \{1, \dots, \mathcal{N}\}. \tag{2.16}$$

Mandelstam-like variables can be defined via

$$s_{i_1 \dots i_K} \equiv - \left( \sum_{i \in S} k_i \right)^2 = \sum_{i \in S} \Delta_i - 2 \sum_{\substack{i, j \in S, \\ i < j}} \gamma_{ij}, \tag{2.17}$$

where  $S = \{i_1, \dots, i_K\} \subset \{1, \dots, \mathcal{N}\}$  is a subset of the set of all external legs. For large  $N$  CFTs, Mellin amplitudes are meromorphic functions of such Mandelstam-like variables, built out of the local zeta function  $\zeta_p$  or  $\zeta_\infty$ , with the poles corresponding to the exchange of single-trace operators (and their descendants in  $\mathbb{R}^n$ ).

---

<sup>6</sup>We thank Brian Trundy for this observation.

**Example (i).** The simplest Mellin amplitudes are the contact amplitudes, represented diagrammatically thus:

$$\mathcal{M}^{\text{contact}} = \begin{array}{c} 2 \\ \diagup \quad \diagdown \\ \circ \\ \diagdown \quad \diagup \\ \mathcal{N} \end{array} \quad . \quad (2.18)$$

In our normalization, the Mellin amplitudes for the contact diagram are given by

$$\begin{aligned} \mathbb{Q}_{p^n}) \quad \mathcal{M}^{\text{contact}} &= \zeta_p \left( \sum_{i=1}^{\mathcal{N}} \Delta_i - n \right), \\ \mathbb{R}^n) \quad \mathcal{M}^{\text{contact}} &= \frac{1}{2} \zeta_\infty \left( \sum_{i=1}^{\mathcal{N}} \Delta_i - n \right). \end{aligned} \quad (2.19)$$

For diagrams with internal lines corresponding to exchange of single-trace operators, it is convenient to express Mellin amplitudes as contour integrals over the so-called *pre-amplitudes* (denoted with a tilde):

$$\begin{aligned} \mathbb{Q}_{p^n}) \quad \mathcal{M} &= \left[ \prod_I \int_{-\frac{i\pi}{\log p}}^{\frac{i\pi}{\log p}} \frac{dc_I}{2\pi i} f_{\Delta_I}(c_I) \right] \widetilde{\mathcal{M}}, \\ \mathbb{R}^n) \quad \mathcal{M} &= \left[ \prod_I \int_{-i\infty}^{i\infty} \frac{dc_I}{2\pi i} f_{\Delta_I}(c_I) \right] \widetilde{\mathcal{M}}, \end{aligned} \quad (2.20)$$

where  $f_\Delta(c)$  is defined in (2.8). The index  $I$  runs over all internal lines in the diagram. Like Mellin amplitudes, pre-amplitudes depend on Mellin variables solely via Mandelstam-like variables, but unlike Mellin amplitudes, pre-amplitudes depend only on external scaling dimensions, not internal ones.

**Example (ii).** The amplitude with exactly one internal line, that is the exchange amplitude, is depicted thus:

$$\mathcal{M}^{\text{exchange}} = i_L \begin{array}{c} \diagdown \quad \diagup \\ \circ \\ \diagup \quad \diagdown \\ \Delta \end{array} i_R \quad . \quad (2.21)$$

The associated Mandelstam invariant  $s$  is given by

$$s = \sum \Delta_{i_L} - 2 \sum \gamma_{i_L j_L} = \sum \Delta_{i_R} - 2 \sum \gamma_{i_R j_R}, \quad (2.22)$$

where the limits of the various sums have been left implicit, but it should be clear from the context what indices are being summed over. For example,  $\sum \Delta_{i_L} = \sum_{i_L} \Delta_{i_L}$  is a sum over all possible values that  $i_L$  takes, and  $\sum \gamma_{i_L j_L} = \sum_{i_L < j_L} \gamma_{i_L j_L}$  where  $i_L, j_L$  are summed over all possible indices that label the external legs to the left of the internal line. The  $p$ -adic and real pre-amplitudes for the exchange diagram are then given by

$$\begin{aligned} \mathbb{Q}_p^n) \quad \widetilde{\mathcal{M}}^{\text{exchange}} &= \zeta_p \left( \sum \Delta_{i_L} + c - h \right) \zeta_p \left( \sum \Delta_{i_R} - c - h \right) \\ &\quad \times \beta_p \left( h + c - s, \sum \Delta_{i_L} - h - c \right) \beta_p \left( h - c - s, \sum \Delta_{i_R} - h + c \right), \\ \mathbb{R}^n) \quad \widetilde{\mathcal{M}}^{\text{exchange}} &= \frac{1}{4} \zeta_\infty \left( \sum \Delta_{i_L} + c - h \right) \zeta_\infty \left( \sum \Delta_{i_R} - c - h \right) \\ &\quad \times \beta_\infty \left( h + c - s, \sum \Delta_{i_L} - h - c \right) \beta_\infty \left( h - c - s, \sum \Delta_{i_R} - h + c \right), \end{aligned} \quad (2.23)$$

where we have defined

$$\mathbb{Q}_p^n) \quad \beta_p(s, t) \equiv \frac{\zeta_p(s) \zeta_p(t)}{\zeta_p(s+t)} = \zeta_p(s) - \zeta_p(-t), \quad \mathbb{R}^n) \quad \beta_\infty(s, t) \equiv \frac{\zeta_\infty(s) \zeta_\infty(t)}{\zeta_\infty(s+t)}. \quad (2.24)$$

The functional similarities between the real and  $p$ -adic results reviewed in this section hint at a framework in which perhaps both real and  $p$ -adic computations can be performed in a unified manner. Indeed as stated in the introduction, we will present in this paper prescriptions for constructing arbitrary-point tree-level Mellin amplitudes for scalars which apply to both the real and  $p$ -adic AdS/CFT frameworks simultaneously, demonstrating the close ties between the formalisms and providing further evidence for a larger universal framework in which the real and  $p$ -adic formulations are treated on the same footing.

## 3 Construction of Mellin Amplitudes

### 3.1 Recursive prescription for $p$ -adic Mellin amplitudes

In Ref. [4], we computed the  $p$ -adic Mellin amplitudes for a general scalar contact diagram, as well as for arbitrary-point tree-level bulk diagrams containing one, two or three internal lines.

A careful comparison of these amplitudes hints at a recursive structure. In this section, we provide a precise formulation of this structure and a prescription for recovering all previously computed Mellin amplitudes from Ref. [4]. In appendices B and C, we prove that this recursive prescription extends to arbitrary tree-level bulk diagrams, and thus can be used to directly write down closed-form expressions for Mellin amplitudes corresponding to tree-level bulk diagrams with an arbitrary number of internal lines admitting scalar exchanges, helping bypass tedious bulk computations.

It is well known that in position space, any tree-level bulk diagram, also referred to as a Witten diagram, is built out of three ingredients: external legs corresponding to bulk-to-boundary propagators, internal lines corresponding to bulk-to-bulk propagators, and interaction vertices corresponding to coupling constants. The same continues to hold true in  $p$ -adic AdS/CFT [2]. The full ( $p$ -adic) position space amplitude is obtained by performing bulk integration over all bulk vertices of an integrand given by the product over all factors associated with the individual ingredients going into the diagram.

In contrast, in Mellin space the closed-form expressions for Mellin amplitudes from Ref. [4] suggest that  $p$ -adic Mellin amplitudes can be written in terms of two basic building blocks, which we represent graphically as:

- Contact vertex:

$$\begin{array}{c} \Delta_2 \\ | \\ \Delta_1 \text{---} \bullet \text{---} \Delta_3 \\ / \quad \backslash \\ \Delta_f \quad \dots \quad \Delta_4 \end{array} \equiv \zeta_p \left( \sum_{i=1}^f \Delta_i - n \right). \quad (3.1)$$

- Internal line:

$$\overline{\quad A \quad} \equiv \zeta_p(s_A - \Delta_A). \quad (3.2)$$

We present two examples.

**Example (iii).** Using the graphical representations above, we can rewrite the closed-form  $p$ -adic Mellin amplitude for the arbitrary-point exchange diagram as

$$\begin{array}{c} \text{---} \bullet \text{---} \bullet \text{---} \\ / \quad \backslash \quad / \quad \backslash \\ i_L \quad \vdots \quad i_R \end{array} \equiv \left( \begin{array}{c} i_L \text{---} \bullet \text{---} A \\ / \quad \backslash \\ \vdots \quad \vdots \end{array} \right) \left( \begin{array}{c} \bullet \text{---} A \text{---} \bullet \\ / \quad \backslash \\ \vdots \quad \vdots \end{array} \right) \left( \begin{array}{c} \bullet \text{---} A \text{---} \bullet \\ / \quad \backslash \\ i_L \text{---} \bullet \text{---} i_R \end{array} \right), \quad (3.3)$$

where we have defined

$$\begin{array}{c} i_U \\ \vdots \\ \diagup \quad \diagdown \\ \text{---} A \text{---} \\ \diagdown \quad \diagup \\ \vdots \\ i_R \end{array} \equiv (-1)^1 \left\{ \left( \text{---} A \text{---} \right) - \left( \begin{array}{c} i_L \quad \vdots \quad i_R \\ \diagdown \quad \diagup \\ \text{---} \\ \diagup \quad \diagdown \end{array} \right) \right\}. \quad (3.4)$$

It is straightforward to verify that this is simply a diagrammatic rewriting of equation (4.42) of Ref. [4] provided we identify the Mandelstam invariant  $s_A$  with the expression in (2.22).

**Example (iv).** Similar to the previous example, the  $p$ -adic Mellin amplitude for a bulk diagram with two internal lines (but arbitrary external insertions) is given by

$$\begin{array}{c} i_U \\ \vdots \\ \diagup \quad \diagdown \\ \text{---} A \text{---} B \text{---} \\ \diagdown \quad \diagup \\ \vdots \\ i_R \end{array} = \left( \begin{array}{c} i_L \quad \vdots \\ \diagdown \quad \diagup \\ \text{---} A \text{---} \end{array} \right) \left( \begin{array}{c} i_U \\ \vdots \\ \diagdown \quad \diagup \\ \text{---} A \text{---} B \text{---} \\ \diagdown \quad \diagup \end{array} \right) \left( \begin{array}{c} \text{---} B \text{---} \\ \diagdown \quad \diagup \\ \vdots \\ i_R \end{array} \right) \left( \begin{array}{c} i_U \\ \vdots \\ \diagup \quad \diagdown \\ \text{---} A \text{---} B \text{---} \\ \diagdown \quad \diagup \\ \vdots \\ i_R \end{array} \right), \quad (3.5)$$

where we have defined

$$\begin{array}{c} i_U \\ \vdots \\ \diagup \quad \diagdown \\ \text{---} A \text{---} B \text{---} \\ \diagdown \quad \diagup \\ \vdots \\ i_R \end{array} \equiv (-1)^2 \left\{ \left( \text{---} A \text{---} \right) \left( \text{---} B \text{---} \right) - \left( \begin{array}{c} i_U \\ \vdots \\ \diagdown \quad \diagup \\ \text{---} A \text{---} \quad \vdots \quad i_R \end{array} \right) (-1)^1 \left( \begin{array}{c} i_U \\ \vdots \\ \diagup \quad \diagdown \\ \text{---} A \text{---} B \text{---} \\ \diagdown \quad \diagup \\ \vdots \\ i_R \end{array} \right) \right. \\ \left. - \left( \begin{array}{c} i_U \\ \vdots \\ \diagdown \quad \diagup \\ \text{---} \quad \vdots \quad \text{---} \\ \diagdown \quad \diagup \\ \vdots \\ i_L \end{array} \right) (-1)^1 \left( \begin{array}{c} i_U \\ \vdots \\ \diagup \quad \diagdown \\ \text{---} B \text{---} \\ \diagdown \quad \diagup \\ \vdots \\ i_R \end{array} \right) - \left( \begin{array}{c} i_U \\ \vdots \\ \diagdown \quad \diagup \\ \text{---} \quad \vdots \quad \text{---} \\ \diagdown \quad \diagup \\ \vdots \\ i_R \end{array} \right) \right\}. \quad (3.6)$$

This reproduces the amplitude given in equation (4.56) of Ref. [4] if we set the Mandelstam-like variables  $s_A, s_B$  to

$$s_A = \sum \Delta_{i_L} - 2 \sum \gamma_{i_L j_L}, \quad s_B = \sum \Delta_{i_R} - 2 \sum \gamma_{i_R j_R}, \quad (3.7)$$

and use (3.4) to further reduce (3.6) to an expression given entirely in terms of vertex and internal line factors (3.1)-(3.2).

The two examples above are suggestive of the recursive procedure for reconstructing  $p$ -adic Mellin amplitudes which we will now describe. In this prescription, no integration is necessary and the basic building blocks are the bulk contact-interaction vertices and internal lines, (3.1) and (3.2) respectively. This recursive procedure will be proven in the appendices.

**Prescription I** ( $p$ -adic Mellin amplitudes). *The Mellin amplitude for a particular bulk diagram is given by the product over a vertex factor (3.1) for each contact vertex in the diagram, times what we will refer to as an “undressed Mellin amplitude” (which we have depicted in red in (3.3) and (3.5)). The undressed amplitudes are constructed recursively as follows:*

- *The undressed amplitude for a bulk diagram with no internal lines is equal to one.*
- *The undressed amplitude for a bulk diagram with one or more internal lines is given by an overall factor of minus one raised to the number of internal lines times the following combination: the product over all internal line factors (3.2) associated with the bulk diagram, minus all possible undressed diagrams associated with bulk diagrams obtained by collapsing all possible subsets of internal lines in the original bulk diagram, with each such subtracted term weighted by minus one raised to the number of remaining internal lines and also weighted by the vertex factor(s) (3.1) associated with any new contact vertex (or vertices) generated upon affecting such a collapse.*

Schematically, this prescription takes the form:

$$\begin{aligned}
 (\text{undressed diagram}) = & (-1)^{\# \text{ internal lines}} \left\{ \prod (\text{internal line factors}) \right. \\
 & - \sum \left[ (-1)^{\# \text{ remaining internal lines}} (\text{new vertex factor(s)}) \right. \\
 & \left. \left. \times (\text{reduced undressed diagram}) \right] \right\}. \tag{3.8}
 \end{aligned}$$

We make two remarks about the prescription described above:

- ★ Each vertex factor is given by the  $p$ -adic local zeta function (3.1) whose argument is given by the sum over the scaling dimensions of all (internal and external) operators incident on the vertex, minus the dimension of the boundary field theory  $n$ .
- ★ In each factor (3.2) associated with an internal line, the Mandelstam variable carried by the line is given by a combination of Mellin variables  $\gamma_{ij}$  and external scaling dimensions  $\Delta_i$  as defined in (2.17), with the subset  $S$  in (2.17) taken to be all the external indices on one side of the internal line in question.

As is clear from the recursive prescription for the undressed amplitudes, the recursion is on the number of internal lines (exchanges), with each undressed amplitude expressible in terms of undressed amplitudes containing fewer internal lines (exchange channels).

It will be often convenient to represent this recursive procedure diagrammatically. To distinguish between the full Mellin amplitudes and undressed Mellin amplitudes, we will use the following convention:

- ★ Mellin amplitudes will be represented like standard Witten diagrams, drawn in black with the Poincaré disk shown explicitly.
- ★ Undressed amplitudes will be represented in red with no Poincaré disk shown, and we will refer to these as “undressed diagrams”.

For illustrative purposes, we apply this procedure to two non-trivial diagrams, namely the two topologically distinct types of diagrams involving three internal lines.

**Example (v).** For the diagram with three internal lines arranged in a series, the recursive procedure leads to the following Mellin amplitude.

$$\begin{aligned}
 & \text{Diagram with three internal lines in series, enclosed in an oval, with external lines } i_L, i_r, \dots \text{ and internal lines } A, B, C. \\
 & = \left( \begin{array}{c} i_L \\ \vdots \\ \text{Diagram 1} \end{array} \right) \left( \begin{array}{c} i_l \\ \vdots \\ \text{Diagram 2} \end{array} \right) \left( \begin{array}{c} i_r \\ \vdots \\ \text{Diagram 3} \end{array} \right) \left( \begin{array}{c} \vdots \\ i_R \\ \text{Diagram 4} \end{array} \right) \left( \begin{array}{c} i_l \quad i_r \\ \vdots \quad \vdots \\ \text{Diagram 5} \end{array} \right), \\
 & \tag{3.9}
 \end{aligned}$$

where the undressed diagram is given by

$$\begin{aligned}
 & \text{Diagram 5 (undressed)} = \\
 & (-1)^3 \left\{ \left( \begin{array}{c} \text{Diagram 6} \end{array} \right) \left( \begin{array}{c} \text{Diagram 7} \end{array} \right) \left( \begin{array}{c} \text{Diagram 8} \end{array} \right) - \left( \begin{array}{c} i_l \\ \vdots \\ \text{Diagram 9} \end{array} \right) (-1)^2 \left( \begin{array}{c} i_l \quad i_r \\ \vdots \quad \vdots \\ \text{Diagram 10} \end{array} \right) \right. \\
 & - \left( \begin{array}{c} i_l \\ \vdots \\ \text{Diagram 11} \end{array} \right) (-1)^2 \left( \begin{array}{c} i_l \\ \vdots \\ \text{Diagram 12} \end{array} \right) - \left( \begin{array}{c} i_r \\ \vdots \\ \text{Diagram 13} \end{array} \right) (-1)^2 \left( \begin{array}{c} i_l \quad i_r \\ \vdots \quad \vdots \\ \text{Diagram 14} \end{array} \right) \\
 & - \left( \begin{array}{c} i_l \\ \vdots \\ \text{Diagram 15} \end{array} \right) (-1)^1 \left( \begin{array}{c} i_l \\ \vdots \\ \text{Diagram 16} \end{array} \right) - \left( \begin{array}{c} i_l \\ \vdots \\ \text{Diagram 17} \end{array} \right) (-1)^1 \left( \begin{array}{c} i_l \\ \vdots \\ \text{Diagram 18} \end{array} \right) \\
 & \left. - \left( \begin{array}{c} i_l \\ \vdots \\ \text{Diagram 19} \end{array} \right) \left( \begin{array}{c} i_r \\ \vdots \\ \text{Diagram 20} \end{array} \right) (-1)^1 \left( \begin{array}{c} i_l \quad i_r \\ \vdots \quad \vdots \\ \text{Diagram 21} \end{array} \right) - \left( \begin{array}{c} i_l \\ \vdots \\ \text{Diagram 22} \end{array} \right) \right\}. \\
 & \tag{3.10}
 \end{aligned}$$



where the undressed diagram is given by

$$\begin{aligned}
& \begin{array}{c} i_U \\ \vdots \\ \text{---} \\ A \quad B \\ \text{---} \\ i_L \quad \vdots \quad i_R \\ | \\ C \\ \text{---} \\ \vdots \\ i_D \end{array} = \\
& (-1)^3 \left\{ \left( \text{---} \right) \left( \text{---} \right) \left( \left| \right. \right) - \left( \begin{array}{c} i_U \\ \vdots \\ \text{---} \\ B \\ \text{---} \\ i_L \quad \vdots \quad i_R \\ | \\ C \end{array} \right) (-1)^2 \left( \begin{array}{c} i_U \\ \vdots \\ \text{---} \\ B \\ \text{---} \\ i_L \quad \vdots \quad i_R \\ | \\ C \\ \text{---} \\ \vdots \\ i_D \end{array} \right) \right. \\
& - \left( \begin{array}{c} i_U \\ \vdots \\ \text{---} \\ A \\ \text{---} \\ i_L \quad \vdots \quad i_R \\ | \\ C \end{array} \right) (-1)^2 \left( \begin{array}{c} i_U \\ \vdots \\ \text{---} \\ A \\ \text{---} \\ i_L \quad \vdots \quad i_R \\ | \\ C \\ \text{---} \\ \vdots \\ i_D \end{array} \right) - \left( \begin{array}{c} i_U \\ \vdots \\ \text{---} \\ A \\ \text{---} \\ i_L \quad \vdots \quad i_R \\ | \\ B \\ \text{---} \\ \vdots \\ i_D \end{array} \right) (-1)^2 \left( \begin{array}{c} i_U \\ \vdots \\ \text{---} \\ A \\ \text{---} \\ i_L \quad \vdots \quad i_R \\ | \\ B \\ \text{---} \\ \vdots \\ i_D \end{array} \right) \\
& - \left( \begin{array}{c} i_U \\ \vdots \\ \text{---} \\ A \\ \text{---} \\ i_L \quad \vdots \quad i_R \\ | \\ B \\ \text{---} \\ \vdots \\ i_D \end{array} \right) (-1)^1 \left( \begin{array}{c} i_U \\ \vdots \\ \text{---} \\ A \\ \text{---} \\ i_L \quad \vdots \quad i_R \\ | \\ C \\ \text{---} \\ \vdots \\ i_D \end{array} \right) - \left( \begin{array}{c} i_U \\ \vdots \\ \text{---} \\ B \\ \text{---} \\ i_L \quad \vdots \quad i_R \\ | \\ C \\ \text{---} \\ \vdots \\ i_D \end{array} \right) (-1)^1 \left( \begin{array}{c} i_U \\ \vdots \\ \text{---} \\ B \\ \text{---} \\ i_L \quad \vdots \quad i_R \\ | \\ C \\ \text{---} \\ \vdots \\ i_D \end{array} \right) \\
& \left. - \left( \begin{array}{c} i_U \\ \vdots \\ \text{---} \\ A \\ \text{---} \\ i_L \quad \vdots \quad i_R \\ | \\ C \\ \text{---} \\ \vdots \\ i_D \end{array} \right) (-1)^1 \left( \begin{array}{c} i_U \\ \vdots \\ \text{---} \\ A \\ \text{---} \\ i_L \quad \vdots \quad i_R \\ | \\ C \\ \text{---} \\ \vdots \\ i_D \end{array} \right) - \left( \begin{array}{c} i_U \\ \vdots \\ \text{---} \\ B \\ \text{---} \\ i_L \quad \vdots \quad i_R \\ | \\ C \\ \text{---} \\ \vdots \\ i_D \end{array} \right) \right\}, \tag{3.13}
\end{aligned}$$

with the Mandelstam-like variables given by

$$\begin{aligned}
s_A &= \sum \Delta_{i_L} - 2 \sum \gamma_{i_L j_L}, \\
s_B &= \sum \Delta_{i_R} - 2 \sum \gamma_{i_R j_R}, \\
s_C &= \sum \Delta_{i_D} - 2 \sum \gamma_{i_D j_D}.
\end{aligned} \tag{3.14}$$

Just like in the previous example, the undressed diagram in (3.13) may recursively be reduced further using expressions (3.4) and (3.6), to give an amplitude expressed solely in terms of the internal line and contact vertex factors. It is again easily verified that this result matches the previously computed amplitude given in equation (4.78) of Ref. [4].

### 3.2 Feynman rules for real Mellin amplitudes

It is interesting to compare the recursive procedure describe above with the so-called Feynman rules for real Mellin amplitudes.

**Prescription II** (Feynman rules for real Mellin amplitudes [6, 7, 8]). *Given a tree-level bulk diagram, (adapted to the conventions and normalization described in section 2) the Feynman rules are:*

- *Label the internal lines with an index  $j$  running from 1 to  $v - 1$  and associate to each internal line an integer  $n_j$  and a factor of*

$$L_j(s_j, \Delta_j, n_j) = \frac{1}{n_j!} \frac{(1 + \Delta_j - h)_{n_j}}{(\Delta_j - s_j)/2 + n_j}, \quad (3.15)$$

where  $s_j$  is the Mandelstam invariant associated to internal leg  $j$ , and  $(a)_{n_j} \equiv \frac{\Gamma(a+n_j)}{\Gamma(a)}$  is the Pochhammer symbol.

- *Label the vertices with an index  $j$  running from one to  $v$ . For a vertex  $j$  connected to  $L$  legs with scaling dimensions  $\Delta_1$  to  $\Delta_L$ , label the internal legs by indices 1 to  $l$  and the external legs by indices  $l + 1$  to  $L$ , let  $n_1$  to  $n_l$  be the integers associated with the internal legs, and associate to the vertex  $j$  a factor of*

$$V_j(\{\Delta_i\}, \{n_i\}) = \frac{1}{2} \zeta_\infty \left( \sum_{i=1}^L \Delta_i - n \right) \times F_A^{(l)} \left( \frac{1}{2} \sum_{i=1}^L \Delta_i - h; \{-n_1, \dots, -n_l\}; \{1 + \Delta_1 - h, \dots, 1 + \Delta_l - h\}; 1, \dots, 1 \right), \quad (3.16)$$

where  $F_A^{(l)}$  is the Lauricella hypergeometric series [43, 44, 45, 7], defined as

$$F_A^{(l)}(g; \{a_1, \dots, a_l\}; \{b_1, \dots, b_l\}; x_1, \dots, x_l) = \left[ \prod_{i=1}^l \sum_{n_i=0}^{\infty} \right] (g)_{\sum_{i=1}^l n_i} \prod_{i=1}^l \frac{(a_i)_{n_i}}{(b_i)_{n_i}} \frac{x_i^{n_i}}{n_i!}. \quad (3.17)$$

- The Mellin amplitude is given by taking the product of all line and vertex factors and then summing over the integers associated with the internal legs:

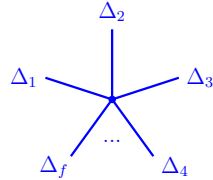
$$\mathcal{M}(\{\gamma_{ij}\}, \{\Delta_i\}) = \left[ \prod_{i=1}^{v-1} \sum_{n_i=0}^{\infty} \right] \left[ \prod_{j=1}^{v-1} L_j(s_j, \Delta_j, n_j) \right] \left[ \prod_{j=1}^v V_j(\{\Delta_i\}, \{n_i\}) \right]. \quad (3.18)$$

These rules are arguably more compact and straightforward than the prescription for obtaining the  $p$ -adic Mellin amplitudes, but this apparent simplicity is deceptive and merely due to the fact that the real Mellin amplitude is left in the form of unevaluated infinite sums, while the prescription in the  $p$ -adic case fully reduces the Mellin amplitudes to finite sums of elementary functions. For this reason, prescriptions I and II do not highlight the similarity in the structure of real and  $p$ -adic Mellin amplitudes. For a unified perspective on real and  $p$ -adic amplitudes, it is useful to turn instead to pre-amplitudes which will be the subject of the next section. However, we do note at this point that as in the  $p$ -adic case, we can decompose both real and  $p$ -adic Mellin amplitudes into a product of contact vertices and an “undressed diagram”:

$$\mathcal{M}(\{\gamma_{ij}\}, \{\Delta_i\}) = (\text{all contact vertices}) \times (\text{undressed diagram}), \quad (3.19)$$

where in the real case the vertex factors are defined as

- Contact vertex:



$$\equiv \frac{1}{2} \zeta_{\infty} \left( \sum_{i=1}^f \Delta_i - n \right). \quad (3.20)$$

With this definition in place, equations (3.3), (3.5), (3.9), and (3.12) continue to apply for real Mellin amplitudes, with the explicit expressions for the undressed diagrams over the  $p$ -adics (given by prescription I) getting replaced by infinite sums over products of Lauricella functions over the reals (given by prescription II). Equation (3.19) serves as the definition of undressed diagrams over reals. We will show in the next section that the undressed diagrams over the reals and the  $p$ -adics are in fact closely related to each other via a concrete relation.

## 4 Construction of Pre-Amplitudes

Mellin amplitudes  $\mathcal{M}$ , real and  $p$ -adic, admit a representation called the Mellin-Barnes representation in terms of a contour integral over a pre-amplitude  $\widetilde{\mathcal{M}}$ , defined in (2.20). Compared to Mellin amplitudes, pre-amplitudes are markedly simpler: they do not depend on internal scaling dimensions, and for any given bulk diagram the corresponding pre-amplitude is simply a product over factors associated with each vertex of the bulk diagram. Furthermore, pre-amplitudes of real and  $p$ -adic AdS/CFT take identical forms, and for this reason we can simultaneously present the prescription for either type of pre-amplitude. In the real case, the prescription essentially follows from Ref. [8] after adjusting overall coefficients to account for our normalization conventions described in section 2. For the  $p$ -adic case, we present an inductive proof of the prescription in appendix B.

**Prescription III** (Pre-amplitudes). *For a diagram with  $v$  vertices labelled by indices  $j \in \{1, \dots, v\}$ , the pre-amplitude is constructed as follows:*

- Associate to each internal leg an orientation and a complex variable  $c_i$ .
- For a vertex  $j$  connected to  $L$  legs with scaling dimensions  $\Delta_1$  to  $\Delta_L$ , let indices 1 to  $l$  label internal legs and let indices  $l+1$  to  $L$  label external leg. Furthermore, define scaling dimensions  $\widetilde{\Delta}_i$  as follows: if  $i \in \{1, \dots, l\}$  so that  $i$  labels an internal leg, define a complex scaling dimension  $\widetilde{\Delta}_i = h \pm c_i$ , where the plus sign is chosen if the orientation of the internal leg is incoming and the minus sign is chosen if the internal leg is outgoing with respect to the vertex; if  $i \in \{l+1, \dots, L\}$  so that  $i$  labels an external leg, define  $\widetilde{\Delta}_i = \Delta_i$ . Also associate to each vertex a factor of:

$$\begin{aligned}
 \mathbb{Q}_p^n) \quad \widetilde{V}_j(\{s_i\}, \{\widetilde{\Delta}_i\}) &= \\
 \zeta_p \left( \sum_{i=1}^L \widetilde{\Delta}_i - n \right) &\left[ \prod_{i=1}^l \frac{2\zeta_p(1)}{|2|_p} \int_{\mathbb{Q}_p^2} \frac{dx_i}{|x_i|_p} |x_i|_p^{\frac{\widetilde{\Delta}_i - s_i}{2}} |1, x_i|_s^{\frac{\widetilde{\Delta}_i + s_i - n}{2}} \right] |1, x_1, \dots, x_l|_s^{\frac{n - \sum_{i=1}^L \widetilde{\Delta}_i}{2}}, \\
 \\
 \mathbb{R}^n) \quad \widetilde{V}_j(\{s_i\}, \{\widetilde{\Delta}_i\}) &= \\
 \frac{1}{2} \zeta_\infty \left( \sum_{i=1}^L \widetilde{\Delta}_i - n \right) &\left[ \prod_{i=1}^l \int_0^\infty \frac{dx_i}{|x_i|} |x_i|^{\frac{\widetilde{\Delta}_i - s_i}{2}} |1 + x_i|^{\frac{\widetilde{\Delta}_i + s_i - n}{2}} \right] \left| 1 + \sum_{i=1}^l x_i \right|^{\frac{n - \sum_{i=1}^L \widetilde{\Delta}_i}{2}}.
 \end{aligned} \tag{4.1}$$

Here  $\{s_i\}$  is the set of Mandelstam-like variables associated with the internal lines and  $\mathbb{Q}_p^2$  denotes the set of  $p$ -adic squares, see (A.8).

- The Mellin pre-amplitude is given by the product of these vertex factors:

$$\widetilde{\mathcal{M}}(\{\gamma_{ij}\}, \{\Delta_{\text{ext},i}\}, \{c_i\}) = \prod_{j=1}^v \widetilde{V}_j(\{s_i\}, \{\widetilde{\Delta}_i\}). \quad (4.2)$$

We point out that the integral representation of the pre-amplitude vertex factor in (4.1) over the  $p$ -adics and the reals is related to undressed diagrams as defined in (3.19). Thus these integrals admit a recursive construction via prescription I for the  $p$ -adics and prescription II for the reals. This point is explained in more detail next.

## 4.1 Obtaining pre-amplitudes from Mellin amplitudes

The reader might have noticed that the contact vertices defined in (3.1) and (3.20) appear in the prescription above for pre-amplitude vertex factors, and as we commented above the remaining factors in (4.1) can be identified with undressed diagrams. Essentially the claim is that pre-amplitudes decompose into products of Mellin amplitudes with a special assignment of internal dimensions, so that the Mellin-Barnes integral representation expresses any Mellin amplitude as a contour integral over simpler Mellin amplitudes.

More precisely, the pre-amplitude vertex factor  $\widetilde{V}_j(\{s_i\}, \{\widetilde{\Delta}_i\})$  from (4.1) associated with a given vertex in a bulk diagram, with internal lines assigned orientations according to prescription III as displayed in black in (4.3), is expressible as a product of a contact vertex and an undressed diagram associated to a full Mellin amplitude, as shown:

$$\widetilde{V}_j(\{s_i\}, \{\widetilde{\Delta}_i\}) = \left( \begin{array}{c} \Delta_L \quad \quad s_1, \Delta_1 \\ \vdots \quad \quad \vdots \\ \Delta_{l+1} \quad \quad s_l, \Delta_l \end{array} \right) : \quad (4.3)$$

$$= \left( \begin{array}{c} \Delta_L \quad \quad h+c_1 \\ \vdots \quad \quad \vdots \\ \Delta_{l+1} \quad \quad h+c_l \end{array} \right) \left( \begin{array}{c} \Delta_L \quad \quad s_1, h-c_1 \\ \vdots \quad \quad \vdots \\ \Delta_{l+1} \quad \quad s_l, h-c_l \end{array} \right),$$

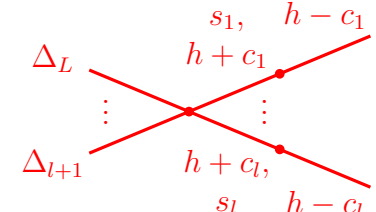
where the contact vertex factor (shown in blue in (4.3)) is given by (3.1) over  $p$ -adics and (3.20) over reals, and the undressed diagram (shown in red in (4.3)) can be explicitly constructed over the  $p$ -adics using the recursive prescription I, while over the reals it is con-

structured using the Feynman rule prescription II.

We point out that the undressed diagram in (4.3) has  $l$  internal lines, with Mandelstam invariants  $s_i$  and propagating complex dimensions  $h + c_i$ . Furthermore, the  $l$  vertices at which operators of dimensions  $h - c_i$  are incident should formally be thought of as contact interaction vertices, each of which has precisely one leg incident on another bulk vertex, while all other legs connect to external operator insertions.

We now prove this non-trivial claim, beginning with the real case. From the Feynman rules and definitions in section 3.2, it follows that

$\mathbb{R}^n$ )



(4.4)

$$\begin{aligned}
&= \left[ \prod_{i=1}^l \sum_{n_i=0}^{\infty} \right] \left[ \prod_{j=1}^l \frac{1}{n_j!} \frac{(1 + \tilde{\Delta}_j - h)_{n_j}}{(\tilde{\Delta}_j - s_j)/2 + n_j} F_A^{(1)} \left( \frac{\tilde{\Delta}_j + h - c_j}{2} - h; \{-n_j\}; \{1 + c_j\}; 1 \right) \right] \\
&\quad \times F_A^{(l)} \left( \frac{1}{2} \sum_{i=1}^L \tilde{\Delta}_i - h; \{-n_1, \dots, -n_l\}; \{1 + c_1, \dots, 1 + c_l\}; 1, \dots, 1 \right).
\end{aligned}$$

Since  $\tilde{\Delta}_j = h + c_j$  for  $j \in \{1, \dots, l\}$ , the Lauricella functions  $F_A^{(1)}$  in the above expression are all equal to unity. Using the definition (3.17) for the Lauricella function as a multiple sum, changing the order of summation between this multiple sum and the sums over  $n_i$ , and applying the identity

$$\sum_{n=0}^{\infty} \frac{(-n)_m (1 + c)_n}{n! (A + n)} = \frac{\Gamma(A + m) \Gamma(-c)}{\Gamma(A - c)} = (A)_m \beta_{\infty}(2A, -2c), \quad (4.5)$$

where  $\beta_{\infty}(\cdot, \cdot)$  is related to the usual Euler Beta function and was defined in (2.24), one can

carry out the sums over the integers  $n_i$  to find,

$$\begin{aligned}
& \mathbb{R}^n) \\
& \begin{array}{c} \Delta_L \\ \vdots \\ \Delta_{l+1} \end{array} \begin{array}{c} s_1, \quad h - c_1 \\ h + c_1 \\ \vdots \\ h + c_l, \\ s_l \quad h - c_l \end{array} \\
& = F_A^{(l)} \left( \frac{\sum_{i=1}^L \tilde{\Delta}_i - n}{2}; \left\{ \frac{\tilde{\Delta}_1 - s_1}{2}, \dots, \frac{\tilde{\Delta}_l - s_l}{2} \right\}; \{1 + c_1, \dots, 1 + c_l\}; 1, \dots, 1 \right) \prod_{i=1}^l \beta_\infty(\tilde{\Delta}_i - s_i, -2c_i) \\
& = \left[ \prod_{i=1}^l \int_0^\infty \frac{dx_i}{|x_i|} |x_i|^{\frac{\tilde{\Delta}_i - s_i}{2}} |1 + x_i|^{\frac{\tilde{\Delta}_i + s_i - n}{2}} \right] \left| 1 + \sum_{i=1}^l x_i \right|^{\frac{n - \sum_{i=1}^L \tilde{\Delta}_i}{2}}, \tag{4.6}
\end{aligned}$$

where the last equality arises from a formal substitution justified via an appropriate analytic continuation; we refer the reader to equation (3.30) of Ref. [8]. This proves (4.3) over  $\mathbb{R}^n$ .

We now turn to the  $p$ -adic case, where we need to prove the identity

$$\begin{aligned}
& \mathbb{Q}_p^n) \\
& \begin{array}{c} \Delta_L \\ \vdots \\ \Delta_{l+1} \end{array} \begin{array}{c} s_1, \quad h - c_1 \\ h + c_1 \\ \vdots \\ h + c_l, \\ s_l \quad h - c_l \end{array} \\
& \stackrel{!}{=} \left[ \prod_{i=1}^l \frac{2 \zeta_p(1)}{|2|_p} \int_{\mathbb{Q}_p^2} \frac{dx_i}{|x_i|_p} |x_i|_p^{\frac{c_i + h - s_i}{2}} |1, x_i|_s^{\frac{c_i + s_i - h}{2}} \right] |1, x_1, \dots, x_l|_s^{\frac{2h - \Delta - \sum_{i=1}^l (c_i + h)}{2}} \equiv \mathcal{D}, \tag{4.7}
\end{aligned}$$

where  $\Delta \equiv \sum_{i=l+1}^L \Delta_i$  and the left-hand side of the equation is obtained using prescription I in section 3.1 and we have introduced the symbol  $\mathcal{D}$  as a convenient shorthand for the right-hand side. As a first step, we change to variables  $t_i \in \mathbb{Q}_p$  satisfying  $x_i = t_i^2$ . Rather than picking a specific root for each  $x_i$ , we can include both roots in the domain of  $t_i$  at the cost of a factor of  $2/|2|_p$  per variable. We get that

$$\mathcal{D} = \prod_{i=1}^l \left[ \zeta_p(1) \int_{\mathbb{Q}_p} \frac{dt_i}{|t_i|_p} |t_i|_p^{h + c_i - s_i} |1, t_i|_s^{c_i + s_i - h} \right] |1, t_1, \dots, t_l|_s^{2h - \Delta - \sum_{i=1}^l (c_i + h)}. \tag{4.8}$$

Starting from this expression one can verify (4.7) when  $l = 1$ :

$$\begin{aligned} \mathcal{D}|_{l=1} &= \zeta_p(1) \int_{\mathbb{Q}_p} \frac{dt}{|t|_p} |t|_p^{h+c_1-s_1} |1, t|_p^{s_1-\Delta} = \zeta_p(\Delta - c_1 - h) - \zeta_p(s_1 - c_1 - h) \\ &= \begin{array}{c} \Delta_L \\ \vdots \\ \Delta_2 \end{array} \begin{array}{c} \diagup \\ \bullet \\ \diagdown \end{array} \begin{array}{c} s_1 \\ \text{---} \\ h+c_1 \quad h-c_1 \end{array}, \end{aligned} \quad (4.9)$$

where we refer the reader to (A.12) for the second equality, and in the final equality we used the expression for the undressed diagram with a single internal leg, given in (3.4).

Having established the base case, we now proceed to prove (4.7) inductively by showing that (4.8) satisfies the same recursion relation as the undressed diagram in (4.7). This can be achieved by partitioning the domain of the multi-dimensional integral in (4.8) into the following sub-domains:

1. the part of the domain where  $|t_1|_p, |t_2|_p, \dots, |t_l|_p \leq 1$ ,
2. the part of the domain where  $|t_1|_p = |t_2|_p = \dots = |t_l|_p > 1$ , and finally
3. for each proper subset  $\{u_1, u_2, \dots, u_g\} \subset \{1, 2, \dots, l\}$ , with complementary set labeled  $\{u_{g+1}, u_{g+1}, \dots, u_l\}$ , the part of the domain where  $|t_{u_1}|_p = |t_{u_2}|_p = \dots = |t_{u_g}|_p > 1, |t_{u_{g+1}}|_p, |t_{u_{g+2}}|_p, \dots, |t_{u_l}|_p \leq 1$ .

For the first part of the domain, the integral in  $\mathcal{D}$  evaluates to

$$\mathcal{D}|_{\text{sub-domain 1}} = \prod_{i=1}^l \left[ \zeta_p(1) \int_{\mathbb{Q}_p} \frac{dt_i}{|t_i|_p} |t_i|_p^{-s_i+h+c_i} \gamma_p(t_i) \right] = \prod_{i=1}^l \zeta_p(-s_i + h + c_i), \quad (4.10)$$

where  $\gamma_p$  is the characteristic function of  $\mathbb{Z}_p$ , defined in (A.1) and we used identity (A.5) to obtain the second equality. The contribution to  $\mathcal{D}$  coming from the second sub-domain evaluates to

$$\mathcal{D}|_{\text{sub-domain 2}} = \zeta_p(1) \int_{\mathbb{Q}_p} \frac{dt}{|t|_p} |t|_p^{2h-\Delta-\sum_{i=1}^l (-c_i+h)} \gamma_p\left(\frac{1}{pt}\right) = -\zeta_p\left(2h - \Delta - \sum_{i=1}^l (-c_i + h)\right). \quad (4.11)$$

For the last type of sub-domain, the contribution to  $\mathcal{D}$  arising from the subset  $\{u_1, \dots, u_g\}$

evaluates to

$$\begin{aligned} \mathcal{D} \Big|_{\substack{\{u_1, \dots, u_g\} \text{ part} \\ \text{of sub-domain 3}}} &= \prod_{i=g+1}^l \left[ \zeta_p(1) \int_{\mathbb{Q}_p} \frac{dt_{u_i}}{|t_{u_i}|_p} |t_{u_i}|_p^{-s_{u_i}+h+c_{u_i}} |1, t_{u_i}|_s^{s_{u_i}-h+c_{u_i}} \right] \\ &\times \zeta_p(1) \int_{\mathbb{Q}_p} \frac{dt}{|t|_p} |t|_p^{2h-\Delta-\sum_{i=1}^g(h-c_{u_i})-\sum_{i=g+1}^l(h+c_{u_i})} \gamma_p \left( \frac{(1, t_{u_{g+1}}, \dots, t_{u_l})_s}{pt} \right). \end{aligned} \quad (4.12)$$

By changing variable from  $t$  to  $u \equiv t/(1, t_{u_{g+1}}, \dots, t_{u_l})_s$ , the  $u$  integral factors out and can immediately be evaluated. One obtains

$$\begin{aligned} \mathcal{D} \Big|_{\substack{\{u_1, \dots, u_g\} \text{ part} \\ \text{of sub-domain 3}}} &= -\zeta_p \left( 2h - \Delta - \sum_{i=1}^g (h - c_{u_i}) - \sum_{i=g+1}^l (h + c_{u_i}) \right) \\ &\times \prod_{i=g+1}^l \left[ \zeta_p(1) \int_{\mathbb{Q}_p} \frac{dt_{u_i}}{|t_{u_i}|_p} |t_{u_i}|_p^{-s_{u_i}+h+c_{u_i}} |1, t_{u_i}|_s^{s_{u_i}-h+c_{u_i}} \right] \\ &\times |1, t_{u_{g+1}}, \dots, t_{u_l}|_s^{2h-\Delta-\sum_{i=1}^g(h-c_{u_i})-\sum_{i=g+1}^l(h+c_{u_i})}. \end{aligned} \quad (4.13)$$

We notice that the above expression is equal to a local zeta function times an integral of the same form as the original integral (4.8) except with  $l - g$  instead of  $l$  internal legs and with  $\Delta - \sum_{i=1}^g (h - c_{u_i})$  substituted for  $\Delta$ . Via an inductive reasoning, we assume that this remaining integral obeys (4.7), that is it is equal to the undressed diagram obtained by collapsing legs indexed by  $u_1$  to  $u_g$  in the undressed diagram on the right-hand side of (4.7), and now proceed to show that this implies the full diagram obeys (4.7) too.

In section 3.1 we defined undressed diagrams as satisfying the recursion relation (3.8). From the decomposition of  $\mathcal{D}$  into sub-domains as described above, we have in fact recovered the same recursive structure except we did not pick up explicit factors of  $(-1)^{\#\text{internal lines}}$  and the local zeta functions in (4.10), (4.11), and (4.13) appear with minus the argument with which they would have appeared in the vertex factors and internal leg factors as prescribed by (3.8). That is, compared to (3.8), we find here

$$\begin{aligned} \mathcal{D} &= \prod (\text{internal line factors w/ opposite sign arguments}) \\ &- \sum (\text{new vertex factors w/ opposite sign arguments}) \times (\text{reduced undressed diagram}). \end{aligned} \quad (4.14)$$

However, the two decompositions (3.8) and (4.14) are in fact equivalent, by virtue of the

$p$ -adic local zeta function identity

$$\zeta_p(x) + \zeta_p(-x) = 1, \quad (4.15)$$

using which one can show that if one flips the sign of 1) the degree of extension  $n$ , 2) all the scaling dimensions  $\Delta_i$ , and 3) all the Mandelstam invariants  $s_i$  inside the arguments of the local zeta functions, then any undressed diagram transform into itself times a factor of  $(-1)^{\#\text{internal legs}}$ . The equivalence of (3.8) and (4.14) follows directly from this, completing the proof of (4.7).

## 4.2 Pre-amplitude examples

In light of the identities for undressed diagrams derived in the previous subsection, the prescription for real and  $p$ -adic pre-amplitudes can be recast in a diagrammatic form that applies to both cases at once. In the contour integrals which follow, it will be understood that in the real case the contours run parallel to the imaginary axis, with limits from  $-i\infty$  to  $i\infty$ , while in the  $p$ -adic case the contour wraps once around the complex cylinder, so that the limits are from  $-\frac{i\pi}{\log p}$  to  $\frac{i\pi}{\log p}$ . With these conventions in place, let us consider some explicit examples for illustrative purposes.

**Example (vii).** The exchange diagram Mellin amplitude and pre-amplitude take the following form:

$$\begin{aligned} \left( \text{Diagram: Ellipse with internal line } s, \text{ vertices } i_L, i_R, \text{ and } \Delta \right) &= \left( \text{Diagram: Blue vertex } i_L, \text{ blue line } \Delta \right) \left( \text{Diagram: Blue vertex } i_R, \text{ blue line } \Delta \right) \left( \text{Diagram: Red vertex } i_L, \text{ red line } s, \text{ red vertex } i_R, \text{ red line } \Delta \right) \\ &= \int \frac{dc}{2\pi i} f_\Delta(c) \left( \text{Diagram: Blue vertex } i_L, \text{ blue line } h+c \right) \left( \text{Diagram: Red vertex } i_L, \text{ red line } s, \text{ red line } h-c \right) \\ &\quad \times \left( \text{Diagram: Blue vertex } i_R, \text{ blue line } h-c \right) \left( \text{Diagram: Red vertex } i_R, \text{ red line } s, \text{ red line } h+c \right), \end{aligned} \quad (4.16)$$

where we remind the reader that  $f_\Delta(c)$  was defined in (2.8), the vertex factors are given by (3.1) over  $p$ -adics and (3.20) over reals, and the undressed diagrams are obtained from prescription I over  $p$ -adics and prescription II over reals. It can be easily checked that this reproduces the pre-amplitudes in (2.23).

**Example (viii).** The Mellin amplitude and pre-amplitude for the diagram with two internal lines, (3.5), are:

$$\begin{aligned}
& \left( \text{Diagram: Ellipse with vertices } i_L, \dots, i_U, \dots, i_R. \text{ Internal lines } s_A, s_B \text{ and triangles } \Delta_A, \Delta_B. \right) \\
&= \left( \text{Diagram: Blue vertex } i_L \text{ with } \Delta_A \text{ triangle} \right) \left( \text{Diagram: Blue vertex } i_U \text{ with } \Delta_A, \Delta_B \text{ triangles} \right) \left( \text{Diagram: Blue vertex } i_R \text{ with } \Delta_B \text{ triangle} \right) \\
&\quad \times \left( \text{Diagram: Red vertex } i_L \text{ with } s_A, s_B \text{ lines and } \Delta_A, \Delta_B \text{ triangles} \right) \\
&= \int \frac{dc_A}{2\pi i} f_{\Delta_A}(c_A) \int \frac{dc_B}{2\pi i} f_{\Delta_B}(c_B) \left( \text{Diagram: Blue vertex } i_L \text{ with } h-c_A \text{ line} \right) \left( \text{Diagram: Red vertex } i_L \text{ with } s_A \text{ line and } h-c_A, h+c_A \text{ lines} \right) \\
&\quad \times \left( \text{Diagram: Blue vertex } i_U \text{ with } h+c_A, h-c_B \text{ lines} \right) \left( \text{Diagram: Red vertex } i_U \text{ with } s_A, s_B \text{ lines and } h-c_A, h+c_A, h-c_B, h+c_B \text{ lines} \right) \\
&\quad \times \left( \text{Diagram: Blue vertex } i_R \text{ with } h+c_B \text{ line} \right) \left( \text{Diagram: Red vertex } i_R \text{ with } s_B \text{ line and } h-c_B, h+c_B \text{ lines} \right).
\end{aligned} \tag{4.17}$$

**Example (ix).** The Mellin amplitude for the diagram with three internal lines arranged in series, (3.9) decomposes into a pre-amplitude thus:

$$\begin{aligned}
& \text{Diagram: } \text{An oval containing three triangles } \Delta_A, \Delta_B, \Delta_C \text{ connected in series. External lines } i_L, \dots, i_r \text{ enter from the top, and } i_L, \dots, i_R \text{ enter from the sides. Internal lines are labeled } s_A, s_B, s_C. \\
& = \int \frac{dc_A}{2\pi i} f_{\Delta_A}(c_A) \int \frac{dc_B}{2\pi i} f_{\Delta_B}(c_B) \int \frac{dc_C}{2\pi i} f_{\Delta_C}(c_C) \\
& \times \left( \begin{array}{c} i_L \vdots \\ \text{Blue vertex} \\ h - c_A \end{array} \right) \left( \begin{array}{c} i_L \vdots \\ \text{Red vertex} \\ s_A \\ h - c_A \quad h + c_A \end{array} \right) \\
& \times \left( \begin{array}{c} i_l \\ \text{Blue vertex} \\ h + c_A \quad h - c_B \end{array} \right) \left( \begin{array}{c} i_l \\ \text{Red vertex} \\ s_A \quad s_B \\ h - c_A \quad h + c_A \quad h - c_B \quad h + c_B \end{array} \right) \\
& \times \left( \begin{array}{c} i_r \\ \text{Blue vertex} \\ h + c_B \quad h - c_C \end{array} \right) \left( \begin{array}{c} i_r \\ \text{Red vertex} \\ s_B \quad s_C \\ h - c_A \quad h + c_B \quad h - c_C \quad h + c_B \end{array} \right) \\
& \times \left( \begin{array}{c} h + c_C \\ \text{Blue vertex} \\ \vdots i_R \end{array} \right) \left( \begin{array}{c} s_C \\ \text{Red vertex} \\ h - c_C \quad h + c_C \\ \vdots i_R \end{array} \right). \tag{4.18}
\end{aligned}$$

**Example (x).** As a final example, consider the Mellin amplitude for the diagram with three internal lines meeting at a center vertex, (3.12). It exhibits the following decomposition into a contour integral over its pre-amplitude:



merged into the single undressed amplitude.

As an example of how this, consider the Mellin amplitude  $\mathcal{M}^{3\text{-int}}$  for the diagram with three internal legs arranged in series as given in equation (4.18). Carrying out the  $c_A$  integral gives the following:

$$\begin{aligned}
\mathcal{M}^{3\text{-int}} &\equiv \int \frac{dc_B}{2\pi i} f_{\Delta_B}(c_B) \int \frac{dc_C}{2\pi i} f_{\Delta_C}(c_C) \\
&\times \left( \begin{array}{c} i_L \vdots \\ \diagup \quad \diagdown \\ \Delta_A \end{array} \right) \left( \begin{array}{c} i_l \quad \dots \\ \diagdown \quad \diagup \\ \Delta_A \quad h-c_B \quad h+c_B \\ i_L \vdots \end{array} \right) \left( \begin{array}{c} i_l \quad \dots \\ \diagdown \quad \diagup \\ \Delta_A \quad h-c_B \end{array} \right) \\
&\times \left( \begin{array}{c} i_r \quad \dots \\ \diagdown \quad \diagup \\ h-c_B \quad h+c_B \quad h-c_C \quad h+c_C \\ i_L \vdots \end{array} \right) \left( \begin{array}{c} i_r \quad \dots \\ \diagdown \quad \diagup \\ h+c_B \quad h-c_C \end{array} \right) \left( \begin{array}{c} \dots \quad i_R \\ \diagdown \quad \diagup \\ h-c_C \quad h+c_C \end{array} \right) \\
&\times \left( \begin{array}{c} \dots \quad i_R \\ \diagdown \quad \diagup \\ h+c_C \end{array} \right).
\end{aligned} \tag{4.20}$$

Carrying out the  $c_B$  integral next, one finds that

$$\begin{aligned}
\mathcal{M}^{3\text{-int}} &= \int \frac{dc_C}{2\pi i} f_{\Delta_C}(c_C) \left( \begin{array}{c} i_L \vdots \\ \diagup \quad \diagdown \\ \Delta_A \end{array} \right) \left( \begin{array}{c} i_l \quad \dots \\ \diagdown \quad \diagup \\ \Delta_A \quad \Delta_B \end{array} \right) \\
&\times \left( \begin{array}{c} i_l \quad \dots \quad i_r \quad \dots \\ \diagdown \quad \diagup \quad \diagdown \quad \diagup \\ \Delta_A \quad \Delta_B \quad h-c_C \quad h+c_C \\ i_L \vdots \quad s_A \quad s_B \end{array} \right) \left( \begin{array}{c} i_r \quad \dots \\ \diagdown \quad \diagup \\ \Delta_B \quad h-c_C \end{array} \right) \\
&\times \left( \begin{array}{c} \dots \quad i_R \\ \diagdown \quad \diagup \\ h-c_C \quad h+c_C \end{array} \right) \left( \begin{array}{c} \dots \quad i_R \\ \diagdown \quad \diagup \\ h+c_C \end{array} \right).
\end{aligned} \tag{4.21}$$

Finally, carrying out the  $c_C$  integral yields

$$\begin{aligned}
\mathcal{M}^{3\text{-int}} = & \left( \begin{array}{c} i_L \vdots \\ \diagup \quad \diagdown \\ \Delta_A \end{array} \right) \left( \begin{array}{c} i_l \\ \diagdown \quad \diagup \\ \Delta_A \quad \Delta_B \end{array} \right) \left( \begin{array}{c} i_r \\ \diagdown \quad \diagup \\ \Delta_B \quad \Delta_C \end{array} \right) \left( \begin{array}{c} \vdots i_R \\ \diagdown \quad \diagup \\ \Delta_C \end{array} \right) \\
& \times \left( \begin{array}{c} i_l \quad i_r \\ \diagdown \quad \diagup \quad \diagdown \quad \diagup \\ s_A \quad s_B \\ \Delta_A \quad \Delta_B \quad \Delta_C \\ i_L \quad \vdots \quad i_R \end{array} \right). \tag{4.22}
\end{aligned}$$

We see that carrying out contour integrals of the form above effectively glues together two of the undressed diagrams defined in section 3. This holds true generally: given a preamplitude,

$$\begin{aligned}
\widetilde{\mathcal{M}} \equiv & \left( \begin{array}{c} F \\ \diagup \quad \diagdown \\ A \quad h-c \\ \vdots \\ i_1 \end{array} \right) \left( \begin{array}{c} i_5 \quad i_6 \\ \diagdown \quad \diagup \quad \diagdown \quad \diagup \\ D \quad E \quad F \\ i_4 \quad \vdots \quad i_3 \\ \vdots \quad i_2 \quad i_1 \\ s \\ h-c \quad h+c \end{array} \right) \\
& \times \left( \begin{array}{c} s \\ \diagdown \quad \diagup \\ h-c \quad h+c \\ \vdots i_7 \end{array} \right) \left( \begin{array}{c} \vdots i_7 \\ \diagdown \quad \diagup \\ h+c \end{array} \right), \tag{4.23}
\end{aligned}$$

the following identity holds,

$$\begin{aligned}
\int \frac{dc}{2\pi i} f_\Delta(c) \widetilde{\mathcal{M}} = & \left( \begin{array}{c} F \\ \diagup \quad \diagdown \\ A \quad \Delta \\ \vdots \\ i_1 \end{array} \right) \left( \begin{array}{c} i_5 \quad i_6 \\ \diagdown \quad \diagup \quad \diagdown \quad \diagup \\ D \quad E \quad F \\ i_4 \quad \vdots \quad i_3 \\ \vdots \quad i_2 \quad i_1 \\ s \\ \Delta \\ \vdots i_7 \end{array} \right) \left( \begin{array}{c} \vdots i_7 \\ \diagdown \quad \diagup \\ \Delta \end{array} \right). \tag{4.24}
\end{aligned}$$

At the real place, this fact follows from the Feynman rules for Mellin amplitudes and preamplitudes that already exist in the literature (see Refs. [6, 7, 8]), and which in this paper we have presented in a manner which highlights the common features that hold true over both

the reals and the  $p$ -adics. At the  $p$ -adic place, this fact requires a proof which is provided in appendix C.

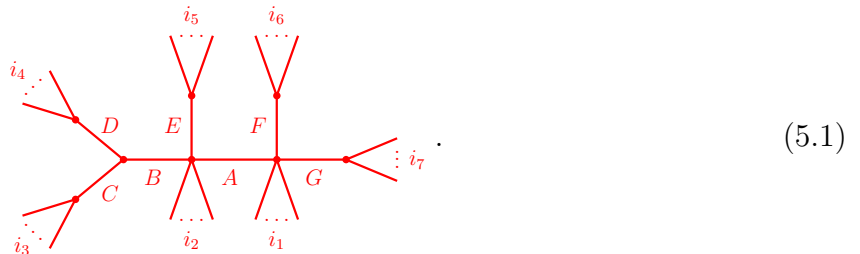
## 5 On-Shell Recursion for Mellin Amplitudes

The recursive structure of  $p$ -adic Mellin amplitudes described in section 3.1 is of a somewhat unusual kind: the amplitude of an  $\mathcal{N}$ -point bulk diagram is expressed in terms of amplitudes of  $\mathcal{N}$ -point diagrams with fewer internal lines. Such a recursion relation invokes interaction vertices of higher and higher degree, that is, interaction terms involving more and more fields. A natural question to ask is whether it is possible to set up a recursive prescription in a form more similar to the familiar on-shell recursions in flat-space, such as the BCFW recursion relation [14], where no new interaction vertices are introduced and a higher-point amplitude is expressed in terms of lower point amplitudes of the same theory. In this section we show that this is indeed possible, though we emphasize that the recursion we formulate in this section applies at the level of *individual* bulk diagrams.

We start in section 5.1 by describing the factorization property of undressed diagrams and explaining how this property allows us to reformulate the recursion relation (3.8) in a manner that will play as a precursor to the on-shell recursion of this section. Then, in section 5.2, we present what we refer to as the “on-shell” recursion relation, following up with a proof that establishes the equivalence between the recursive prescription I of section 3 and the on-shell prescription of this section. At the end of this section we comment on its connection with the Feynman rules for real Mellin amplitudes stated earlier as prescription II, and in appendix D, with the help of two explicit examples, we demonstrate the similarities (and differences) between this prescription and flat-space BCFW recursion.

### 5.1 Factorization property of undressed diagrams

Consider an arbitrary undressed diagram:



It follows from the recursive prescription I of section 3.1 that the sum of all the terms of the undressed amplitude proportional to the internal line factor  $\zeta_p(s_G - \Delta_G)$  is itself given by an undressed diagram:

$$-\zeta_p(s_G - \Delta_G) \left( \begin{array}{c} \text{Diagram with internal line } G \end{array} \right). \quad (5.2)$$

More generally, the coefficient of an internal line factor in an undressed diagram is given by the product of the left- and right-hand (undressed) diagrams obtained by cutting the diagram across the chosen internal line, and assigning the off-shell internal leg dimension to the newly generated external legs of the left- and right-hand undressed diagrams. For example, in the diagram (5.1), adding together all the terms containing the internal line factor  $\zeta_p(s_A - \Delta_A)$  gives,

$$-\zeta_p(s_A - \Delta_A) \left( \begin{array}{c} \text{Diagram with internal line } A \end{array} \right) \left( \begin{array}{c} \text{Diagram with internal line } A \end{array} \right). \quad (5.3)$$

The procedure generalizes straightforwardly if one wants to pick out terms containing multiple propagator factors:

$$\begin{aligned} & \left( \text{terms in undressed diagram } D \text{ containing propagator factors } \zeta_p(s_1 - \Delta_1) \dots \zeta_p(s_f - \Delta_f) \right) \\ &= (-1)^f \left[ \prod_{I=1}^f \zeta_p(s_I - \Delta_I) \right] \times \left( \begin{array}{c} \text{product of undressed diagrams resulting from} \\ \text{removing internal legs 1 to } f \text{ from } D \end{array} \right). \end{aligned} \quad (5.4)$$

For example, in diagram (5.1), the terms containing both factors  $\zeta_p(s_A - \Delta_A)$  and  $\zeta_p(s_B - \Delta_B)$  sum to

$$(-1)^2 \zeta_p(s_A - \Delta_A) \zeta_p(s_B - \Delta_B) \left( \begin{array}{c} \text{Diagram 1} \\ \text{Diagram 2} \\ \text{Diagram 3} \end{array} \right) \quad (5.5)$$

These observations reflect the meromorphic nature of arbitrary Mellin amplitudes, which have simple poles at values of Mandelstam-like invariants that put any internal leg “on-shell”. For  $p$ -adic Mellin amplitudes it is clear from the above that such poles occur in the internal leg factor (3.2) when the Mandelstam invariant of the associated leg equals the conformal dimension of the bulk field propagating along the leg. These poles correspond to the exchange of single-trace operators in the boundary theory. Thus  $p$ -adic Mellin amplitudes have the right factorization properties of (AdS) scattering amplitudes.

Another property of undressed diagrams that follows immediately from the recursive prescription I is that the momentum independent terms (i.e. terms independent of any Mandelstam variable  $s_I$  and thereby also independent of the Mellin variables  $\gamma_{ij}$ ) are in one-to-one correspondence with the terms exhibiting momentum dependence. If for a given undressed diagram one takes all the momentum-dependent terms, sets all internal leg factors  $\zeta_p(s - \Delta)$  to unity (which can be achieved by sending all Mandelstam variables  $s$  to infinity), and multiplies with an overall factor of  $(-1) \times \zeta_p(\Sigma)$ , where  $\Sigma$  is the sum of all external scaling dimensions minus  $n = 2h$ ,

$$\Sigma \equiv \sum \Delta_{\text{external}} - 2h, \quad (5.6)$$

then one exactly recovers the momentum independent part of the undressed diagram:

$$(\text{momentum independent terms}) = -\zeta_p(\Sigma) \lim_{\forall s \rightarrow \infty} (\text{momentum dependent terms}). \quad (5.7)$$

By applying the inclusion-exclusion principle to these two properties we can derive yet another recursive formula for undressed diagrams, as we now explain: As discussed above, given any diagram, we can, for each internal leg  $I$ , sum over the terms proportional to  $\zeta_p(s_I - \Delta_I)$ , the sum of which gives us  $-\zeta_p(s_I - \Delta_I)$  times a smaller diagram or a product of two smaller diagrams. Summing  $-\zeta_p(s_I - \Delta_I)$  times these smaller diagrams over all  $I$ , we obtain a sum containing all momentum-dependent terms. But in doing so, terms containing two factors

of  $\zeta_p(s - \Delta)$  (i.e. terms proportional to  $\zeta_p(s_I - \Delta_I)\zeta_p(s_J - \Delta_J)$  for  $I \neq J$ ) have been double-counted. This over-counting can be compensated for by subtracting off all terms with the two factors of  $\zeta_p(s - \Delta)$ , which by the factorization property above, are also given in terms of smaller diagrams. But now terms containing three factors of  $\zeta_p(s - \Delta)$  haven't been included at all, so we add those terms back in. Carrying out this alternating sum until one reaches the one term that contains the product of  $\zeta_p(s_I - \Delta_I)$  over all  $I$ , we get an expression for all the momentum-dependent terms. (Note that the alternating sign of the inclusion-exclusion principle is cancelled by the  $(-1)^f$  prefactor in (5.4) so that each term comes with a minus sign.) We then add in the momentum-independent terms to get an expression for the full undressed diagram under consideration, by adding  $-\zeta_p(\Sigma)$  times the momentum-dependent terms, except with all Mandelstam variables set to infinity. Thus we arrive at the formula

$$\begin{aligned}
(\text{undressed diagram}) = & - \sum_{\ell=1}^{\# \text{ of internal legs}} \sum_{\text{all possible sets of } \ell \text{ internal legs } \{I_1, \dots, I_\ell\}} \\
& \times \left[ \prod_{i=1}^{\ell} \zeta_p(s_{I_i} - \Delta_{I_i}) - \zeta_p(\Sigma) \lim_{\forall s \rightarrow \infty} \right] \\
& \times (\text{undressed diagrams left after removing legs } \{I_1, \dots, I_\ell\}),
\end{aligned} \tag{5.8}$$

where by “removing a leg” we mean cutting or factorizing the diagram across the particular leg. Concretely, writing out the first couple of terms on the right-hand side as well as the last term, this formula says that

$$\begin{aligned}
(\text{undressed diagram}) = & - \sum_I \left[ \zeta_p(s_I - \Delta_I) - \zeta_p(\Sigma) \lim_{\forall s \rightarrow \infty} \right] \\
& \times (\text{undressed diagrams left after removing leg } I) \\
& - \sum_{I < J} \left[ \zeta_p(s_I - \Delta_I)\zeta_p(s_J - \Delta_J) - \zeta_p(\Sigma) \lim_{\forall s \rightarrow \infty} \right] \\
& \times (\text{undressed diagrams left after removing legs } I, J) \\
& - \sum_{I < J < K} \left[ \zeta_p(s_I - \Delta_I)\zeta_p(s_J - \Delta_J)\zeta_p(s_K - \Delta_K) - \zeta_p(\Sigma) \lim_{\forall s \rightarrow \infty} \right] \\
& \times (\text{undressed diagrams left after removing legs } I, J, K) \\
& \vdots \qquad \qquad \qquad \vdots \qquad \qquad \qquad \vdots \\
& - \left[ \prod_{\text{internal legs } I} \zeta_p(s_I - \Delta_I) - \zeta_p(\Sigma) \right].
\end{aligned} \tag{5.9}$$



## 5.2 $p$ -adic on-shell recursion relation and proof

Motivated by the factorization properties and the on-shell recursive structure observed for simple examples in appendix D, we propose the following recursive prescription for  $p$ -adic Mellin amplitudes:

**Prescription IV** (On-shell recursion for  $p$ -adic Mellin amplitudes). *The following recursive relation is obeyed by  $p$ -adic Mellin amplitudes,*

$$\mathcal{M}(\{s_I\}) = - \sum_{\text{internal leg } I} \mathcal{M}_{\text{left}}(\{s_{\text{left}}\}) \beta_p(s_I - \Delta_I, n - \sum_i \Delta_i) \mathcal{M}_{\text{right}}(\{s_{\text{right}}\}) \Big|_{\forall J \neq I: s_J \rightarrow s_J - s_I + \Delta_I} . \quad (5.11)$$

*This formula is to be understood as follows. For an arbitrary tree-level bulk diagram:*

- *For each internal leg  $I$  with the associated Mandelstam invariant  $s_I$ , and which is propagating a scalar field of conformal dimension  $\Delta_I$ , include a “propagator” factor of  $\beta_p(s_I - \Delta_I, n - \sum_i \Delta_i)$  defined in (2.24), times the Mellin amplitudes for the left and right sub-amplitudes separated by the internal leg  $I$ , where all Mandelstam invariants of the two sub-amplitudes have been shifted by  $(-s_I + \Delta_I)$ . In referring to the Mandelstam-dependence of the left (right) sub-amplitude as  $\{s_{\text{left}}\}$  ( $\{s_{\text{right}}\}$ ), we mean to say that the Mandelstam invariants of the sub-amplitude can be constructed entirely out of the Mellin variables  $\gamma_{ij}$  and external scaling dimensions  $\Delta_i$  indexed by numbers  $i$  and  $j$  that label external legs to the left (right) of the internal leg  $I$  in question (and which, as described above, must be shifted further by  $-s_I + \Delta_I$ ).*
- *We sum over all such terms (times an overall factor of minus one).*

An alternate formulation of this prescription (in auxiliary momentum space) is provided in appendix D. Before demonstrating the equivalence between prescriptions IV and I, let us consider a few examples. The derivation of (5.11) for the case of four- and five-point diagrams is discussed in significant detail in appendix D, using the familiar technique of complexifying the amplitude and BCFW-shifting the (auxiliary) momenta. We focus here on the final decomposition for two six-point examples to illustrate how to apply (5.11).

**Example (xii).** For the six-point series diagram, the on-shell recursion (5.11) dictates

$$\begin{aligned}
& \text{Diagram 1} = \\
& - \text{Diagram 2} \beta_p(s_A - \Delta_A, n - \Delta_\Sigma) - \text{Diagram 3} \\
& - \text{Diagram 4} \beta_p(s_B - \Delta_B, n - \Delta_\Sigma) - \text{Diagram 5} \\
& - \text{Diagram 6} \beta_p(s_C - \Delta_C, n - \Delta_\Sigma) \text{Diagram 7},
\end{aligned} \tag{5.12}$$

where we have defined  $\Delta_\Sigma \equiv \sum_{i=1}^6 \Delta_i$ , and the Mandelstam variables are

$$\begin{aligned}
s_A &\equiv \Delta_1 + \Delta_2 - 2\gamma_{12}, & s_C &\equiv \Delta_3 + \Delta_4 - 2\gamma_{34}, \\
s_B &\equiv s_A + \Delta_6 - 2\gamma_{16} - 2\gamma_{26} = s_C + \Delta_5 - 2\gamma_{35} - 2\gamma_{45},
\end{aligned} \tag{5.13}$$

where the Mellin variables  $\gamma_{ij}$  satisfy (2.13) for  $\mathcal{N} = 6$ . Further, in (5.12), we have indicated the Mandelstam variables associated with the internal legs on top of the lines, and in the r.h.s. in the sub-amplitudes, we have explicitly displayed the shifted Mandelstam variables.

**Example (xiii).** Likewise, for the six-point star diagram, (5.11) gives

$$\begin{aligned}
& \text{Diagram 1} = - \text{Diagram 2} \beta_p(s_A - \Delta_A, n - \Delta_\Sigma) - \text{Diagram 3} \beta_p(s_B - \Delta_B, n - \Delta_\Sigma) - \text{Diagram 4} \beta_p(s_C - \Delta_C, n - \Delta_\Sigma) \\
& \text{Diagram 5} - \text{Diagram 6} \beta_p(s_B - \Delta_B, n - \Delta_\Sigma) \text{Diagram 7} \\
& \text{Diagram 8} - \text{Diagram 9} \beta_p(s_C - \Delta_C, n - \Delta_\Sigma) \text{Diagram 10} ,
\end{aligned} \tag{5.14}$$

where this time

$$s_A \equiv \Delta_1 + \Delta_2 - 2\gamma_{12}, \quad s_B \equiv \Delta_3 + \Delta_4 - 2\gamma_{34}, \quad s_C \equiv \Delta_5 + \Delta_6 - 2\gamma_{56}. \tag{5.15}$$

Equations (5.12) and (5.14) can be reduced further by repeated application of (5.11) (see e.g. equations (D.30) and (D.52) in appendix D) to expressions which involve only (in this case, three-point) contact interactions, whose Mellin amplitudes are given simply by the respective vertex factors (3.1). It is straightforward to confirm that (5.12) and (5.14) agree with the Mellin amplitudes for diagrams with three internal legs computed from first principles in Ref. [4] and rederived here in examples (v)-(vi) using prescription I.

We now prove that prescription IV is mathematically equivalent to the recursive prescription I described in section 3. (We will later prove prescription I in appendix C.) Starting with a Mellin amplitude  $\mathcal{M}$  given in terms of the recursive prescription I, let  $\mathcal{M}(z)$  be the complex deformation obtained by replacing each Mandelstam invariant  $s_I$  with  $s_I(z) \equiv s_I - z$ . In that case the function,

$$\mathcal{I}(z) \equiv \log p \left[ \zeta_p(z) - \zeta_p \left( \sum_i \Delta_i - n \right) \right] \mathcal{M}(z), \tag{5.16}$$

is defined on a “complex cylinder” where the imaginary axis wraps around a circle of radius  $1/\log p$ . In other words  $z \in \mathbb{R} \times \left[-\frac{\pi}{\log p}, \frac{\pi}{\log p}\right)$ . From here on, we will use the shorthand  $\mathcal{M} = \mathcal{M}(0)$ . Consider now the sum

$$S(r) \equiv \int_{r-\frac{i\pi}{\log p}}^{r+\frac{i\pi}{\log p}} dz \mathcal{I}(z) + \int_{-r+\frac{i\pi}{\log p}}^{-r-\frac{i\pi}{\log p}} dz \mathcal{I}(z), \quad (5.17)$$

where  $r$  is some positive number. In the limit as  $r$  tends to infinity,  $S(r)$  tends to zero as we will now show. As the real part of  $z$  tends to plus or minus infinity, the integrands in (5.17) become constant, and the integrals evaluate to  $2\pi/\log p$  (which is the circumference of the cylindrical manifold) times the constant integrand. This asymptotic behavior follows from the fact that  $\mathcal{I}(z)$  depends on  $z$  solely through the arguments of  $p$ -adic local zeta-functions, which themselves have the asymptotic behavior

$$\zeta_p(z) \rightarrow \begin{cases} 1 & \text{as } \text{Re}[z] \rightarrow \infty, \\ 0 & \text{as } \text{Re}[z] \rightarrow -\infty. \end{cases} \quad (5.18)$$

We see then that when  $r \rightarrow \infty$ , the first term in (5.17) gives

$$\begin{aligned} \int_{\infty-\frac{i\pi}{\log p}}^{\infty+\frac{i\pi}{\log p}} dz \mathcal{I}(z) &= 2\pi \left[ 1 - \zeta_p\left(\sum_i \Delta_i - n\right) \right] \mathcal{M}(z = \infty) \\ &= 2\pi \left[ 1 - \zeta_p\left(\sum_i \Delta_i - n\right) \right] \left( \text{the momentum-independent terms of } \mathcal{M} \right). \end{aligned} \quad (5.19)$$

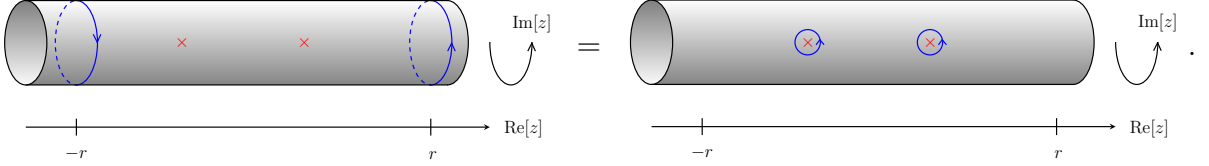
For the second term in (5.17), noting that the contour runs in the opposite direction, we get

$$\int_{-\infty+\frac{i\pi}{\log p}}^{-\infty-\frac{i\pi}{\log p}} dz \mathcal{I}(z) = 2\pi \zeta_p\left(\sum_i \Delta_i - n\right) \mathcal{M}(z = -\infty). \quad (5.20)$$

We split the expression (5.20) into two parts:

1. A part proportional to the momentum-independent part of  $\mathcal{M}$ : this part exactly cancels the second term inside the square brackets in the second line of (5.19).
2. A part proportional to the momentum-dependent part of  $\mathcal{M}$ : since  $z$  is taken to minus infinity, all factors of  $\zeta_p$  in  $\mathcal{M}$  which carry Mandelstam variable dependence tend to unity. Using equation (5.7), this part is seen to exactly cancel with the first term inside square brackets in the second line of (5.19).

We see then that  $\lim_{r \rightarrow \infty} S(r) = 0$ . But from this it follows that the sum over all residues of  $\mathcal{I}(z)$  defined in (5.16) vanishes. For we may shift the contour of the first term in (5.17) from  $\int_{r+\frac{i\pi}{\log p}}^{r-\frac{i\pi}{\log p}}$  to  $\int_{-r+\frac{i\pi}{\log p}}^{-r-\frac{i\pi}{\log p}}$  so that this term cancels with the second term, provided we add in  $2\pi i$  times the sum of all the residues in the strip  $-r < \text{Re}[z] < r$ :



The residue of  $\mathcal{I}(z)$  at  $z = 0$  equals  $\mathcal{M} = \mathcal{M}(0)$ , the original un-deformed amplitude. Since  $\mathcal{M}(z)$  is obtained from  $\mathcal{M}$  by replacing in  $\mathcal{M}$  each factor of  $\zeta_p(s_I - \Delta_I)$  with  $\zeta_p(s_I - \Delta_I - z)$ , we see that the remaining residues of  $\mathcal{M}(z)$  occur at  $z_* = s_I - \Delta_I$ , exactly when the complex-shifted internal leg goes on shell, i.e.  $s_I(z_*) = \Delta_I$ . Furthermore, from (5.16) we conclude that each of these residues is equal to a factor of  $\left[ \zeta_p(s_I - \Delta_I) - \zeta_p(\sum_i \Delta_i - n) \right] = \beta_p(s_I - \Delta_I, n - \sum_i \Delta_i)$  times the (on-shell) left and the right sub-amplitudes (evaluated at  $z = z_*$ ), as follows from the factorization property described in section 5.1.

Thus upon equating the residue of  $\mathcal{I}(z)$  at  $z = 0$  with minus the sum of all remaining residues, we recover the on-shell recursion formula (5.11), proving prescription IV assuming prescription I.

Given the strong similarities between the structure of real and  $p$ -adic Mellin amplitudes as illuminated in this paper so far, it is natural to wonder if the on-shell recursion relations presented in this section also have a real counterpart. It turns out (a trivial restatement of) the Feynman rules for real Mellin amplitudes (as given in prescription II) provides the closest analog, with an important subtlety: The on-shell recursion given in prescription IV has a particularly simple form owing to the absence of descendant fields in the  $p$ -adic setup, which is no longer the case over the reals. Thus (5.11) continues to hold for real Mellin amplitudes, provided we additionally assign to each internal leg  $I$  an integer  $m_I$ , replace the propagator factor  $\beta_p(\cdot, \cdot)$  above by the propagator factor  $L(s_I, \Delta_I, m_I)$  defined in (3.15), update the Mandelstam shift operation in (5.11) to be  $s_J \rightarrow s_J - s_I + \Delta_I + 2m_I$ , and finally include infinite sums over all integers  $m_I \in [0, \infty)$  in (5.11). The fact that this prescription reduces to the Feynman rules trivially follows from the partial fraction identity,

$$\frac{1}{D_1 \dots D_f} = \sum_{i=1}^f \frac{1}{D_i} \left[ \prod_{j \neq i} \frac{1}{D_j - D_i} \right], \quad (5.21)$$

applied to the product of factors  $1/(s_I - \Delta_I - 2m_I)$  appearing in the propagator factors  $L(s_I, \Delta_I, m_I)$ .

## 6 Outlook

In this paper we completed the task, initiated in Ref. [4], of computing  $p$ -adic Mellin amplitudes for all tree-level, arbitrary-point bulk diagrams involving scalars. This is achieved by establishing various prescriptions for constructing Mellin amplitudes which overcome the need to perform bulk integrations altogether:

- Prescription I provides an effective computational strategy, recursive on the number of internal lines;
- Prescription IV provides an even more effective “on-shell” strategy;
- Prescription III (along with (4.3)) provides a recipe for directly writing down the Mellin pre-amplitudes defined via Mellin-Barnes contour integrals in (2.20).

In fact, we showed further that the pre-amplitude prescription III of section 4 applies simultaneously to both  $p$ -adic *and* real Mellin pre-amplitudes, and provides a precise, unified recipe for obtaining the pre-amplitudes from full Mellin amplitudes. This demonstrates the close ties between the real and  $p$ -adic formulations of AdS/CFT.

While the real and  $p$ -adic Mellin amplitudes share many common properties, such as the recursion relations mentioned above, physical factorization properties, the analytic form of the pre-amplitudes, and the fact that they are meromorphic functions which carry simple poles corresponding to exchange of single-trace operators, the  $p$ -adic amplitudes are significantly simpler than the real amplitudes owing to the fact that the  $p$ -adic CFTs we are studying lack descendants [5, 30]. The simplicity of  $p$ -adic Mellin amplitudes as compared to their real cousins is for example highlighted in the structure of the on-shell recursion relation IV described in section 5, which is related to, though simpler than the Feynman rules prescription II for real Mellin amplitudes. Thus the  $p$ -adic formulation provides a promising, powerful computational tool for investigating the harder to work with real Mellin amplitudes.

Part of our motivation for studying  $p$ -adic Mellin space is the hope that the simplicity and tractability of the  $p$ -adic setting may lead to new inspiration and results for real Mellin amplitudes. We should like to think of the relation between real Mellin amplitudes and the corresponding real pre-amplitudes from section 4.1 as an instantiation of this hope; it may

be worthwhile to also investigate whether such relations exist for spinning amplitudes and loop amplitudes.

Another promising avenue is the study of  $p$ -adic Mellin amplitudes involving bulk fermions [39] and amplitudes at loop level. It is tempting to note that the real Mellin loop-amplitudes, especially in the Mellin-Barnes integral form for pre-amplitudes [10, 11], are expressible in terms of the local zeta function  $\zeta_\infty$ , which naturally suggests analogous candidates for  $p$ -adic loop amplitudes. It would be interesting to explore this connection more systematically. We also wonder whether (possibly a generalization of) the recursion relations put forward in this paper extend to loop amplitudes.

In this paper we have restricted ourselves to computing Mellin amplitudes associated to individual bulk diagrams. It remains to see whether it is possible to lift the on-shell recursion of section 5, which is applicable at the level of individual diagrams, to one which applies to total amplitudes, i.e. the sums over constitutive diagrams of a bulk theory, and to other bulk theories over reals. Nevertheless, the techniques of this paper should still prove useful in extending the construction of the putative bulk dual of the free  $p$ -adic  $O(N)$  model, at least at tree-level [30].

On a closing note, we emphasize that at present the mounting number of remarkable similarities between the conventional (real) and  $p$ -adic AdS/CFT formulations are still mathematical curiosities which remain to be fully understood. It is tempting to wonder whether one may think of the real and  $p$ -adic formulations as “local formulations” of AdS/CFT at the place at infinity and the finite places, respectively. This immediately leads to the question [46]: Is there an adelic formulation of AdS/CFT, i.e. a “global” formulation which subsumes the real and  $p$ -adic formulations in a single field-independent (field in the mathematics sense) framework? Such a unified formulation would constitute an important conceptual step forward in understanding as yet undiscovered mathematical aspects of AdS/CFT.

## Acknowledgments

C. B. J. and S. P. thank Steven S. Gubser, Matilde Marcolli, and Brian Trundy for useful discussions and encouragement. S. P. thanks Perimeter Institute for their kind hospitality while this work was in progress. The work of C. B. J. was supported in part by the Department of Energy under Grant No. DE-FG02-91ER40671, by the US NSF under Grant No. PHY-1620059, and by the Simons Foundation, Grant 511167 (SSG). The work of S. P. was supported in part by Perimeter Institute for Theoretical Physics. Research at Perimeter

Institute is supported by the Government of Canada through the Department of Innovation, Science and Economic Development and by the Province of Ontario through the Ministry of Research, Innovation and Science.

## A Useful Formulae and Conventions

We now recall some useful functions and formulae from Ref. [4], to which we refer for further details. The characteristic function takes a  $p$ -adic argument, and is defined to be

$$\gamma_p(x) = \frac{2 \log p}{2\pi i} \int_{\epsilon - \frac{i\pi}{2 \log p}}^{\epsilon + \frac{i\pi}{2 \log p}} d\gamma \frac{\zeta_p(2\gamma)}{|x|_p^{2\gamma}} = \begin{cases} 1 & \text{for } |x|_p \leq 1, \\ 0 & \text{otherwise.} \end{cases} \quad (\text{A.1})$$

It plays the role of the Gaussian function for  $p$ -adic variables. If we let  $\{S_1, \dots, S_{\mathcal{N}}\}$  denote a finite set of  $p$ -adic numbers and let  $m$  be an index such that  $|S_m|_p = \sup\{|S_1|_p, \dots, |S_{\mathcal{N}}|_p\}$ , then it follows from the definition of the characteristic function that it satisfies the factorization property

$$\gamma_p(S_1) \dots \gamma_p(S_{\mathcal{N}}) = \gamma_p(S_m). \quad (\text{A.2})$$

Furthermore, letting  $\{x_1, \dots, x_{\mathcal{N}}\}$  denote another set of  $p$ -adic numbers of equal cardinality, it follows from the ultra-metricity of the  $p$ -adic norm that

$$\prod_{\substack{i=1 \\ i \neq m}}^{\mathcal{N}} \gamma_p(S_i(x_i - x_m)^2) = \prod_{1 \leq i < j \leq \mathcal{N}} \gamma_p\left(\frac{S_i S_j}{S_m}(x_i - x_j)^2\right). \quad (\text{A.3})$$

An integral identity for characteristic functions that comes in handy in the context of  $p$ -adic Mellin amplitudes is

$$\int_{\mathbb{Q}_p^n} dx \left[ \prod_i \gamma_p(S_i(x - x_i)^2) \right] = \frac{1}{|S_m|_p^{n/2}} \left[ \prod_{i \neq m} \gamma_p(S_i(x_i - x_m)^2) \right]. \quad (\text{A.4})$$

Some useful integration formulae, which we collectively refer to as the “ $p$ -adic Schwinger parameter trick” are listed below:

$$\frac{1}{|x|_p^\Delta} = \frac{\zeta_p(n)}{\zeta_p(\Delta)} \int_{\mathbb{Q}_p^n} \frac{dS}{|S|_p^n} |S|_p^\Delta \gamma_p(xS) \quad \text{for } x \in \mathbb{Q}_p^n, \quad (\text{A.5})$$

$$\frac{1}{|x|_p^\Delta} = \frac{2}{|2|_p} \frac{\zeta_p(1)}{\zeta_p(2\Delta)} \int_{\mathbb{Q}_p^2} \frac{dS}{|S|_p} |S|_p^\Delta \gamma_p(xS) \quad \text{for } x \in \mathbb{Q}_p^2, \quad (\text{A.6})$$

$$\frac{1}{|x|_p^\Delta} = \frac{2}{|2|_p} \frac{\zeta_p(1)}{\zeta_p(2\Delta)} \int_{p\mathbb{Q}_p^2} \frac{dS}{|S|_p} |S|_p^\Delta \gamma_p(xS) \quad \text{for } x \in p\mathbb{Q}_p^2, \quad (\text{A.7})$$

where

$$\mathbb{Q}_p^2 \equiv \{x \in \mathbb{Q}_p : x = y^2 \text{ for some } y \in \mathbb{Q}_p\}. \quad (\text{A.8})$$

$$p\mathbb{Q}_p^2 \equiv \{x \in \mathbb{Q}_p : x = py^2 \text{ for some } y \in \mathbb{Q}_p\}. \quad (\text{A.9})$$

The  $p$ -adic version of the Symanzik star integration formula takes the form,

$$\int [d\gamma] \prod_{1 \leq i < j \leq \mathcal{N}} \frac{\zeta_p(2\gamma_{ij})}{|x_{ij}|_p^{2\gamma_{ij}}} = \sum_{a \in \{1,p\}} \prod_{i=1}^{\mathcal{N}} \left( \frac{2\zeta_p(1)}{|2|_p} \int_{a\mathbb{Q}_p^2} \frac{ds_i}{|s_i|_p} |s_i|_p^{\Delta_i} \right) \prod_{1 \leq i < j \leq \mathcal{N}} \gamma_p(s_i s_j x_{ij}^2). \quad (\text{A.10})$$

An integral identity from which, with the help of the Symanzik formula, the contact amplitude may be extracted is,

$$\sum_{(z_0, z) \in \mathcal{T}_{p^n}} \prod_{i=1}^{\mathcal{N}} K_{\Delta_i}(z_0, z; x_i) = \sum_{a \in \{1,p\}} \zeta_p \left( \sum_i \Delta_i - n \right) \prod_{i=1}^{\mathcal{N}} \left( \frac{2\zeta_p(1)}{|2|_p} \int_{a\mathbb{Q}_p^2} \frac{ds_i}{|s_i|_p} |s_i|_p^{\Delta_i} \right) \prod_{i < j} \gamma_p(s_i s_j x_{ij}^2). \quad (\text{A.11})$$

A  $p$ -adic integral that has appeared at some instances in this paper is

$$\begin{aligned} \int_{\mathbb{Q}_p} \frac{dt}{|t|_p} |t|_p^a |1, t|_p^b &= \sum_{n \in \mathbb{Z}} \int_{p^{-n}\mathbb{U}_p} \frac{dt}{|t|_p} |t|_p^a |1, t|_p^b = \sum_{n=-\infty}^0 \int_{p^{-n}\mathbb{U}_p} \frac{dt}{|t|_p} |t|_p^a + \sum_{n=1}^{\infty} \int_{p^{-n}\mathbb{U}_p} \frac{dt}{|t|_p} |t|_p^{a+b} \\ &= \frac{1}{\zeta(1)} \left( \sum_{n=-\infty}^0 p^{an} + \sum_{n=1}^{\infty} p^{(a+b)n} \right) = \frac{\zeta_p(a) - \zeta_p(a+b)}{\zeta_p(1)}. \end{aligned} \quad (\text{A.12})$$

## B Inductive Proof of Prescription III for Pre-Amplitudes

### B.1 Outline of the proof

In this section we prove that at tree-level any  $p$ -adic Mellin amplitude is given in terms of a multiple contour integral over a pre-amplitude according to prescription III of section 4. Subsequently, in the next appendix we prove that the performing all the contour integrals

over a pre-amplitude reproduces the Mellin amplitude given by the recursive prescription I presented in section 3.1.

The proof for the pre-amplitude prescription is inductive. A possible inductive approach one might attempt to adopt is weak induction on the number of internal legs. However, given the pre-amplitude for an arbitrary bulk diagram, it turns out to be technically difficult to find the pre-amplitude for a diagram obtained by inserting an extra internal leg at an arbitrary position in the diagram. It is significantly more tractable to attach extra internal legs to a special kind of bulk vertex, one that only has one internal leg attached to it. Thus our inductive strategy will be to assume that the pre-amplitude prescription III is satisfied by an arbitrary bulk diagram  $D_L$ , and a bulk diagram  $D_R$  built from  $f$  internal lines all connected to the same vertex:

$$D_L = \left( \text{Diagram with } V_1 \text{ and } R_0 \right), \quad D_R = \left( \text{Diagram with } R_0, R_1, \dots, R_f \right). \quad (\text{B.1})$$

Here the grey circles each indicate an arbitrary number of vertices and internal lines that form part of the diagram  $D_L$ , and we have omitted drawing the external lines, of which an arbitrary number may be connected to any vertex. We will then consider the bulk diagram  $D_M$  obtained by merging the two diagrams by fusing the two vertices labelled  $R_0$  in (B.1), to get

$$D_M = \left( \text{Merged Diagram with } V_1, R_0, R_1, \dots, R_f \right), \quad (\text{B.2})$$

where the merged diagram has a set of external legs which is the union of the set of external legs for  $D_L$  and  $D_R$ . Using the inductive assumptions we will demonstrate that this

bulk-diagram has a Mellin amplitude given by the pre-amplitude prescription III, thereby completing the inductive proof.

## B.2 Details of the proof

**The “left-hand diagram”  $D_L$ .** As a first step in the proof, we will recast the pre-amplitude for  $D_L$  in a more useful form. To this end, it is useful to first consider a smaller diagram  $D_l$ , namely the one obtained by removing the vertex  $R_0$  and the internal line connected to it (i.e. collapsing the internal line joining  $R_0$  to  $V_1$  in  $D_L$ ). We keep the number and dimensions of external legs attached to vertex  $V_1$  in  $D_l$  arbitrary for now but fix them later. The smaller diagram takes the following form, where this time we show a subset of the external legs,

The diagram  $D_l$  is a circular bulk diagram. It features five vertices labeled  $V_I, V_J, V_K, V_1, V_g$  arranged in a roughly circular pattern. Vertex  $V_1$  is at the center. Vertices  $V_I, V_J, V_K$  are on the left side, and  $V_g$  is at the bottom. Vertex  $V_1$  is connected to  $V_I, V_J, V_K, V_g$ . External legs are shown as lines extending from the vertices to the boundary of the circle. The legs from  $V_I$  are labeled  $i_{V_I}$ . The legs from  $V_J$  are labeled  $i_{V_J}$ . The legs from  $V_K$  are labeled  $i_{V_K}$ . The legs from  $V_1$  are labeled  $i_{V_1}$ . The legs from  $V_g$  are labeled  $i_{V_g}$ . Ellipses indicate additional legs and vertices.

$$D_l = \text{Diagram} \quad (\text{B.3})$$

The vertices of this diagram are labelled  $V_1, V_2, \dots, V_g$ , and the external legs are labelled by the lower-case alphabet  $i$  or  $j$ , where we sometimes put a subscript on them to indicate which vertex they are incident on. Specifically the label  $i_{V_I}$  runs over the external legs incident on vertex  $V_I$ , and  $i_V$  runs over all labels  $i_{V_1}, i_{V_2}, \dots, i_{V_g}$ . We posit that the position space pre-amplitude  $\tilde{\mathcal{A}}_l$  for  $D_l$ , denoted with a tilde and defined via

$$\mathcal{A}(x) \equiv \left( \prod_I \int \frac{dc}{2\pi i} f_{\Delta_I}(c_I) \right) \tilde{\mathcal{A}}(x), \quad (\text{B.4})$$

can be written in the form<sup>7</sup>

$$\begin{aligned} \tilde{\mathcal{A}}_l = \mathcal{L} & \left[ \prod_{L=1}^{2g-2} \int_{\mathbb{Q}_p} \frac{dt_L}{|t_L|_p} \right] \mathcal{G}(\{t_L\}) \sum_{a \in \{1,p\}} \left[ \prod_{i_V} \frac{2\zeta_p(1)}{|2|_p} \int_{a\mathbb{Q}_p^2} \frac{ds_{i_V}}{|s_{i_V}|_p} |s_{i_V}|_p^{\sum \Delta_{i_V}} \right] \\ & \times \left[ \prod_{1 \leq I \leq J \leq g} \prod_{i_{V_I}, i_{V_J}} \gamma_p \left( f_{IJ}(\{t_L\}) s_{i_{V_I}} s_{i_{V_J}} x_{i_{V_I} i_{V_J}}^2 \right) \right] \end{aligned} \quad (\text{B.5})$$

where  $\mathcal{G}(\{t_L\})$  and  $f_{IJ}(\{t_L\})$  are, respectively, real and  $p$ -adic valued functions whose exact form we will not need, except for the fact that the functions  $f_{IJ}$  are valued in  $\mathbb{Q}_p^2$ .  $\mathcal{L}$  and  $\mathcal{G}(\{t_L\})$  also depend on external scaling dimensions  $\Delta_{i_V}$ , the degree of the field extension  $n$ , and complex variables  $c_I$ , but we suppress such dependencies. The fact that the  $\tilde{\mathcal{A}}_l$  has the form (B.5) can be seen inductively. For the initial step, we note that equations (4.34) and (4.48) in Ref. [4] show that the diagrams with one and two internal legs have a position space pre-amplitude of the form (B.5). We will now assume (B.5) and show that the diagram  $D_L$  (with one additional internal leg) has a pre-amplitude of the same form as well.

Applying the split representation (2.6) to the internal leg connecting vertices  $V_1$  and  $R_0$  in  $D_L$ ,

$$D_L = \int \frac{dc}{2\pi i} f_\Delta(c) \int_{\mathbb{P}^1(\mathbb{Q}_p^n)} dx \quad \begin{array}{c} \text{Diagram of } D_L \text{ in } \mathbb{P}^1(\mathbb{Q}_p^n) \\ \text{A circular diagram with vertices } V_1, R_0, \text{ and } i_{V_I}, i_{V_J}, i_{V_K}, i_{V_g}, i_{V_1}, i_{R_0}. \\ \text{Internal legs connect } V_1 \text{ to } i_{V_I}, i_{V_J}, i_{V_K}, i_{V_g}, \text{ and } R_0. \\ \text{External legs are incident at } i_{V_I}, i_{V_J}, i_{V_K}, i_{V_g}, i_{V_1}, \text{ and } i_{R_0}. \\ \text{Angles } h-c \text{ and } h+c \text{ are indicated near } V_1. \end{array} \quad , \quad (\text{B.6})$$

we find that the position space pre-amplitude  $\tilde{\mathcal{A}}_L$  is given by a boundary integral over the product of 1) the pre-amplitude  $\tilde{\mathcal{A}}_l$  as written in (B.5) with appropriately chosen external dimensions incident at  $V_1$ , and 2) a contact amplitude associated to the vertex  $R_0$ . We fix the dimension of one of the external legs incident at  $V_1$  in  $D_L$  to a complex-shifted value consistent

<sup>7</sup>We are allowing for the possibility of vertices  $V_I$  with no external legs incident to them. Such vertices have no associated variables  $s_{i_{V_I}}$  as  $i_{V_I}$  runs over the empty set. But the total number of  $t_L$  variables remains  $2g - 2$  where  $g$  is the total number of vertices, with or without incident external legs.

with the split representation, and assign the rest of the external legs the dimensions of the external operators originally incident on  $V_1$  in  $D_L$ . Label the complex-shifted dimension  $\Delta_1$ . We define

$$\tilde{\mathcal{L}} = \mathcal{L}|_{\Delta_1 \rightarrow h-c}, \quad \tilde{\mathcal{G}}(\{t_L\}) = \mathcal{G}(\{t_L\})|_{\Delta_1 \rightarrow h-c}, \quad (\text{B.7})$$

and rename the integration variable  $s_1$  associated to this external leg to  $t$ . Furthermore, we will now take the set  $\{i_{V_1}\}$  to not include the index  $i = 1$  associated to this leg. For the contact amplitude associated to the vertex  $R_0$ , we apply the identity (A.11). Again we must assign a complex value to the dimension of an external leg consistent with the split representation, and we call the integration variable associated with this external leg  $u$ , while the other external legs (with real scaling dimensions) are labelled by an index  $i_{R_0}$ . The split representation then leads to

$$\begin{aligned} \tilde{\mathcal{A}}_L &= \int_{\mathbb{Q}_p^n} dx \tilde{\mathcal{L}} \left[ \prod_{L=1}^{2g-2} \int_{\mathbb{Q}_p} \frac{dt_L}{|t_L|_p} \right] \tilde{\mathcal{G}}(\{t_L\}) \\ &\times \sum_{a \in \{1,p\}} \left[ \prod_{i_V} \frac{2\zeta_p(1)}{|2|_p} \int_{a\mathbb{Q}_p^2} \frac{ds_{i_V}}{|s_{i_V}|_p} |s_{i_V}|_p^{\sum \Delta_{i_V}} \right] \frac{2\zeta_p(1)}{|2|_p} \int_{a\mathbb{Q}_p^2} \frac{dt}{|t|_p} |t|_p^{h-c} \\ &\times \left[ \prod_{1 \leq I \leq J \leq g} \prod_{i_{V_I}, i_{V_J}} \gamma_p \left( f_{IJ}(t_L) s_{i_{V_I}} s_{i_{V_J}} x_{i_{V_I} i_{V_J}}^2 \right) \right] \\ &\times \left[ \prod_{1 \leq I \leq g} \prod_{i_{V_I}} \gamma_p \left( f_{1I}(t_L) t s_{i_{V_I}} (x - x_{i_{V_I}})^2 \right) \right] \quad (\text{B.8}) \\ &\times \zeta_p \left( \sum \Delta_{i_{R_0}} - h + c \right) \\ &\times \sum_{b \in \{1,p\}} \left[ \prod_{i_{R_0}} \frac{2\zeta_p(1)}{|2|_p} \int_{b\mathbb{Q}_p^2} \frac{ds_{i_{R_0}}}{|s_{i_{R_0}}|_p} |s_{i_{R_0}}|_p^{\sum \Delta_{i_{R_0}}} \right] \frac{2\zeta_p(1)}{|2|_p} \int_{b\mathbb{Q}_p^2} \frac{du}{|u|_p} |u|_p^{h+c} \\ &\times \left[ \prod_{i_{R_0} < j_{R_0}} \gamma_p \left( s_{i_{R_0}} s_{j_{R_0}} x_{i_{R_0} j_{R_0}}^2 \right) \right] \left[ \prod_{i_{R_0}} \gamma_p \left( u s_{i_{R_0}} (x - x_{i_{R_0}})^2 \right) \right]. \end{aligned}$$

Performing the changes of variables  $s_{i_{R_0}} \rightarrow \frac{s_{i_{R_0}}}{u}$  and  $s_{i_{V_I}} \rightarrow \frac{s_{i_{V_I}}}{f_{1I}(t_L) t}$  and letting  $m$  denote an index such that  $|s_m|_p = \sup(|s_{i_{V_1}}|_p, |s_{i_{V_2}}|_p, \dots, |s_{i_{V_g}}|_p, |s_{i_{R_0}}|_p)$ , we can carry out the  $x$  integral with the integral formula (A.4). Applying this formula, and re-expressing the domains of

integration of  $t$  and  $u$  to all of  $\mathbb{Q}_p$  at the cost of two factors of  $\frac{2}{|2|_p}$ , we find that

$$\begin{aligned}
\tilde{\mathcal{A}}_L &= \tilde{\mathcal{L}} \left[ \prod_{L=1}^{2g-2} \int_{\mathbb{Q}_p} \frac{dt_L}{|t_L|_p} \right] \tilde{\mathcal{G}}(\{t_L\}) \\
&\times \left[ \prod_{i_V} \frac{2\zeta_p(1)}{|2|_p} \int_{\mathbb{Q}_p^2} \frac{ds_{i_V}}{|s_{i_V}|_p} |s_{i_V}|_p^{\sum \Delta_{i_V}} \right] \zeta_p(1) \int_{\mathbb{Q}_p} \frac{dt}{|t|_p} |t|_p^{-\sum \Delta_{i_V} + h - c} \\
&\times \left[ \prod_{1 \leq I \leq J \leq g} \prod_{i_{V_I}, i_{V_J}} \gamma_p \left( \frac{s_{i_{V_I}} s_{i_{V_J}} f_{IJ}(t_L)}{t^2 f_{1I}(t_L) f_{1J}(t_L)} x_{i_{V_I} i_{V_J}}^2 \right) \right] \\
&\times \left( \prod_{1 \leq I \leq g} |f_{1I}(t_L)|_p^{-\sum \Delta_{i_{V_I}}} \left[ \prod_{i_{V_I}} \gamma_p(s_{i_{V_I}} (x_m - x_{i_{V_I}})^2) \right] \right) \\
&\times \zeta_p \left( \sum \Delta_{i_{R_0}} - h + c \right) \\
&\times \left[ \prod_{i_{R_0}} \frac{2\zeta_p(1)}{|2|_p} \int_{\mathbb{Q}_p^2} \frac{ds_{i_{R_0}}}{|s_{i_{R_0}}|_p} |s_{i_{R_0}}|_p^{\sum \Delta_{i_{R_0}}} \right] \zeta(1) \int_{\mathbb{Q}_p} \frac{du}{|u|_p} |u|_p^{-\sum \Delta_{i_{R_0}} + h + c} \\
&\times \left[ \prod_{i_{R_0} < j_{R_0}} \gamma_p \left( \frac{s_{i_{R_0}} s_{j_{R_0}}}{u^2} x_{i_{R_0} j_{R_0}}^2 \right) \right] \left[ \prod_{i_{R_0}} \gamma_p(s_{i_{R_0}} (x_m - x_{R_0})^2) \right] |s_m|_p^{-h}.
\end{aligned} \tag{B.9}$$

Next, we change variables  $t \rightarrow t\sqrt{s_m}$  and  $u \rightarrow u\sqrt{s_m}$ , and then change variables  $s_i \rightarrow s_i\sqrt{s_m}$  for all  $i \neq m$ , and lastly change variable  $s_m \rightarrow s_m^2$ :

$$\begin{aligned}
\tilde{\mathcal{A}}_L &= \tilde{\mathcal{L}} \left[ \prod_{L=1}^{2g-2} \int_{\mathbb{Q}_p} \frac{dt_L}{|t_L|_p} \right] \tilde{\mathcal{G}}(\{t_L\}) \\
&\times \sum_{a \in \{1, p\}} \left[ \prod_{i_V} \frac{2\zeta_p(1)}{|2|_p} \int_{a\mathbb{Q}_p^2} \frac{ds_{i_V}}{|s_{i_V}|_p} |s_{i_V}|_p^{\sum \Delta_{i_V}} \right] \zeta_p(1) \int_{\mathbb{Q}_p} \frac{dt}{|t|_p} |t|_p^{-\sum \Delta_{i_V} + h - c} \\
&\times \left( \prod_{1 \leq I \leq J \leq g} \left[ \prod_{i_{V_I}, i_{V_J}} \gamma_p \left( \frac{s_{i_{V_I}} s_{i_{V_J}} f_{IJ}(t_L)}{t^2 f_{1I}(t_L) f_{1J}(t_L)} x_{i_{V_I} i_{V_J}}^2 \right) \right] \right) \\
&\times \left( \prod_{1 \leq I \leq g} |f_{1I}(t_L)|_p^{-\sum \Delta_{i_{V_I}}} \left[ \prod_{i_{V_I}} \gamma_p(s_{i_{V_I}} s_m (x_m - x_{i_{V_I}})^2) \right] \right) \\
&\times \zeta_p \left( \sum \Delta_{i_{R_0}} - h + c \right) \\
&\times \left[ \prod_{i_{R_0}} \frac{2\zeta_p(1)}{|2|_p} \int_{a\mathbb{Q}_p^2} \frac{ds_{i_{R_0}}}{|s_{i_{R_0}}|_p} |s_{i_{R_0}}|_p^{\sum \Delta_{i_{R_0}}} \right] \zeta_p(1) \int_{\mathbb{Q}_p} \frac{du}{|u|_p} |u|_p^{-\sum \Delta_{i_{R_0}} + h + c} \\
&\times \left[ \prod_{i_{R_0} < j_{R_0}} \gamma_p \left( \frac{s_{i_{R_0}} s_{j_{R_0}}}{u^2} x_{i_{R_0} j_{R_0}}^2 \right) \right] \left[ \prod_{i_{R_0}} \gamma_p(s_{i_{R_0}} s_m (x_m - x_{R_0})^2) \right].
\end{aligned} \tag{B.10}$$

The above expression for  $\tilde{\mathcal{A}}_L$  exhibits an explicit dependence on  $s_m$ , which is inexpedient for

further manipulations. But let  $i$  denote an index that runs over all the indices  $i_{V_I}$  and  $i_{R_0}$ . Using (A.3), one can show that

$$\left[ \prod_{1 \leq I \leq g} \prod_{i_{V_I}} \gamma_p(s_{i_{V_I}} s_m (x_m - x_{i_{V_I}})^2) \right] \left[ \prod_{i_{R_0}} \gamma_p(s_{i_{R_0}} s_m (x_m - x_{R_0})^2) \right] = \prod_{i,j} \gamma_p(s_i s_j x_{ij}^2). \quad (\text{B.11})$$

After using this formula, we note that equation (B.10) is of the same form as equation (B.5), and so, as promised, we have demonstrated inductively that the position space pre-amplitude  $\tilde{A}_L$  could indeed be cast in the form (B.5). This completes the inductive proof that any arbitrary tree-level diagram, in particular the diagram in (B.3) corresponding to the position space pre-amplitude  $\tilde{A}_l$ , takes the form described in (B.5).

Applying the  $p$ -adic Symanzik star integration formula (A.10) to (B.10) after invoking (B.11), we obtain

$$\begin{aligned} \tilde{A}_L &= \tilde{\mathcal{L}} \zeta_p(\sum \Delta_{i_{R_0}} - h + c) \left[ \prod_{L=1}^{2g-2} \int_{\mathbb{Q}_p} \frac{dt_L}{|t_L|_p} \right] \tilde{\mathcal{G}}(\{t_L\}) \left[ \prod_{1 \leq I \leq g} |f_{1I}(t_L)|_p^{-\sum \Delta_{i_{V_I}}} \right] \\ &\times \int [d\gamma] \left[ \prod_{i < j} \frac{\zeta_p(2\gamma_{ij})}{|x_{ij}|_p^{2\gamma_{ij}}} \right] \zeta_p(1) \int_{\mathbb{Q}_p} \frac{du}{|u|_p} |u|_p^{-\sum \Delta_{i_{R_0}} + h + c} \left[ \prod_{i_{R_0} < j_{R_0}} \left| 1, \frac{1}{u} \right|_s^{-2\gamma_{i_{R_0} j_{R_0}}} \right] \\ &\times \zeta_p(1) \int_{\mathbb{Q}_p} \frac{dt}{|t|_p} |t|_p^{-\sum \Delta_{i_V} + h - c} \left[ \prod_{1 \leq I \leq J \leq g} \prod_{i_{V_I}, i_{V_J}} \left| 1, \frac{f_{IJ}(t)}{t^2 f_{1I}(t) f_{1J}(t)} \right|_s^{-\gamma_{i_{V_I} i_{V_J}}} \right]. \end{aligned} \quad (\text{B.12})$$

The factor of  $\zeta_p(\sum \Delta_{i_{R_0}} - h + c)$  gives us the vertex factor (3.1) associated with the vertex  $R_0$  in the diagram  $D_L$ . The  $u$  integral evaluates to (see (A.12) in appendix A)

$$\frac{-1}{\zeta_p(1)} \left[ \zeta_p(\sum \Delta_{R_0} - 2 \sum \gamma_{i_{R_0}, j_{R_0}} - h - c) - \zeta_p(\sum \Delta_{i_{R_0}} - h - c) \right], \quad (\text{B.13})$$

which is the undressed diagram associated with the vertex  $R_0$  (recall identity (4.3)). We are making the inductive assumption that expression (B.12) is equal to the position space pre-amplitude for diagram  $D_L$  according to prescription III of section 4, and this assumption implies that the remaining part of the right-hand side of (B.12) is equal to the product of all the vertex factors and undressed diagrams associated with the remaining vertices of  $D_L$ ,

that is,

$$\begin{aligned}
& \tilde{\mathcal{L}} \left[ \prod_{L=1}^{2g-2} \int_{\mathbb{Q}_p} \frac{dt_L}{|t_L|_p} \right] \tilde{\mathcal{G}}(\{t_L\}) \left[ \prod_{1 \leq I \leq g} |f_{1I}(t_L)|_p^{-\sum \Delta_{i_{V_I}}} \right] \\
& \times \zeta_p(1) \int_{\mathbb{Q}_p} \frac{dt}{|t|_p} |t|_p^{-\sum \Delta_{i_V} + h - c} \left[ \prod_{1 \leq I \leq J \leq g} \prod_{i_{V_I}, i_{V_J}} \left| 1, \frac{f_{IJ}(t_L)}{t^2 f_{1I}(t_L) f_{1J}(t_L)} \right|_s^{-\gamma_{i_{V_I} i_{V_J}}} \right] \\
& = \left[ \prod_{I=1}^g (\text{vertex factor for vertex } V_I) (\text{undressed diagram for vertex } V_I) \right].
\end{aligned} \tag{B.14}$$

**The “right-hand diagram”  $D_R$ .** Now we turn our attention to the position space pre-amplitude  $\tilde{\mathcal{A}}_R$  for diagram  $D_R$  in (B.1). According to prescription III and (4.3) of section 4, this Mellin pre-amplitude is given by the following product of vertex factors and undressed diagrams:

$$\begin{aligned}
\tilde{\mathcal{M}}_R &= \left( \begin{array}{c} \text{blue diagram} \\ \vdots \\ i_{R_0} \vdots \\ \vdots \\ h+c_1 \\ \vdots \\ h+c_f \end{array} \right) \left( \begin{array}{c} \text{red diagram} \\ \vdots \\ i_{R_0} \vdots \\ \vdots \\ h+c_f \\ \vdots \\ h-c_f \end{array} \right) \\
&\times \prod_{I=1}^f \left[ \left( \begin{array}{c} \text{blue diagram} \\ \vdots \\ h-c_I \\ \vdots \\ i_{R_I} \end{array} \right) \left( \begin{array}{c} \text{red diagram} \\ \vdots \\ h+c_I \quad h-c_I \\ \vdots \\ i_{R_I} \end{array} \right) \right].
\end{aligned} \tag{B.15}$$

From this diagrammatic decomposition, we can obtain an expression for the Mellin amplitude by applying to it equations (3.1) and (4.7)-(4.8). We find it useful, however, to recast the integral expression (4.7)-(4.8) for undressed diagrams by changing variables to  $u_i \equiv \frac{1}{\sqrt{x_i}}$ :

$$\begin{aligned}
& \left( \begin{array}{c} \text{red diagram} \\ \vdots \\ \Delta_L \quad s_1, \quad h-c_1 \\ \vdots \\ \vdots \\ \vdots \\ \Delta_{l+1} \quad h+c_l, \\ \vdots \\ s_l \quad h-c_l \end{array} \right) \\
& = \left[ \prod_{i=1}^l \zeta_p(1) \int_{\mathbb{Q}_p^2} \frac{du_i}{|u_i|_p} |u_i|_p^{-2c_i} \left| 1, u_i \right|_s^{s_i+c_i-h} \right] \left| 1, \frac{1}{u_1}, \dots, \frac{1}{u_l} \right|_s^{2h - \sum_{i=1}^l (c_i+h) - \sum_{i=l+1}^L \Delta_i}.
\end{aligned} \tag{B.16}$$

Writing out the vertex factors in terms of their  $p$ -adic zeta functions and using the above integral form for the undressed diagrams, (B.15) can be rewritten as

$$\begin{aligned}
\tilde{\mathcal{A}}_R &= \zeta_p \left( \sum \Delta_{I_{R_0}} + \sum_{I=1}^f (h + c_I) - 2h \right) \int [d\gamma] \left[ \prod_{i < j} \frac{\zeta_p(2\gamma_{ij})}{|x_{ij}|_p^{2\gamma_{ij}}} \right] \\
&\times \left[ \prod_{I=1}^f \zeta_p \left( \sum \Delta_{i_{R_I}} - h - c_I \right) \zeta_p(1) \int_{\mathbb{Q}_p} \frac{dv_I}{|v_I|} |v_I|_p^{\sum \Delta_{i_{R_I}} - h + c_I} \left| 1, v_I \right|_s^{-2\sum \gamma_{i_{R_I} j_{R_I}}} \right] \\
&\times \left[ \prod_{I=1}^f \zeta_p(1) \int_{\mathbb{Q}_p} \frac{du_I}{|u_I|} |u_I|_p^{-2c_I} \left| 1, u_I \right|_s^{\sum \Delta_{i_{R_I}} - h + c_I - 2\sum \gamma_{i_{R_I} j_{R_I}}} \right] \\
&\times \left| 1, \frac{1}{u_1}, \frac{1}{u_2}, \dots, \frac{1}{u_f} \right|_s^{2h - \sum \Delta_{i_{R_0}} - \sum_{I=1}^f (c_I + h)}.
\end{aligned} \tag{B.17}$$

where  $i, j$  run over all external leg indices  $i_{R_0}, i_{R_1}, \dots, i_{R_f}$ . Lumping together the vertex factors into one symbol

$$\mathcal{R} \equiv \zeta_p \left( \sum \Delta_{I_{R_0}} + \sum_{I=1}^f (h + c_I) - 2h \right) \left[ \prod_{I=1}^f \zeta_p \left( \sum \Delta_{i_{R_I}} - h - c_I \right) \right], \tag{B.18}$$

and using the Symanzik star integration formula (A.10), one finds that the position space pre-amplitude for diagram  $D_R$  is given by

$$\begin{aligned}
\tilde{\mathcal{A}}_R &= \mathcal{R} \sum_{b \in \{1, p\}} \left[ \prod_{i_R} \frac{2\zeta_p(1)}{|2|_p} \int_{b\mathbb{Q}_p^2} \frac{ds_{i_R}}{|s_{i_R}|_p} |s_{i_R}|_p^{\sum \Delta_{i_R}} \right] \\
&\times \left[ \prod_{I=1}^f \zeta_p(1) \int_{\mathbb{Q}_p} \frac{du_I}{|u_I|} |u_I|_p^{-2c_I} \left| 1, u_I \right|_s^{\sum \Delta_{i_{R_I}} - h + c_I} \zeta_p(1) \int_{\mathbb{Q}_p} \frac{dv_I}{|v_I|} |v_I|_p^{\sum \Delta_{i_{R_I}} - h + c_I} \right] \\
&\times \left| 1, \frac{1}{u_1}, \frac{1}{u_2}, \dots, \frac{1}{u_f} \right|_s^{2h - \sum \Delta_{i_{R_0}} - \sum_{I=1}^f (c_I + h)} \left[ \prod_{i_R, j_R} \gamma_p(s_{i_R} s_{j_R} x_{i_R j_R}^2) \right] \\
&\times \left[ \prod_{I=1}^f \prod_{i_{R_I} < j_{R_I}} \gamma_p(s_{i_{R_I}} s_{j_{R_I}} (1, u_I)_s^2 (1, v_I)_s^2 x_{i_{R_I} j_{R_I}}^2) \right],
\end{aligned} \tag{B.19}$$

where the index  $i_R$  runs over  $i_{R_0}, i_{R_1}, \dots, i_{R_f}$  and

$$(1, u)_s \equiv \begin{cases} 1, & \text{when } |u|_p \leq 1, \\ u, & \text{when } |u|_p > 1. \end{cases} \tag{B.20}$$

**The “merged diagram”  $D_M$ .** By strong induction we are making the assumption that diagrams  $D_I$ ,  $D_L$ , and  $D_R$  satisfy prescription III. The inductive step we shall undertake in order to prove the pre-amplitude prescription is that under this assumption, the position space pre-amplitude of diagram  $D_M$ , which we call  $\tilde{\mathcal{A}}_M$ , evaluates to the appropriate product of vertex factors and undressed diagrams as prescribed by prescription III.

Applying the split representation to the internal leg connecting vertices  $V_1$  and  $R_0$  in  $D_M$ , we can express  $\tilde{\mathcal{A}}_M$  as a boundary integral over the pre-amplitudes for the left- and right-hand diagrams, for which we may use equations (B.5) and (B.19). However, in using each of these two equations, we once again need to assign a complex scaling dimension to one of the external legs. For the left-hand part of the diagram we assign a complex value  $h - c$  to the scaling dimension of an external leg connected to vertex  $V_1$  and once again rename the integration variable  $s_{i_{V_1}}$  as  $t$ . For the right-hand part of the diagram, we assign the value  $h + c$  to the scaling dimension, call it  $\Delta_0$ , of an external leg connected to vertex  $R_0$ . Furthermore, we rename the integration variable  $s_{i_{R_0}}$  as  $u$  and define  $\tilde{\mathcal{R}} \equiv \mathcal{R}|_{\Delta_0=h+c}$ .

We arrive, then, at the following expression for the position space pre-amplitude of  $D_M$ :

$$\begin{aligned}
\tilde{\mathcal{A}}_M &= \int_{\mathbb{Q}_p^n} dx \tilde{\mathcal{L}} \left[ \prod_{L=1}^{2g-2} \int_{\mathbb{Q}_p} \frac{dt_L}{|t_L|_p} \right] \tilde{\mathcal{G}}(\{t_L\}) \\
&\times \sum_{a \in \{1,p\}} \left[ \prod_{i_V} \frac{2\zeta_p(1)}{|2|_p} \int_{a\mathbb{Q}_p^2} \frac{ds_{i_V}}{|s_{i_V}|_p} |s_{i_V}|_p^{\sum \Delta_{i_V}} \right] \frac{2\zeta_p(1)}{|2|_p} \int_{a\mathbb{Q}_p^2} \frac{dt}{|t|_p} |t|_p^{h-c} \\
&\times \left[ \prod_{1 \leq I \leq J \leq g} \prod_{i_{V_I}, i_{V_J}} \gamma_p(f_{IJ}(t_L) s_{i_{V_I}} s_{i_{V_J}} x_{i_{V_I} i_{V_J}}^2) \right] \\
&\times \left[ \prod_{1 \leq I \leq g} \prod_{i_{V_I}} \gamma_p(f_{1I}(t_L) t s_{i_{V_I}} (x - x_{i_{V_I}})^2) \right] \\
&\times \tilde{\mathcal{R}} \sum_{b \in \{1,p\}} \left[ \prod_{i_R} \frac{2\zeta_p(1)}{|2|_p} \int_{b\mathbb{Q}_p^2} \frac{ds_{i_R}}{|s_{i_R}|_p} |s_{i_R}|_p^{\sum \Delta_{i_R}} \right] \\
&\times \frac{2\zeta_p(1)}{|2|_p} \int_{b\mathbb{Q}_p^2} \frac{du}{|u|_p} |u|_p^{h+c} \left[ \prod_{i_R} \gamma_p(u s_{i_R} (x - x_{i_R})^2) \right] \\
&\times \left[ \prod_{I=1}^f \zeta_p(1) \int_{\mathbb{Q}_p} \frac{du_I}{|u_I|_p} |u_I|_p^{-2c_I} |1, u_I|_s^{\sum \Delta_{i_{R_I}} - h + c_I} \zeta_p(1) \int_{\mathbb{Q}_p} \frac{dv_I}{|v_I|_p} |v_I|_p^{\sum \Delta_{i_{R_I}} - h + c_I} \right] \\
&\times \left| 1, \frac{1}{u_1}, \frac{1}{u_2}, \dots, \frac{1}{u_f} \right|_s^{2h - \sum \Delta_{i_{R_0}} - \sum_{I=1}^f (c_I + h) - h - c} \left[ \prod_{i_R, j_R} \gamma_p(s_{i_R} s_{j_R} x_{i_R j_R}^2) \right] \\
&\times \left[ \prod_{I=1}^f \prod_{i_{R_I} < j_{R_I}} \gamma_p(s_{i_{R_I}} s_{j_{R_I}} (1, u_I)_s^2 (1, v_I)_s^2 x_{i_{R_I} j_{R_I}}^2) \right].
\end{aligned} \tag{B.21}$$

Changing variables,  $s_{i_{V_I}} \rightarrow \frac{s_{i_{V_I}}}{t f_{1I}(t_L)}$  and  $s_{i_R} \rightarrow \frac{s_{i_R}}{u}$ , re-expressing the domains of the  $t$  and  $u$  integrals, letting  $m$  denote an index such that  $|s_m|_p = \sup_i |s_i|_p$ , and carrying out the  $x$  integral, we get

$$\begin{aligned}
\tilde{\mathcal{A}}_M &= \tilde{\mathcal{L}} \left[ \prod_{L=1}^{2g-2} \int_{\mathbb{Q}_p} \frac{dt_L}{|t_L|_p} \right] \tilde{\mathcal{G}}(t_L) \\
&\times \left[ \prod_{i_V} \frac{2\zeta_p(1)}{|2|_p} \int_{\mathbb{Q}_p^2} \frac{ds_{i_V}}{|s_{i_V}|_p} |s_{i_V}|_p^{\sum \Delta_{i_V}} \right] \zeta_p(1) \int_{\mathbb{Q}_p} \frac{dt}{|t|_p} |t|_p^{-\sum \Delta_{i_V} + h - c} \\
&\times \left[ \prod_{1 \leq I \leq J \leq g} \prod_{i_{V_I}, i_{V_J}} \gamma_p \left( \frac{f_{IJ}(t_L) s_{i_{V_I}} s_{i_{V_J}}}{t^2 f_{1I}(t_L) f_{1J}(t_L)} x_{i_{V_I} i_{V_J}}^2 \right) \right] \\
&\times \left( \prod_{1 \leq I \leq g} |f_{1I}(t_L)|_p^{-\sum \Delta_{i_{V_I}}} \left[ \prod_{i_{V_I}} \gamma_p \left( s_{i_{V_I}} (x_m - x_{i_{V_I}})^2 \right) \right] \right) \\
&\times \tilde{\mathcal{R}} \left[ \prod_{i_R} \frac{2\zeta_p(1)}{|2|_p} \int_{\mathbb{Q}_p^2} \frac{ds_{i_R}}{|s_{i_R}|_p} |s_{i_R}|_p^{\sum \Delta_{i_R}} \right] \\
&\times \zeta_p(1) \int_{\mathbb{Q}_p} \frac{du}{|u|_p} |u|_p^{-\sum \Delta_{i_R} + h + c} \left[ \prod_{i_R} \gamma_p \left( s_{i_R} (x_m - x_{i_R})^2 \right) \right] |s_m|_p^{-h} \\
&\times \left[ \prod_{I=1}^f \zeta_p(1) \int_{\mathbb{Q}_p} \frac{du_I}{|u_I|_p} |u_I|_p^{-2c_I} |1, u_I|_s^{\sum \Delta_{i_{R_I}} - h + c_I} \zeta_p(1) \int_{\mathbb{Q}_p} \frac{dv_I}{|v_I|_p} |v_I|_p^{\sum \Delta_{i_{R_I}} - h + c_I} \right] \\
&\times \left| 1, \frac{1}{u_1}, \frac{1}{u_2}, \dots, \frac{1}{u_f} \right|_s^{2h - \sum \Delta_{i_{R_0}} - \sum_{I=1}^f (c_I + h) - h - c} \left[ \prod_{i_R, j_R} \gamma_p \left( \frac{s_{i_R} s_{j_R}}{u^2} x_{i_R j_R}^2 \right) \right] \\
&\times \left[ \prod_{I=1}^f \prod_{i_{R_I} < j_{R_I}} \gamma_p \left( \frac{s_{i_{R_I}} s_{j_{R_I}}}{u^2} (1, u_I)_s^2 (1, v_I)_s^2 x_{i_{R_I} j_{R_I}}^2 \right) \right].
\end{aligned} \tag{B.22}$$

Changing variables  $t \rightarrow \sqrt{s_m} t$ ,  $u \rightarrow \sqrt{s_m} u$ , and  $s_i \rightarrow \sqrt{s_m} s_i$  for  $i \neq m$ , and then changing variable  $s_i \rightarrow s_i^2$  gives:

$$\begin{aligned}
\tilde{\mathcal{A}}_M &= \tilde{\mathcal{L}} \left[ \prod_{L=1}^{2g-2} \int_{\mathbb{Q}_p} \frac{dt_L}{|t_L|_p} \right] \tilde{\mathcal{G}}(t_L) \\
&\times \sum_{a \in \{1,p\}} \left[ \prod_{i_V} \frac{2\zeta_p(1)}{|2|_p} \int_{a\mathbb{Q}_p^2} \frac{ds_{i_V}}{|s_{i_V}|_p} |s_{i_V}|_p^{\sum \Delta_{i_V}} \right] \zeta_p(1) \int_{\mathbb{Q}_p} \frac{dt}{|t|_p} |t|_p^{-\sum \Delta_{i_V} + h - c} \\
&\times \left[ \prod_{1 \leq I \leq J \leq g} \prod_{i_{V_I}, i_{V_J}} \gamma_p \left( \frac{f_{IJ}(t_L) s_{i_{V_I}} s_{i_{V_J}}}{t^2 f_{1I}(t_L) f_{1J}(t_L)} x_{i_{V_I} i_{V_J}}^2 \right) \right] \\
&\times \left( \prod_{1 \leq I \leq g} |f_{1I}(t_L)|_p^{-\sum \Delta_{i_{V_I}}} \left[ \prod_{i_{V_I}} \gamma_p (s_m s_{i_{V_I}} (x_m - x_{i_{V_I}})^2) \right] \right) \\
&\times \tilde{\mathcal{R}} \left[ \prod_{i_R} \frac{2\zeta_p(1)}{|2|_p} \int_{a\mathbb{Q}_p^2} \frac{ds_{i_R}}{|s_{i_R}|_p} |s_{i_R}|_p^{\sum \Delta_{i_R}} \right] \\
&\times \zeta_p(1) \int_{\mathbb{Q}_p} \frac{du}{|u|_p} |u|_p^{-\sum \Delta_{i_R} + h + c} \left[ \prod_{i_R} \gamma_p (s_m s_{i_R} (x_m - x_{i_R})^2) \right] \\
&\times \left[ \prod_{I=1}^f \zeta_p(1) \int_{\mathbb{Q}_p} \frac{du_I}{|u_I|_p} |u_I|_p^{-2c_I} |1, u_I|_s^{\sum \Delta_{i_{R_I}} - h + c_I} \zeta_p(1) \int_{\mathbb{Q}_p} \frac{dv_I}{|v_I|_p} |v_I|_p^{\sum \Delta_{i_{R_I}} - h + c_I} \right] \\
&\times \left| 1, \frac{1}{u_1}, \frac{1}{u_2}, \dots, \frac{1}{u_f} \right|_s^{2h - \sum \Delta_{i_{R_0}} - \sum_{I=1}^f (c_I + h) - h - c} \left[ \prod_{i_R, j_R} \gamma_p \left( \frac{s_{i_R} s_{j_R}}{u^2} x_{i_R j_R}^2 \right) \right] \\
&\times \left[ \prod_{I=1}^f \prod_{i_{R_I} < j_{R_I}} \gamma_p \left( \frac{s_{i_{R_I}} s_{j_{R_I}}}{u^2} (1, u_I)_s^2 (1, v_I)_s^2 x_{i_{R_I} j_{R_I}}^2 \right) \right].
\end{aligned} \tag{B.23}$$

Introducing redundant characteristic functions to remove the explicit  $s_m$  dependence like in (B.11), and then invoking the Symanzik star integration formula (A.10), we obtain

$$\begin{aligned}
\tilde{A}_M &= \int [d\gamma] \left[ \prod_{i < j} \frac{\zeta(2\gamma_{ij})}{|x_{ij}|_p^{2\gamma_{ij}}} \right] \\
&\times \tilde{\mathcal{L}} \left[ \prod_{L=1}^{2g-2} \int_{\mathbb{Q}_p} \frac{dt_L}{|t_L|_p} \right] \tilde{\mathcal{G}}(t_L) \left[ \prod_{1 \leq I \leq g} |f_{1I}(t_L)|_p^{-\sum \Delta_{i_{V_I}}} \right] \\
&\times \zeta_p(1) \int_{\mathbb{Q}_p} \frac{dt}{|t|_p} |t|_p^{-\sum \Delta_{i_V} + h - c} \left[ \prod_{1 \leq I \leq J \leq g} \prod_{i_{V_I}, i_{V_J}} \left| 1, \frac{f_{IJ}(t_L)}{t^2 f_{1I}(t_L) f_{1J}(t_L)} \right|_s^{-\gamma_{i_{V_I} i_{V_J}}} \right] \\
&\times \tilde{\mathcal{R}} \zeta_p(1) \int_{\mathbb{Q}_p} \frac{du}{|u|_p} |u|_p^{-\sum \Delta_{i_R} + h + c} \left| 1, \frac{1}{u} \right|_s^{-2 \sum \gamma_{i_{R_0} j_{R_0}}} \left[ \prod_{0 \leq I < J \leq f} \left| 1, \frac{1}{u} \right|_s^{-2 \sum \gamma_{i_{R_I} j_{R_J}}} \right] \\
&\times \left[ \prod_{I=1}^f \zeta_p(1) \int_{\mathbb{Q}_p} \frac{du_I}{|u_I|_p} |u_I|_p^{-2c_I} \left| 1, u_I \right|_p^{\sum \Delta_{i_{R_I}} - h + c_I} \zeta_p(1) \int_{\mathbb{Q}_p} \frac{dv_I}{|v_I|_p} |v_I|_p^{\sum \Delta_{i_{R_I}} - h + c_I} \right] \\
&\times \left| 1, \frac{1}{u_1}, \frac{1}{u_2}, \dots, \frac{1}{u_f} \right|_s^{2h - \sum \Delta_{i_{R_0}} - \sum_{I=1}^f (c_I + h) - h - c} \left[ \prod_{I=1}^f \left| 1, \frac{(1, u_I)_s (1, v_I)_s}{u} \right|_s^{-2 \sum \gamma_{i_{R_I} j_{R_I}}} \right], \tag{B.24}
\end{aligned}$$

where by the sum  $\sum \gamma_{i_{R_I} j_{R_I}}$  we mean  $\sum_{i_{R_i} < j_{R_j}} \gamma_{i_{R_i} j_{R_j}}$ , that is, no double-counting. Comparing the second and third lines of (B.24) with (B.14), we see that the Mellin amplitude of  $D_M$  by the inductive assumption includes the vertex factors and undressed diagrams of all the vertices  $V_I$  on the left-hand side of diagram  $D_M$ . What remains for us to show is that the bottom three lines of (B.24), denote them  $\tilde{M}_R$ , equal the vertex factors and undressed diagrams of the vertices  $R_I$  of the right-hand diagram. Changing the variable  $u$  to its reciprocal, the bottom three lines can be rewritten as

$$\begin{aligned}
\tilde{M}_R &= \tilde{\mathcal{R}} \zeta_p(1) \int_{\mathbb{Q}_p} \frac{du}{|u|_p} |u|_p^{\sum \Delta_{i_R} - h - c} \left| 1, u \right|_s^{-2 \sum \gamma_{i_{R_0} j_{R_0}}} \left[ \prod_{0 \leq I < J \leq f} \left| 1, u \right|_s^{-2 \sum \gamma_{i_{R_I} j_{R_J}}} \right] \\
&\times \left[ \prod_{I=1}^f \zeta_p(1) \int_{\mathbb{Q}_p} \frac{du_I}{|u_I|_p} |u_I|_p^{-2c_I} \left| 1, u_I \right|_p^{\sum \Delta_{i_{R_I}} - h + c_I} \zeta_p(1) \int_{\mathbb{Q}_p} \frac{dv_I}{|v_I|_p} |v_I|_p^{\sum \Delta_{i_{R_I}} - h + c_I} \right] \\
&\times \left| 1, \frac{1}{u_1}, \frac{1}{u_2}, \dots, \frac{1}{u_f} \right|_s^{2h - \sum \Delta_{i_{R_0}} - \sum_{I=1}^f (c_I + h) - h - c} \left[ \prod_{I=1}^f \left| 1, u, uu_I, u(1, u_I)_s v_I \right|_s^{-2 \sum \gamma_{i_{R_I} j_{R_I}}} \right]. \tag{B.25}
\end{aligned}$$

Noting that  $\sum \Delta_{i_R} = \sum \Delta_{i_{R_0}} + \sum_{I=1}^f \sum \Delta_{i_{R_I}}$  and changing variables  $v_I \rightarrow \frac{(1, u, uu_I)_s}{u(1, u_I)_s} v_I$ ,

we obtain

$$\begin{aligned}
\widetilde{M}_R &= \widetilde{\mathcal{R}} \zeta_p(1) \int_{\mathbb{Q}_p} \frac{du}{|u|_p} |u|_p^{\sum \Delta_{i_{R_0}} + \sum_{I=1}^f (h-c_I) - h - c} |1, u|_s^{-2 \sum \gamma_{i_{R_0} j_{R_0}}} \left[ \prod_{0 \leq I < J \leq f} |1, u|_s^{-2 \sum \gamma_{i_{R_I} i_{R_J}}} \right] \\
&\times \left[ \prod_{I=1}^f \zeta_p(1) \int_{\mathbb{Q}_p} \frac{du_I}{|u_I|_p} |u_I|_p^{-2c_I} |1, u, uu_I|_s^{\sum \Delta_{i_{R_I}} - 2 \sum \gamma_{i_{R_I} j_{R_I}} - h + c_I} \right] \\
&\times \left[ \zeta_p(1) \int_{\mathbb{Q}_p} \frac{dv_I}{|v_I|_p} |v_I|_p^{\sum \Delta_{i_{R_I}} - h + c_I} |1, v_I|_s^{-2 \sum \gamma_{i_{R_I} j_{R_I}}} \right] \\
&\times \left| 1, \frac{1}{u_1}, \frac{1}{u_2}, \dots, \frac{1}{u_f} \right|_s^{2h - \sum \Delta_{i_{R_0}} - \sum_{I=1}^f (c_I + h) - h - c}.
\end{aligned} \tag{B.26}$$

Carrying out the  $v_I$  integrals using (A.12) and changing variables  $u_I \rightarrow \frac{(1, u)_s}{u} u_I$ , the pre-amplitude simplifies to

$$\begin{aligned}
\widetilde{M}_R &= \widetilde{\mathcal{R}} \left[ \prod_I (-1) \left( \zeta_p(\sum \Delta_{i_{R_I}} - 2 \sum \gamma_{i_{R_I} j_{R_I}} - h + c_I) - \zeta_p(\sum \Delta_{i_{R_I}} - h + c_I) \right) \right] \\
&\times \zeta_p(1) \int_{\mathbb{Q}_p} \frac{du}{|u|_p} |u|_p^{-2c} |1, u|_s^{\sum \Delta_{i_R} - 2 \sum \gamma_{i_{R_0} j_{R_0}} - h + c} \left[ \prod_{0 \leq I < J \leq f} |1, u|_s^{-2 \sum \gamma_{i_{R_I} i_{R_J}}} \right] \\
&\times \left[ \prod_{I=1}^f \zeta_p(1) \int_{\mathbb{Q}_p} \frac{du_I}{|u_I|_p} |u_I|_p^{-2c_I} |1, u_I|_s^{\sum \Delta_{i_{R_I}} - 2 \sum \gamma_{i_{R_I} j_{R_I}} - h + c_I} |1, u|_s^{-2 \sum \gamma_{i_{R_I} j_{R_I}}} \right] \\
&\times \left| 1, \frac{1}{u}, \frac{1}{u_1}, \frac{1}{u_2}, \dots, \frac{1}{u_f} \right|_s^{2h - \sum \Delta_{i_{R_0}} - \sum_{I=1}^f (c_I + h) - h - c}.
\end{aligned} \tag{B.27}$$

Let  $s_I$  denote the Mandelstam invariant associated with the internal leg connecting vertices  $R_0$  and  $R_I$ , and let  $s_0$  denote the Mandelstam invariant associated with the internal leg connecting vertices  $V_1$  and  $R_1$ . Then we have that

$$\begin{aligned}
s_I &= \sum \Delta_{i_{R_I}} - 2 \sum \gamma_{i_{R_I} j_{R_I}}, \\
s_0 &= \sum \Delta_{i_R} - 2 \sum_{0 \leq I < J \leq f} \sum \gamma_{i_{R_I} i_{R_J}} - 2 \sum \gamma_{i_{R_0} j_{R_0}} - 2 \sum_{I=1}^f \sum \gamma_{i_{R_I} j_{R_I}},
\end{aligned} \tag{B.28}$$

using which equation (B.27) can be rewritten as

$$\begin{aligned}
\widetilde{M}_R &= \widetilde{\mathcal{R}} \left[ \prod_I (-1) \left( \zeta_p(s_I - h + c_I) - \zeta_p(\sum \Delta_{i_{R_I}} - h + c_I) \right) \right] \\
&\times \zeta_p(1) \int_{\mathbb{Q}_p} \frac{du}{|u|_p} |u|_p^{-2c} |1, u|_s^{s_0 - h + c} \left[ \prod_{I=1}^f \zeta_p(1) \int_{\mathbb{Q}_p} \frac{du_I}{|u_I|_p} |u_I|_p^{-2c_I} |1, u_I|_s^{s_I - h + c_I} \right] \\
&\times \left| 1, \frac{1}{u}, \frac{1}{u_1}, \frac{1}{u_2}, \dots, \frac{1}{u_f} \right|_s^{2h - \sum \Delta_{i_{R_0}} - \sum_{I=1}^f (c_I + h) - h - c}.
\end{aligned} \tag{B.29}$$

In the first line of this equation,  $\widetilde{\mathcal{R}}$  is the product of vertex factors associated with the vertices  $R_0, R_1, \dots, R_f$  of diagram  $D_M$  and the product over  $I$  gives the product of undressed diagrams associated with vertices  $R_1, R_2, \dots, R_f$ . Comparing with (B.16), we recognize in lines two and three of (B.29) the integral form of the undressed diagram associated with vertex  $R_0$ . We conclude that  $\widetilde{\mathcal{M}}_R$  is equal to the product of vertex factors and undressed diagrams associated with vertices  $R_0, R_1, \dots, R_f$ , and so the full pre-amplitude for  $D_M$  is equal to the product of vertex factors and undressed diagrams associated with all the vertices of this diagram. This completes the proof of prescription III.

## C Inductive Proof of Prescription I for Mellin Amplitudes

In order to obtain a  $p$ -adic Mellin amplitude from a pre-amplitude one must carry out a contour integral around a cylindrical manifold for each internal leg of the diagram. In section 4.3 we proved that such contour integrals over pre-amplitudes, given according to prescription III of section 4, correctly reproduce Mellin amplitudes as defined in (2.12). What remains to be shown to demonstrate that the recursion relations of section 3.1 are true is that carrying out the contour integrals over the pre-amplitudes exactly reproduces the Mellin amplitudes given by prescription I. In this appendix we prove this for arbitrary tree-level bulk diagrams.

Consider first the exchange amplitude. The fact that carrying out the contour integral over its pre-amplitude yields the appropriate Mellin amplitude (see (4.16)) relies mathemat-

ically on the following identity:

$$\begin{aligned}
& \frac{\log p}{2\pi i} \int_{-\frac{i\pi}{\log p}}^{\frac{i\pi}{\log p}} dc \frac{\zeta_p(A+c)\zeta_p(A-c)\zeta_p(B-c)\zeta_p(C+c)}{\zeta_p(2c)\zeta_p(-2c)} \\
& \times \left( \zeta_p(D-c) + \zeta_p(B+c) - 1 \right) \left( \zeta_p(D+c) + \zeta_p(C-c) - 1 \right) \\
& = 2 \zeta_p(A+B)\zeta_p(A+C) \left( \zeta_p(B+C) + \zeta_p(A+D) - 1 \right),
\end{aligned} \tag{C.1}$$

where  $A, B, C, D > 0$ . This identity is a rewriting of equation (4.39) in Ref. [4].

For the bulk diagram with two internal lines, the fact that carrying out the contour integral over the pre-amplitude yields the desired Mellin amplitude (see (4.17)) follows from (C.1) and the following identity:

$$\begin{aligned}
& \frac{\log p}{2\pi i} \int_{-\frac{i\pi}{\log p}}^{\frac{i\pi}{\log p}} dc \frac{\zeta_p(A+c)\zeta_p(A-c)\zeta_p(B-c)\zeta_p(C+c)}{\zeta_p(2c)\zeta_p(-2c)} \left( \zeta_p(D-c) + \zeta_p(B+c) - 1 \right) \\
& \times \left( \zeta_p(E+c)\zeta_p(D+c) + \zeta_p(C-c)\zeta_p(E-c) + \zeta_p(E+c)\zeta_p(E-c) - \zeta_p(E+c) - \zeta_p(E-c) \right) \\
& = 2\zeta_p(A+B)\zeta_p(A+C) \left( \zeta_p(B+C)\zeta_p(B+E) + \zeta_p(A+E)\zeta_p(A+D) \right. \\
& \quad \left. + \zeta_p(A+E)\zeta_p(B+E) - \zeta_p(A+E) - \zeta_p(B+E) \right).
\end{aligned} \tag{C.2}$$

In fact in general, the fact that the pre-amplitudes given by prescription III of section 4 integrate to the appropriate Mellin amplitudes given by prescription I of section 3.1 hinges mathematically on an infinite tower of increasingly convoluted contour integral identities for the local zeta function  $\zeta_p$ .<sup>8</sup> In the diagrammatic notation we have employed in this paper, it turns out these integral identities have a simple interpretation, expressed in the form of identity (4.24). In fact such a diagrammatic interpretation holds true for both real as well as  $p$ -adic Mellin amplitudes. In this appendix we will prove identity (4.24) over the  $p$ -adics.

---

<sup>8</sup>The factors of two on the r.h.s sides of equations (C.1) and (C.2) arise non-trivially: If one computes the contour integrals on the left-hand sides by summing over the residues, it is only the full sum of residues that conspire to yield two times a sum of zeta functions. This holds true for all identities in the previously mentioned infinite tower of identities.



already has two internal lines incident on it:

$$\begin{aligned}
& \sum_{z^* \in \{\Delta_C, \Delta_{i_D}\}} \text{Res}_{z^*} \left[ \zeta_p(\Delta_{i_U} + \Delta_A + \Delta_B + z - n) \left( \begin{array}{c} i_U \\ \vdots \\ \text{---} \\ s_A \quad s_B \\ \Delta_A \quad \Delta_B \\ \text{---} \\ z \end{array} \right) \right. \\
& \quad \left. \times \zeta_p(\Delta_{i_D} - z) \zeta_p(\Delta_C - z) \right] \\
& = -\zeta_p(\Delta_A + \Delta_B + \Delta_C + \Delta_{i_U} - n) \lim_{s_C \rightarrow -\infty} \left( \begin{array}{c} i_U \\ \vdots \\ \text{---} \\ s_A \quad s_B \\ \Delta_A \quad \Delta_B \\ s_C \quad \Delta_C \\ \text{---} \\ i_D \end{array} \right).
\end{aligned} \tag{C.5}$$

These examples demonstrate how the operation of “adding an extra internal line” works. Assuming that such an operation exists for any undressed diagram, it is easy to prove that the type of contour integral displayed in the preceding subsection can be employed to glue together any two undressed diagrams. This proof is carried out in the next subsection. Then, in the subsection after the next, we justify the above-mentioned assumption by proving inductively that the “internal leg adding operation” can be applied to any undressed diagram, and in so doing we complete the proof of the recursive prescription I.

## C.2 Integrating pre-amplitudes using “leg addition”

Given an arbitrary undressed diagram parametrized by the complex number  $c$ ,

$$\mathcal{D} \equiv \left( \begin{array}{c} i_5 \quad i_6 \\ \vdots \quad \vdots \\ \text{---} \quad \text{---} \\ D \quad E \quad F \\ \text{---} \quad \text{---} \quad s \\ C \quad B \quad A \quad h-c \quad h+c \\ \vdots \quad \vdots \quad \vdots \\ i_3 \quad i_2 \quad i_1 \end{array} \right), \tag{C.6}$$



$$\begin{aligned}
\mathcal{D}_2 &= \lim_{s_E \rightarrow -\infty} \mathcal{D} = \lim_{s_E \rightarrow -\infty} \left( \begin{array}{c} \text{Diagram 1} \end{array} \right) \\
&= - \sum_{z^* \in \{\Delta_E, \Delta_{i_2}\}} \text{Res}_{z^*} \left[ \zeta_p(\Delta_A + \Delta_B + \Delta_{i_2} + z - n) \right. \\
&\quad \left. \times \zeta_p(\Delta_{i_5} - z) \zeta_p(\Delta_E - z) \right] \frac{1}{\zeta_p(\Delta_A + \Delta_B + \Delta_E + \Delta_{i_2} - n)}, \tag{C.10}
\end{aligned}$$

where we used the “leg adding operation” from the previous subsection to write the final equality above. (The validity of such a leg adding operation is proven in full generality in the next subsection.)

Essentially, the point of this exercise was to re-express  $\mathcal{D}_1$  and  $\mathcal{D}_2$  (and thus in turn  $\mathcal{D}$ ) in terms of a diagram with one fewer internal line than the original undressed diagram  $\mathcal{D}$ . Having done that, we can now carry out the contour integral in (C.8) by breaking  $\widetilde{\mathcal{M}}$  into two terms, each of which, using the assumption of our inductive setup, admits an extra internal line to be glued on.

Explicitly, splitting up the integrated amplitude  $\mathcal{M} = \mathcal{M}_1 + \mathcal{M}_2$  into the parts coming from  $\mathcal{D}_1$  and  $\mathcal{D}_2$ , respectively, the inductive assumption allows us to straightforwardly evaluate the two parts. The first part is given by

$$\begin{aligned}
\mathcal{M}_1 &\equiv \int_{-\frac{i\pi}{\log p}}^{\frac{i\pi}{\log p}} \frac{dc}{2\pi i} f_\Delta(c) \left( \begin{array}{c} F \\ | \\ \text{---} A \text{---} h-c \\ | \\ \dots \\ | \\ i_1 \end{array} \right) \left( \begin{array}{c} s \\ \text{---} h-c \text{---} h+c \text{---} \\ | \\ \dots \\ | \\ i_R \end{array} \right) \left( \begin{array}{c} \text{---} h+c \text{---} \\ | \\ \dots \\ | \\ i_7 \end{array} \right) \mathcal{D}_1 \\
&= - \left( \begin{array}{c} F \\ | \\ \text{---} A \text{---} \Delta \\ | \\ \dots \\ | \\ i_1 \end{array} \right) \zeta_p(s_E - \Delta_E) \left( \begin{array}{c} i_4 \dots \\ | \\ \text{---} D \text{---} E \text{---} F \text{---} s \text{---} i_7 \\ | \quad | \quad | \quad | \\ \dots \quad \dots \quad \dots \quad \dots \\ | \quad | \quad | \quad | \\ i_3 \quad i_2 \quad i_1 \quad \Delta \end{array} \right) \\
&\quad \times \left( \begin{array}{c} \text{---} \Delta \text{---} \\ | \\ \dots \\ | \\ i_7 \end{array} \right).
\end{aligned} \tag{C.11}$$

And the second part is given by

$$\mathcal{M}_2 \equiv \int_{-\frac{i\pi}{\log p}}^{\frac{i\pi}{\log p}} \frac{dc}{2\pi i} f_\Delta(c) \left( \begin{array}{c} F \\ | \\ \text{---} A \text{---} h-c \\ | \\ \dots \\ | \\ i_1 \end{array} \right) \left( \begin{array}{c} s \\ \text{---} h-c \text{---} h+c \text{---} \\ | \\ \dots \\ | \\ i_7 \end{array} \right) \left( \begin{array}{c} \text{---} h+c \text{---} \\ | \\ \dots \\ | \\ i_7 \end{array} \right) \mathcal{D}_2, \tag{C.12}$$

which, using the leg adding operation, we may re-express as

$$\begin{aligned}
\mathcal{M}_2 = & - \sum_{z^* \in \{\Delta_E, \Delta_{i_5}\}} \text{Res}_{z^*} \left[ \zeta_p(\Delta_A + \Delta_B + \Delta_{i_2} + z - n) \int_{-\frac{i\pi}{\log p}}^{\frac{i\pi}{\log p}} \frac{dc}{2\pi} f_\Delta(c) \left( \begin{array}{c} F \\ | \\ A \text{---} \text{---} h-c \\ | \\ \dots \\ i_1 \end{array} \right) \right. \\
& \times \left( \begin{array}{c} s \\ | \\ h-c \text{---} h+c \\ | \\ \dots \\ i_7 \end{array} \right) \left( \begin{array}{c} \dots \\ | \\ h+c \\ | \\ \dots \\ i_7 \end{array} \right) \\
& \times \left( \begin{array}{c} \dots \\ | \\ i_4 \dots \\ | \\ D \\ | \\ \dots \\ | \\ i_3 \end{array} \begin{array}{c} z \\ | \\ B \\ | \\ \dots \\ i_2 \end{array} \begin{array}{c} \dots \\ | \\ i_6 \dots \\ | \\ F \\ | \\ s \\ | \\ h-c \text{---} h+c \end{array} \right) \\
& \left. \times \zeta_p(\Delta_{i_5} - z) \zeta_p(\Delta_E - z) \right] \frac{1}{\zeta_p(\Delta_A + \Delta_B + \Delta_E + \Delta_{i_2} - n)}. \tag{C.13}
\end{aligned}$$

Here we have made use of the fact that the leg adding operation commutes with the contour integral so that we may choose to first carry out the contour integral, which is easily done using the inductive assumption:

$$\begin{aligned}
\mathcal{M}_2 = & - \sum_{z^* \in \{\Delta_E, \Delta_{i_5}\}} \text{Res}_{z^*} \left[ \zeta_p(\Delta_A + \Delta_B + \Delta_{i_2} + z - n) \right. \\
& \times \left( \begin{array}{c} F \\ | \\ A \text{---} \Delta \\ | \\ \dots \\ i_1 \end{array} \right) \left( \begin{array}{c} \dots \\ | \\ i_4 \dots \\ | \\ D \\ | \\ \dots \\ | \\ i_3 \end{array} \begin{array}{c} z \\ | \\ B \\ | \\ \dots \\ i_2 \end{array} \begin{array}{c} \dots \\ | \\ i_6 \dots \\ | \\ F \\ | \\ s \\ | \\ \Delta \end{array} \begin{array}{c} \dots \\ | \\ \dots \\ | \\ i_7 \end{array} \right) \left( \begin{array}{c} \dots \\ | \\ \Delta \\ | \\ \dots \\ i_7 \end{array} \right) \\
& \left. \times \zeta_p(\Delta_{i_5} - z) \zeta_p(\Delta_E - z) \right] \frac{1}{\zeta_p(\Delta_A + \Delta_B + \Delta_E + \Delta_{i_2} - n)}. \tag{C.14}
\end{aligned}$$

At this point we can use the leg adding operation as described in the previous subsection to

re-express  $\mathcal{M}_2$  in terms of a larger diagram:

$$\mathcal{M}_2 = \left( \begin{array}{c} F \\ | \\ \text{---} A \text{---} \Delta \\ | \\ \dots \\ i_1 \end{array} \right) \lim_{s_E \rightarrow -\infty} \left( \begin{array}{c} i_4 \dots \\ \diagdown \quad \diagup \\ D \\ | \\ \dots \\ i_3 \dots \\ \diagup \quad \diagdown \\ C \end{array} \text{---} \begin{array}{c} i_5 \dots \\ \diagdown \quad \diagup \\ E \\ | \\ \dots \\ i_2 \dots \\ \diagup \quad \diagdown \\ B \end{array} \text{---} \begin{array}{c} i_6 \dots \\ \diagdown \quad \diagup \\ F \\ | \\ \dots \\ i_1 \dots \\ \diagup \quad \diagdown \\ A \end{array} \text{---} \begin{array}{c} s \\ \text{---} \Delta \end{array} \text{---} \begin{array}{c} \dots \\ \diagdown \quad \diagup \\ i_7 \end{array} \right) \left( \begin{array}{c} \dots \\ \diagdown \quad \diagup \\ \Delta \end{array} \text{---} \begin{array}{c} \dots \\ \diagdown \quad \diagup \\ i_7 \end{array} \right). \quad (\text{C.15})$$

Comparing the final expressions for  $\mathcal{M}_1$  and  $\mathcal{M}_2$ , we see that up to a common pre-factor,  $\mathcal{M}_2$  is given by the  $s_E$ -independent terms of a diagram, and  $\mathcal{M}_1$  is given by the  $s_E$ -dependent terms of the same diagram. We thus conclude that their sum is equal to

$$\mathcal{M} = \left( \begin{array}{c} F \\ | \\ \text{---} A \text{---} \Delta \\ | \\ \dots \\ i_1 \end{array} \right) \left( \begin{array}{c} i_4 \dots \\ \diagdown \quad \diagup \\ D \\ | \\ \dots \\ i_3 \dots \\ \diagup \quad \diagdown \\ C \end{array} \text{---} \begin{array}{c} i_5 \dots \\ \diagdown \quad \diagup \\ E \\ | \\ \dots \\ i_2 \dots \\ \diagup \quad \diagdown \\ B \end{array} \text{---} \begin{array}{c} i_6 \dots \\ \diagdown \quad \diagup \\ F \\ | \\ \dots \\ i_1 \dots \\ \diagup \quad \diagdown \\ A \end{array} \text{---} \begin{array}{c} s \\ \text{---} \Delta \end{array} \text{---} \begin{array}{c} \dots \\ \diagdown \quad \diagup \\ i_7 \end{array} \right) \left( \begin{array}{c} \dots \\ \diagdown \quad \diagup \\ \Delta \end{array} \text{---} \begin{array}{c} \dots \\ \diagdown \quad \diagup \\ i_7 \end{array} \right), \quad (\text{C.16})$$

which is precisely what we wanted to show in (C.8).

### C.3 Proof of the general “leg adding” operation

The last task that remains to be accomplished to have a complete proof of the recursive prescription for  $p$ -adic Mellin amplitudes is to show that the leg adding operation works generally. That is, given an arbitrary undressed diagram

$$\mathfrak{D} \equiv \left( \begin{array}{c} i_4 \dots \\ \diagdown \quad \diagup \\ D \\ | \\ \dots \\ i_3 \dots \\ \diagup \quad \diagdown \\ C \end{array} \text{---} \begin{array}{c} i_6 \dots \\ \diagdown \quad \diagup \\ F \\ | \\ \dots \\ i_2 \dots \\ \diagup \quad \diagdown \\ B \end{array} \text{---} \begin{array}{c} i_1 \dots \\ \diagup \quad \diagdown \\ A \\ | \\ \dots \\ i_1 \dots \\ \diagup \quad \diagdown \\ G \end{array} \text{---} \begin{array}{c} \dots \\ \diagdown \quad \diagup \\ i_7 \end{array} \right), \quad (\text{C.17})$$

we need to show that we can obtain a diagram with an extra internal leg (more precisely, the part of the diagram that does not depend on a particular Mandelstam variable), by taking an appropriate sum of residues of  $\mathfrak{D}$ . Concretely, we need to show that the following sum of

residues,

$$\begin{aligned}
B \equiv & \sum_{z^* \in \{\Delta_E, \Delta_{i_5}\}} \text{Res}_{z^*} \left[ \zeta_p(\Delta_A + \Delta_B + \Delta_{i_2} + z - n) \left( \begin{array}{c} \text{Diagram} \end{array} \right) \right] \\
& \times \zeta_p(\Delta_{i_5} - z) \zeta_p(\Delta_E - z) \end{aligned} \tag{C.18}$$

is equal to the following limit,

$$C \equiv -\zeta_p(\Delta_A + \Delta_B + \Delta_E + \Delta_{i_2} - n) \lim_{s_E \rightarrow -\infty} \left( \begin{array}{c} \text{Diagram} \end{array} \right). \tag{C.19}$$

We will show this by strong induction on the number of internal lines. The idea is to apply the formula (5.8) to the undressed diagram in equation (C.18) in order to re-cast it in terms of diagrams with fewer internal lines and then use induction to evaluate the contribution to  $B$  from these smaller diagrams. Specifically, applying the formula (5.8) to the diagram in (C.18), we may decompose  $B$  as

$$\begin{aligned}
B = & -B_A - B_B - B_C - B_D - B_F - B_G \\
& -B_{AB} - B_{AC} - B_{AD} - \cdots - B_{FG} \\
& -B_{ABC} - B_{ABD} - B_{ABF} - \cdots - B_{DFG} \\
& \vdots \\
& -B_{ABCDEFG}, \end{aligned} \tag{C.20}$$

where  $B_{I_{i_1} \dots I_{i_f}}$  represents the contribution to  $B$  arising from the term in the sum in (5.8) which has  $l = f$  and  $I_1 = I_{i_1}, \dots, I_f = I_{i_f}$ . For example,

$$\begin{aligned}
B_A = & \sum_{z^* \in \{\Delta_E, \Delta_{i_5}\}} \operatorname{Res}_{z^*} \left[ \zeta_p(\Delta_A + \Delta_B + \Delta_{i_2} + z - n) \zeta_p(\Delta_{i_5} - z) \zeta_p(\Delta_E - z) \right. \\
& \times \left[ \zeta_p(s_A - \Delta_A) - \zeta_p(\Delta_{i_1 i_2 i_3 i_4 i_6 i_7}, + z - n) \lim_{\sqrt{s} \rightarrow \infty} \right] \left( \begin{array}{c} \text{Diagram 1} \end{array} \right) \\
& \times \left( \begin{array}{c} \text{Diagram 2} \end{array} \right) \left. \right], \tag{C.21}
\end{aligned}$$

where we are using the convention,

$$\Delta_{i_1 \dots i_k, i_{k+1} \dots i_\ell} \equiv \sum_{j=1}^k \Delta_{i_j} - \sum_{j=k+1}^{\ell} \Delta_{i_j}. \tag{C.22}$$

so that

$$\Delta_{i_1 i_2 i_3 i_4 i_6 i_7}, = \Delta_{i_1} + \Delta_{i_2} + \Delta_{i_3} + \Delta_{i_4} + \Delta_{i_6} + \Delta_{i_7}. \tag{C.23}$$

and summation is implied over each of the terms on the r.h.s. It may be remarked right away that we can decompose  $C$  in a similar manner:

$$\begin{aligned}
C = & -C_A - C_B - C_C - C_D - C_E - C_F - C_G \\
& -C_{AB} - C_{AC} - C_{AD} - \dots - C_{FG} \\
& -C_{ABC} - C_{ABD} - C_{ABE} - \dots - C_{EFG} \\
& \vdots \\
& -C_{ABCDEFG}, \tag{C.24}
\end{aligned}$$

where, introducing the definition

$$\Sigma \equiv \Delta_{i_1 i_2 i_3 i_4 i_5 i_6 i_7}, - n, \tag{C.25}$$

the term  $C_A$ , for example, is given by

$$C_A = -\zeta_p(\Delta_{ABEi_2}, -n) \lim_{s_E \rightarrow -\infty} \left[ \zeta_p(s_A - \Delta_A) - \zeta_p(\Sigma) \lim_{\forall s \rightarrow \infty} \right] \left( \left( \begin{array}{c} \text{Diagram 1} \end{array} \right) \left( \begin{array}{c} \text{Diagram 2} \end{array} \right) \right) \quad (\text{C.26})$$

The two limits  $s_E \rightarrow -\infty$  and  $\forall s \rightarrow \infty$  do not commute, since any term containing a factor of  $\zeta_p(s_E - \Delta_E)$  is killed off if the  $s_E \rightarrow -\infty$  is taken first but not if it is taken last. We can therefore commute the two limits only if we add back in these terms. That is, we may write  $C_A = C_{A,1} + C_{A,2}$ , where

$$C_{A,1} = -\zeta_p(\Delta_{ABEi_2}, -n) \left[ \zeta_p(s_A - \Delta_A) - \zeta_p(\Sigma) \lim_{\forall s \rightarrow \infty} \right] \lim_{s_E \rightarrow -\infty} \left( \left( \begin{array}{c} \text{Diagram 1} \end{array} \right) \left( \begin{array}{c} \text{Diagram 2} \end{array} \right) \right), \quad (\text{C.27})$$

$$C_{A,2} = -\zeta_p(\Delta_{ABEi_2}, -n) \zeta_p(\Sigma) \lim_{\forall s \rightarrow \infty} \left( \left( \begin{array}{c} \text{Diagram 1} \end{array} \right) \left( \begin{array}{c} \text{Diagram 2} \end{array} \right) \right). \quad (\text{C.28})$$

In equation (C.24) we get extra terms as compared to (C.20) because the diagram in (C.19) has an extra internal line, but we should remember that the  $s_E \rightarrow -\infty$  limit in (C.19) kills off the part of any term  $C_{I_1 \dots I_f}$  that contains a factor of  $\zeta_p(s_E - \Delta_E)$ .

Let us now look more closely at the contribution  $B_A$ . It is straightforward to check that

$$\zeta_p(\Delta_{i_5} - z)\zeta_p(\Delta_{i_1 i_2 i_3 i_4 i_6 i_7} + z - n) = \zeta_p(\Sigma) \left( \zeta_p(\Delta_{i_5} - z) + \zeta_p(\Delta_{i_1 i_2 i_3 i_4 i_6 i_7} + z - n) - 1 \right). \quad (\text{C.29})$$

Using this, we write  $B_A = B_{A,1} + B_{A,2}$ , where the first part is given by

$$B_{A,1} = \sum_{z^* \in \{\Delta_E, \Delta_{i_5}\}} \text{Res}_{z^*} \left[ \zeta_p(\Delta_A + \Delta_B + \Delta_{i_2} + z - n) \zeta_p(\Delta_{i_5} - z) \zeta_p(\Delta_E - z) \right. \\ \left. \times \left[ \zeta_p(s_A - \Delta_A) - \zeta_p(\Sigma) \lim_{\forall s \rightarrow \infty} \right] \left( \begin{array}{c} i_4 \dots \\ \diagdown \\ D \\ \diagup \\ C \\ i_3 \dots \end{array} \begin{array}{c} z \\ | \\ B \\ | \\ i_2 \dots \end{array} \begin{array}{c} A \\ \hline \end{array} \right) \left( \begin{array}{c} i_6 \dots \\ \diagdown \\ F \\ \diagup \\ G \\ i_1 \dots \end{array} \begin{array}{c} A \\ \hline \end{array} \begin{array}{c} \vdots \\ i_7 \end{array} \right) \right], \quad (\text{C.30})$$

and the second part of  $B_A$  is given by

$$B_{A,2} = - \sum_{z^* \in \{\Delta_E, \Delta_{i_5}\}} \text{Res}_{z^*} \left[ \zeta_p(\Delta_A + \Delta_B + \Delta_{i_2} + z - n) \zeta_p(\Delta_E - z) \right. \\ \left. \times \zeta_p(\Sigma) \left( \zeta_p(\Delta_{i_1 i_2 i_3 i_4 i_6 i_7} + z - n) - 1 \right) \lim_{\forall s \rightarrow \infty} \left( \begin{array}{c} i_4 \dots \\ \diagdown \\ D \\ \diagup \\ C \\ i_3 \dots \end{array} \begin{array}{c} z \\ | \\ B \\ | \\ i_2 \dots \end{array} \begin{array}{c} A \\ \hline \end{array} \right) \left( \begin{array}{c} i_6 \dots \\ \diagdown \\ F \\ \diagup \\ G \\ i_1 \dots \end{array} \begin{array}{c} A \\ \hline \end{array} \begin{array}{c} \vdots \\ i_7 \end{array} \right) \right]. \quad (\text{C.31})$$

Using the fact that the  $s \rightarrow \infty$  limit commutes with the sum over residues and invoking the inductive assumption, the first part is seen to equal

$$B_{A,1} = - \zeta_p(\Delta_A + \Delta_B + \Delta_E + \Delta_{i_2} - n) \\ \times \left[ \zeta_p(s_A - \Delta_A) - \zeta_p(\Sigma) \lim_{\forall s \rightarrow \infty} \right] \lim_{s_E \rightarrow -\infty} \left( \begin{array}{c} i_4 \dots \\ \diagdown \\ D \\ \diagup \\ C \\ i_3 \dots \end{array} \begin{array}{c} i_5 \dots \\ \diagdown \\ E \\ \diagup \\ B \\ | \\ i_2 \dots \end{array} \begin{array}{c} A \\ \hline \end{array} \right) \left( \begin{array}{c} i_6 \dots \\ \diagdown \\ F \\ \diagup \\ G \\ i_1 \dots \end{array} \begin{array}{c} A \\ \hline \end{array} \begin{array}{c} \vdots \\ i_7 \end{array} \right). \quad (\text{C.32})$$

We notice that  $B_{A,1}$  is exactly equal to  $C_{A,1}$ . And this observation does not depend on any special property of  $B_A$  not shared with any of the other terms on the r.h.s. of (C.20): we

may decompose any term  $B_{I_1\dots I_f}$  on the r.h.s. of (C.20) into two parts, called  $B_{I_1\dots I_f,1}$  and  $B_{I_1\dots I_f,2}$ , such that  $B_{I_1\dots I_f,1} = C_{I_1\dots I_f,1}$ . So we have now matched some of (C.18) with some of (C.19).

What remains to be shown is that the remaining part of  $B$  is equal to the remaining part of  $C$ . The remaining part of  $C$  consists of 1) terms  $C_{I_1\dots I_f,2}$  where  $I_i \neq E$  for all  $i \in \{1, 2, \dots, f\}$  and, 2) terms  $C_{I_1\dots I_f}$  for which  $I_i = E$  for some  $i \in \{1, 2, \dots, f\}$ . However, note that the sum of all these terms admits a simple diagrammatic interpretation, as we now explain. It was pointed out in section 5.1 that for any undressed diagram, the momentum-independent terms are in one-to-one correspondence with the terms proportional to internal line factors  $\zeta_p(s - \Delta)$ . Thus in (C.19) when we take the limit  $s_E \rightarrow -\infty$ , although we kill off the terms proportional to  $\zeta_p(s_E - \Delta_E)$ , we do not kill off the momentum-independent terms which are in one-to-one correspondence with these killed-off terms. It is exactly these surviving, unpartnered momentum-independent terms that we have yet to account for. But as these remaining terms stand in one-to-one correspondence with the killed-off terms containing the propagator factor  $\zeta_p(s_E - \Delta)$ , the factorization property of undressed diagrams from section 5.1 allows us to express these remaining unaccounted terms of  $C$  as

$$\zeta_p(\Delta_A + \Delta_B + \Delta_E + \Delta_{i_2} - n) \zeta_p(\Sigma) \lim_{\forall s \rightarrow \infty} \left( \text{Diagram} \right). \quad (\text{C.33})$$

Let's return to the second part of  $B_A$ . We see in the expression for  $B_{A,2}$  in (C.31) that there is no longer a pole at  $z = \Delta_{i_5}$ , so that  $B_{A,2}$  is simply equal to the residue at  $\Delta_E$ . Thus, we have

$$B_{A,2} = -\zeta_p(\Delta_A + \Delta_B + \Delta_E + \Delta_{i_2} - n) \zeta_p(\Sigma) \times \left( 1 - \zeta_p(\Delta_{i_1 i_2 i_3 i_4 i_6 i_7} + \Delta_E - n) \right) \lim_{\forall s \rightarrow \infty} \left( \text{Diagram 1} \right) \left( \text{Diagram 2} \right). \quad (\text{C.34})$$

We can rewrite this expression in a more suggestive form as

$$\begin{aligned}
B_{A,2} &= -\zeta_p(\Delta_A + \Delta_B + \Delta_E + \Delta_{i_2} - n) \zeta_p(\Sigma) \\
&\times \lim_{\forall s \rightarrow \infty} \left( \zeta_p(s_A - \Delta_A) - \zeta_p(\Delta_{i_1 i_2 i_3 i_4 i_6 i_7} + \Delta_E - n) \right) \left( \begin{array}{c} \text{Diagram 1} \\ \text{Diagram 2} \end{array} \right) \\
&\times \left( \begin{array}{c} \text{Diagram 3} \end{array} \right), \tag{C.35}
\end{aligned}$$

where now the symbol  $\forall s \rightarrow \infty$  also includes the limit  $s_A \rightarrow \infty$ . We recognize the above as exactly the contribution from the  $l = 1, I = A$  term if we apply the formula (5.8) to the undressed diagram in (C.33). Again there is nothing special about the  $B_A$  term. In general when we split a term  $B_{I_1 \dots I_f}$  on the right-hand side of (C.21) into  $B_{I_1 \dots I_f, 1}$  and  $B_{I_1 \dots I_f, 2}$ , the second term  $B_{I_1 \dots I_f, 2}$  exactly reproduces the term with  $l = f, I_1 = I_1, \dots, I_f = I_f$  on applying the formula (5.8) to (C.33). We conclude that the sum over these contributions coming from all the terms on the right-hand side of (C.20), that is, the sum

$$\begin{aligned}
&- B_{A,2} - B_{B,2} - B_{C,2} - B_{D,2} - B_{E,2} - B_{G,2} \\
&- B_{AB,2} - B_{AC,2} - B_{AD,2} - \dots - B_{FG,2} \\
&- B_{ABC,2} - B_{ABD,2} - B_{ABE,2} - \dots - B_{DFG,2} \\
&\vdots \\
&- B_{ABCDEFG,2}
\end{aligned} \tag{C.36}$$

is exactly equal to (C.33), which shows that  $B$  exactly reproduces all of  $C$ .

This concludes the proof of the leg adding operation, and in turn proves the recursion prescription I from section 3.

## D BCFW-Shifts of Auxiliary Momenta

In this appendix, we provide an alternative but equivalent form of the recursive prescription (5.11) from section 5, in auxiliary momentum space. The  $p$ -adic Mellin amplitude of a tree-level bulk diagram with external legs labeled  $\{1, \dots, \mathcal{N}\}$  and auxiliary momenta (defined in section 2) labeled  $\{k_1, \dots, k_{\mathcal{N}}\}$ , can be written as

$$\mathcal{M} = - \sum_{\text{partitions } I} \mathcal{M}(I, -\hat{k}_I)(z_I) \times (\text{propagator}) \times \mathcal{M}(I^c, \hat{k}_I)(z_I), \quad (\text{D.1})$$

where the partition of external legs,  $I$  is a subset  $I \subset \{1, \dots, \mathcal{N}\}$  such that it can be obtained by splitting the diagram into two by cutting across any chosen internal line, and  $I^c$  is the complement of  $I$ . The hatted momenta are defined to be  $\hat{k}_I \equiv -\sum_{a \in I} k_a(z)$ , where  $k_a(z)$  are the complex-shifted external momenta which are on-shell at all values of  $z \in \mathbb{C}$ , while  $\hat{k}_I$  goes on-shell only at  $z = z_I$ .

The amplitude  $\mathcal{M}(I, -\hat{k}_I)(z)$  is one of the  $z$ -dependent sub-amplitudes obtained by splitting the original diagram into two by cutting across the chosen internal line, and the factor of “(propagator)” is the Mellin space “propagator”  $\beta_p(-k_I^2 - \Delta_I, n - \sum_{i=1}^{\mathcal{N}} \Delta_i)$  defined in (2.24), where the unhatted momentum  $k_I = -\sum_{a \in I} k_a$  is constructed out of *un-shifted* external momentum variables, and  $\Delta_I$  is the conformal dimension of the bulk field propagating along the chosen internal line.<sup>9</sup>

From here on, we will sometimes refer to the on-shell recursion above as BCFW-type recursion because of the similarity of (D.1) with the usual BCFW decomposition, but we stress that we are working at the level of individual diagrams. We note that the recursion in (D.1) is identical to the recursion relation (5.11) except (5.11) is written without any direct reference to auxiliary momenta. We now explain this recursive prescription in detail with the help of two illustrative examples.

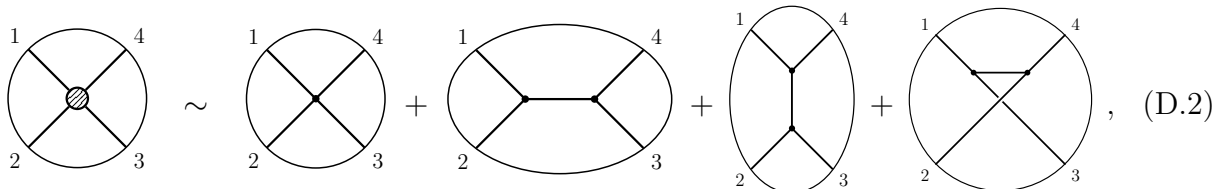
### D.1 Four-point exchange diagram

We start by demonstrating the BCFW-type recursion (D.1) for the simplest case, the four-point function. The full tree-level four-point bulk (Witten) diagram for a theory with cubic

---

<sup>9</sup>Here we have made the implicit assumption that *all* internal lines get complex-shifted – to ensure this is true in general, a “multi-line BCFW-shift” of the external momenta may be required. The final Mellin amplitude  $\mathcal{M}$  will be independent of the choice of the particular BCFW-shift employed, as long as all internal lines develop a  $z$ -dependence and consequently can be put on-shell at particular values of  $z$ .

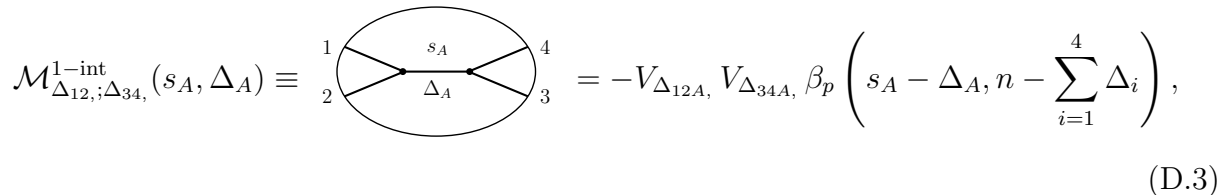
and quartic interaction vertices is given by



where we must sum over all fields which can propagate in the intermediate channels in the  $s$ -,  $t$ - and  $u$ -channel exchange diagrams. We will be suppressing coupling constants and any symmetry factors associated with the diagrams. These details depend on the specifics of the bulk theory, particularly the bulk Lagrangian. We now show that *each individual* diagram in (D.2) in Mellin space admits a BCFW-type recursion relation, with the basic building blocks of the recursion being the contact diagrams. Consequently, we'll find the four-point contact diagram in (D.2) is already in its 'maximally reduced' form.

Let's focus on the  $s$ -channel exchange where a scalar field dual to a (single-trace) operator of conformal dimension  $\Delta_A$  propagates along the internal leg.<sup>10</sup> It turns out the form of the Mellin amplitude for the ( $s$ -channel) four-point exchange diagram as written in example (iii) is, rather trivially, already in the desired BCFW-type on-shell recursion form. However in this subsection, we will take the time to describe in detail the various ingredients which go into recognizing the BCFW-type recursion structure, as they illuminate how this works with more complicated higher-point diagrams.

Define



where the vertex factor  $V_{\Delta_{12A}}$ , defined using the convention (C.22), via (3.1),

$$V(\Delta_{1\dots f},) \equiv \zeta_p(\Delta_{1\dots f}, -n), \quad (\text{D.4})$$

is the Mellin amplitude associated with the 3-point contact diagram between operators of

<sup>10</sup>A similar analysis can be done for the  $t$ - and  $u$ -channel exchange diagrams.

dimensions  $\Delta_1$ ,  $\Delta_2$  and  $\Delta_A$ . Further, we have defined

$$s_A \equiv \Delta_1 + \Delta_2 - 2\gamma_{12} = \Delta_3 + \Delta_4 - 2\gamma_{34}, \quad (\text{D.5})$$

and  $\beta_p$  is defined in (2.24). To go to the auxiliary momentum space, described in section 2, we assign to each external leg of the four-point  $s$ -channel exchange diagram an auxiliary momentum, as shown below:

$$\mathcal{M}_{\Delta_{12}; \Delta_{34}}^{1-\text{int}}(s_A, \Delta_A) = \begin{array}{c} \text{---} k_1 \text{---} \\ \diagdown \quad \diagup \\ \text{---} k_2 \text{---} \\ \diagup \quad \diagdown \\ \text{---} k_3 \text{---} \\ \diagdown \quad \diagup \\ \text{---} k_4 \text{---} \end{array} \equiv \mathcal{M}_{-k_1^2 - k_2^2; -k_3^2 - k_4^2}^{1-\text{int}}(-k_A^2, \Delta_A), \quad (\text{D.6})$$

where the external momenta are on-shell,

$$-k_i^2 = \Delta_i \quad i = 1, \dots, 4, \quad (\text{D.7})$$

while the internal momentum is not, and momentum is conserved at each vertex. We are suppressing the Lorentz indices on the momentum variables. To obtain a BCFW-type relation for the exchange diagram, we begin by complexifying some of the external momenta in such a way that the complex-shifted external legs remain on-shell and still satisfy momentum conservation at each vertex for all values of the complex parameter, and as a result of the shift the momentum along the internal leg gets complex-shifted as well. For instance, we may choose the following “two-line shift” that preserves momentum conservation,

$$k_1 \rightarrow k_1(z) \equiv k_1 + zq, \quad k_4 \rightarrow k_4(z) \equiv k_4 - zq, \quad (\text{D.8})$$

where  $z \in \mathbb{C}$ , and  $q$  is a constrained momentum variable which will in general be complex-valued. The constraints on  $q$  arise from the following on-shell requirements,

$$-k_1(z)^2 = \Delta_1, \quad -k_4(z)^2 = \Delta_4, \quad \forall z \in \mathbb{C}. \quad (\text{D.9})$$

As desired, the momentum running through the internal leg gets complex-shifted as well,

$$k_A \rightarrow k_A(z) \equiv k_1(z) + k_2. \quad (\text{D.10})$$

The conditions (D.9) are met if  $q$  satisfies

$$q^2 = 0 \quad q \cdot k_1 = 0 \quad q \cdot k_4 = 0. \quad (\text{D.11})$$

Momentum conservation along with the constraints above then imply

$$q \cdot k_2 = -q \cdot k_3. \quad (\text{D.12})$$

Owing to the fact that the auxiliary momenta  $k_i$  are not null, it is in general not possible to specify in a Lorentz covariant manner the momentum variable  $q$  satisfying (D.11).<sup>11</sup> However, the explicit form for  $q$  will not be important in the following;  $q$  will enter in the calculations via its dot-product with various momenta and it will be sufficient for us to inquire how these dot-products are related to each other without establishing the explicit form for any of them.

The complex-shifts (D.8) transform the Mandelstam invariant  $s_A$  as well,

$$s_A \rightarrow s_A(z) \equiv -(k_1(z) + k_2)^2 = s_A - 2zq \cdot k_2 = -2q \cdot k_2(z - z_A) + \Delta_A, \quad (\text{D.13})$$

where we have defined

$$z_A \equiv \frac{s_A - \Delta_A}{2q \cdot k_2}. \quad (\text{D.14})$$

From this it is clear that the complex-shifted momentum running through the internal leg,  $k_A(z)$  goes on-shell at  $z = z_A$ . Consequently the complexified Mellin amplitude is given by<sup>12</sup>

$$\mathcal{M}(z) \equiv -V_{\Delta_{12A}}, V_{\Delta_{34A}}, \beta_p \left( s_A(z) - \Delta_A, n - \sum_{i=1}^4 \Delta_i \right), \quad (\text{D.15})$$

so that the original Mellin amplitude is recovered upon setting  $z = 0$ ,

$$\mathcal{M}(0) = \mathcal{M}_{\Delta_{12}; \Delta_{34}}^{1-\text{int}}(s_A, \Delta_A). \quad (\text{D.16})$$

Consider now the integral

$$I \equiv \oint_{\mathcal{C}} \frac{dz}{2\pi i} \frac{\mathcal{M}(z)}{z}, \quad (\text{D.17})$$

---

<sup>11</sup>The momentum variables  $k_i$  and  $q$  are respectively, real and complex valued  $(n+1)$ -dimensional Lorentz vectors with a Lorentzian inner product. If  $(n+1) = 3$ , then only  $q = 0$  satisfies (D.11) for arbitrary  $k_1, k_4$ . Thus we need at least  $(n+1) \geq 4 = \mathcal{N}$  to admit a non-vanishing complex-deformation  $zq$ . This requirement is consistent with the inequality mentioned in section 2.

<sup>12</sup>Note that the complex Mellin amplitude  $\mathcal{M}(z)$  in this appendix is different from the one defined in section 5 above (5.16).

where the contour  $\mathbf{C}$  is chosen to be a circle of infinite radius centered at origin. The integrand has simple poles at

$$z = 0, \quad z = z_A + \frac{1}{2q \cdot k_2} \frac{2\pi im}{\log p} \quad m \in \mathbb{Z}, \quad (\text{D.18})$$

where the infinite sequence of poles arises from the factor of  $\zeta_p(s_A(z) - \Delta_A)$  in the  $\beta_p$  function. We will now apply the residue theorem to obtain an expression for the original amplitude in terms of the residues from the remaining poles. It is clear that the residue at  $z = 0$  is precisely the original amplitude  $\mathcal{M}(0)$ . The residue at the remaining poles takes the form

$$\text{Res}_{\substack{z=z_A \\ + \frac{1}{2q \cdot k_2} \frac{2\pi im}{\log p}}} \left( \frac{\mathcal{M}(z)}{z} \right) = \frac{V_{\Delta_{12A}}, V_{\Delta_{34A}}}{(s_A - \Delta_A) \log p + 2\pi im} \quad m \in \mathbb{Z}. \quad (\text{D.19})$$

Thus we conclude that

$$I = \mathcal{M}(0) + V_{\Delta_{12A}}, V_{\Delta_{34A}} \sum_{m=-\infty}^{+\infty} \frac{1}{(s_A - \Delta_A) \log p + 2\pi im}. \quad (\text{D.20})$$

At this point, one hopes that  $\mathcal{M}(z)$  falls off sufficiently fast at large  $z$ , so that the contour integral  $I = 0$ , i.e. the boundary term vanishes. The infinite sum in (D.20) evaluates to give

$$\sum_{m=-\infty}^{+\infty} \frac{1}{(s_A - \Delta_A) \log p + 2\pi im} = \zeta_p(s_A - \Delta_A) - \frac{1}{2}, \quad (\text{D.21})$$

so the claim that  $I = 0$  becomes

$$\begin{aligned} \mathcal{M}(0) &\stackrel{?}{=} -V_{\Delta_{12A}} \left( \zeta_p(s_A - \Delta_A) - \frac{1}{2} \right) V_{\Delta_{34A}}, \\ &\stackrel{?}{=} -\mathcal{M}(k_1(z), k_2, -k_1(z) - k_2) \Big|_{z=z_A} \left( \zeta_p(s_A - \Delta_A) - \frac{1}{2} \right) \mathcal{M}(k_1(z) + k_2, k_3, k_4(z)) \Big|_{z=z_A}, \end{aligned} \quad (\text{D.22})$$

where in the second line above we have defined the sub-amplitude

$$\mathcal{M}(k_a, k_b, k_c) \equiv V_{-k_a^2, -k_b^2, -k_c^2} \quad (\text{D.23})$$

with  $k_a + k_b + k_c = 0$ . Consider the sub-amplitude

$$\mathcal{M}(k_1(z), k_2, -k_1(z) - k_2) = V_{\Delta_1, \Delta_2, s_A(z)}. \quad (\text{D.24})$$

It represents an “off-shell” three-point contact interaction with incoming momenta  $k_1(z), k_2$  and  $-k_1(z) - k_2$ . At generic values of  $z$ , two of the three external legs are on-shell, while the third one is off-shell, but the third leg goes on-shell at  $z = z_A$ , and we write

$$\mathcal{M}(k_1(z_A), k_2, -k_1(z_A) - k_2) = \begin{array}{c} \begin{array}{c} k_1(z_A) \\ \swarrow \quad \searrow \\ \bullet \\ \uparrow \\ -k_1(z_A) - k_2 \end{array} \\ \text{---} \end{array} . \quad (\text{D.25})$$

Thus if it is true that  $I = 0$ , we can interpret the second line of (D.22) as the claim that we have rewritten the original Mellin amplitude for the  $s$ -channel four-point exchange diagram as a product of two on-shell sub-amplitudes obtained by cutting across the internal leg of the original diagram along which the field dual to an operator of dimension  $\Delta_A$  propagates, times a putative “propagator” running across the internal leg given by the expression  $\zeta_p(s_A - \Delta_A) - 1/2$ .

However, it can be explicitly checked that the boundary contribution in (D.20) does *not* vanish, as the complex Mellin amplitude  $\mathcal{M}(z)$  does not vanish at infinity. Instead, we find

$$\begin{aligned} I &= \frac{1}{2} V_{\Delta_{12A}}, V_{\Delta_{34A}}, V_{\Delta_{1234}}, (1 + p^{n-\Delta_{1234}}) \\ &= \mathcal{M}(k_1(z), k_2, -k_1(z) - k_2) \Big|_{z=z_A} \left( \frac{V_{\Delta_{1234}} (1 + p^{n-\Delta_{1234}})}{2} \right) \mathcal{M}(k_1(z) + k_2, k_3, k_4(z)) \Big|_{z=z_A}, \end{aligned} \quad (\text{D.26})$$

where the second line is merely a suggestive rewriting of the first line. Taking the boundary term into account, the corrected version of (D.22) is then given by

$$\begin{aligned} \mathcal{M}(0) &= -\mathcal{M}(k_1(z), k_2, -k_1(z) - k_2) \Big|_{z=z_A} \left( \zeta_p(s_A - \Delta_A) - \frac{1}{2} \right) \mathcal{M}(k_1(z) + k_2, k_3, k_4(z)) \Big|_{z=z_A} \\ &\quad + \mathcal{M}(k_1(z), k_2, -k_1(z) - k_2) \Big|_{z=z_A} \left( \frac{V_{\Delta_{1234}} (1 + p^{n-\Delta_{1234}})}{2} \right) \mathcal{M}(k_1(z) + k_2, k_3, k_4(z)) \Big|_{z=z_A}, \end{aligned} \quad (\text{D.27})$$

which simplifies to the compact expression

$$\begin{aligned} \mathcal{M}(0) &= -\mathcal{M}(k_1(z), k_2, -k_1(z) - k_2) \Big|_{z=z_A} \beta_p(s_A - \Delta_A, n - \Delta_{1234}) \mathcal{M}(k_1(z) + k_2, k_3, k_4(z)) \Big|_{z=z_A}. \end{aligned} \quad (\text{D.28})$$

The amplitude in (D.28) is, indeed, mathematically identical to the starting point (D.3), and in fact is a special case of (D.1). More importantly, we see the boundary contribution does not destroy the nice decomposition of the amplitude first observed in (D.22); instead it combines nicely with the residue from the poles of the complexified Mellin amplitude in such a way that the original amplitude is still given by a product of two on-shell sub-amplitudes obtained by cutting across the internal leg, times a propagator running across the same internal leg, which we refer to as the ‘‘Mellin space propagator’’ joining the left and right sub-amplitudes. We comment on the appearance of non-vanishing boundary terms at the end of this appendix.

Diagrammatically, we may write (D.28) as

$$\text{Diagrammatic representation of (D.28)} \quad (\text{D.29})$$

We may also equivalently depict the identity (D.28) as

$$\text{Diagrammatic representation of (D.30)} \quad (\text{D.30})$$

which avoids reference to the auxiliary momentum space and any BCFW-shifts altogether, and takes the form presented in (5.11).

Admittedly, the example of the four-point exchange diagram is quite special in that the sub-amplitudes turn out to be contact diagrams and thus have no Mandelstam dependence. Nevertheless, we demonstrate in the next subsection that the BCFW-type decomposition (D.1) holds, rather non-trivially, for the Mellin amplitude of the five-point diagram with two internal exchanges.

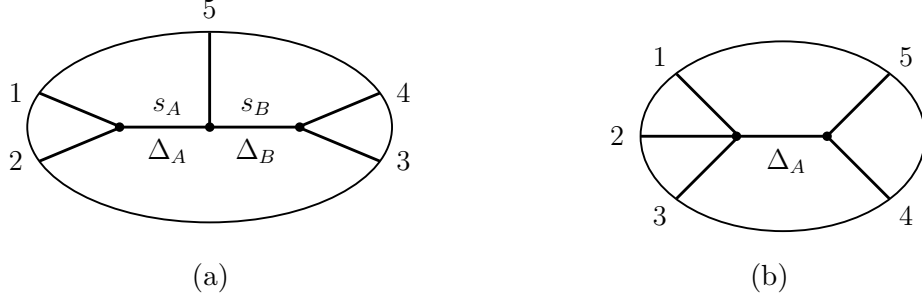


Figure 1: (a) A five-point diagram built out of cubic interaction vertices. The Mandelstam variables  $s_A$  and  $s_B$  are defined in (D.33). (b) A five-point diagram built out of cubic and quartic interaction vertices.

## D.2 Five-point diagram with two internal lines

In a bulk theory with cubic interaction vertices, five-point diagrams of the kind shown in figure 1a, with two internal legs, are allowed. Further, if the theory contains quartic interaction vertices as well, exchange diagrams of the kind shown in figure 1b are also possible. However, exchange diagrams like the one in figure 1b fall in the category of diagrams discussed in the previous subsection, and results obtained there extend trivially to arbitrary exchange diagrams (that is, bulk diagrams with exactly one internal line).

So in this subsection, we focus on the tree-level five-point diagram built solely from cubic vertices. A BCFW-type recursion can be set up in each channel *individually*, so just like in the previous subsection, we will restrict attention to a particular channel, which will be the one shown in figure 1a; an identical analysis will hold in all other channels.

As with the four-point exchange diagram, we start with the Mellin amplitude for the diagram in figure 1a, which is a special case of the diagram evaluated in example (iv),

$$\begin{aligned}
\mathcal{M}_{\Delta_{12}, \Delta_5; \Delta_{34}}^{2\text{-int}}(s_A, \Delta_A; s_B, \Delta_B) &\equiv \text{Diagram (a)} \\
&= V_{\Delta_{12A}}, V_{\Delta_{A5B}}, V_{\Delta_{34B}}, \left[ \zeta_p(s_A - \Delta_A) \zeta_p(s_B - \Delta_B) \right. \\
&\quad \left. - V_{\Delta_{345A}}, \beta_p(s_A - \Delta_A, n - \Delta_\Sigma) - V_{\Delta_{125B}}, \beta_p(s_B - \Delta_B, n - \Delta_\Sigma) \right. \\
&\quad \left. - V_{\Delta_\Sigma} \right], \tag{D.31}
\end{aligned}$$

where the contact amplitudes  $V_{\Delta_{i_1\dots i_f}}$ , were defined in (D.4),  $\beta_p$  was defined in (2.24), and we are using the shorthand

$$\Delta_\Sigma \equiv \sum_{i=1}^5 \Delta_i = \Delta_{12345}, . \quad (\text{D.32})$$

Furthermore, with the help of the Mellin variable constraints (2.13) for  $\mathcal{N} = 5$ , we have defined

$$\begin{aligned} s_A &\equiv \Delta_1 + \Delta_2 - 2\gamma_{12} = \Delta_3 + \Delta_4 + \Delta_5 - 2\gamma_{34} - 2\gamma_{35} - 2\gamma_{45} \\ s_B &\equiv \Delta_3 + \Delta_4 - 2\gamma_{34} = \Delta_1 + \Delta_2 + \Delta_5 - 2\gamma_{12} - 2\gamma_{15} - 2\gamma_{25} . \end{aligned} \quad (\text{D.33})$$

Unlike the case of the four-point exchange diagram, it is not immediately clear that the amplitude in (D.31) admits a BCFW-type decomposition; in the rest of this appendix we show precisely how this works out.

We start by passing to the auxiliary momentum space, with the momentum assignments as shown:

$$\mathcal{M}_{\Delta_{12};\Delta_5;\Delta_{34}}^{2\text{-int}}(s_A, \Delta_A; s_B, \Delta_B) = \text{Diagram} , \quad (\text{D.34})$$

where, like before, the external momenta are on-shell,

$$-k_i^2 = \Delta_i \quad i = 1, \dots, 5, \quad (\text{D.35})$$

and momentum is conserved at each vertex. Once again we employ a complex-shift of momenta; specifically we apply the two-line BCFW-shift (D.8) subject to the on-shell constraints (D.9). The on-shell conditions lead us to constraints on  $q$  as written down in (D.11). Momentum conservation along with constraints (D.11) further implies

$$q \cdot (k_2 + k_3 + k_5) = 0. \quad (\text{D.36})$$

Looking ahead, it will be convenient to set

$$q \cdot k_5 = 0. \quad (\text{D.37})$$

We are free to make this choice and still have (at least one) non-vanishing solution for the complex momentum variable  $q$ , as long as  $(n+1) \geq 5$ , since (D.11) and (D.37) amount to 4

conditions on the  $(n+1)$ -component vector  $q$ . This proviso is consistent with the requirement  $(n+1) \geq \mathcal{N} = 5$  which ensures there are precisely  $\mathcal{N}(\mathcal{N}-3)/2 = 5$  independent Mandelstam variables.

Applying momentum conservation for the complex-shifted momenta vertex by vertex, the shifted internal momenta are given by

$$k_A \rightarrow k_A(z) \equiv k_1(z) + k_2, \quad k_B \rightarrow k_B(z) \equiv k_3 + k_4(z), \quad (\text{D.38})$$

which allows the possibility of setting the internal legs on-shell at specific (non-zero) values of the complex parameter  $z$ . In particular,

$$\begin{aligned} s_A(z) &\equiv -k_A(z)^2 = s_A - 2zq \cdot k_2 = -2q \cdot k_2(z - z_A) + \Delta_A \\ s_B(z) &\equiv -k_B(z)^2 = s_B + 2zq \cdot k_3 = 2q \cdot k_3(z - z_B) + \Delta_B, \end{aligned} \quad (\text{D.39})$$

where we have defined

$$z_A \equiv \frac{s_A - \Delta_A}{2q \cdot k_2}, \quad z_B \equiv -\frac{s_B - \Delta_B}{2q \cdot k_3}. \quad (\text{D.40})$$

We conclude that  $k_A(z)$  goes on-shell at  $z = z_A$ , while  $k_B(z)$  goes on-shell at  $z = z_B$ . Equation (D.39) also suggests what the complex-shifted Mellin amplitude should look like,

$$\mathcal{M}(z) \equiv M_{\Delta_{12}; \Delta_5; \Delta_{34}}^{2-\text{int}}(s_A(z), \Delta_A; s_B(z), \Delta_B), \quad (\text{D.41})$$

that is, we simply promote the Mandelstam variables  $s_A$  and  $s_B$  in (D.31) to their complex-shifted versions.

Like in the previous subsection, consider now the contour integral

$$I \equiv \oint_{\mathcal{C}} \frac{dz}{2\pi i} \frac{\mathcal{M}(z)}{z}, \quad (\text{D.42})$$

where the contour  $\mathcal{C}$  is a circle of infinite radius centered at origin. It is clear from the explicit form in (D.31) that the integrand in (D.42) has simple poles at

$$z = 0, \quad z = z_A + \frac{1}{2q \cdot k_2} \frac{2\pi i m}{\log p}, \quad z = z_B + \frac{1}{2q \cdot k_3} \frac{2\pi i m}{\log p} \quad m \in \mathbb{Z}. \quad (\text{D.43})$$

We will first apply the residue theorem to evaluate (D.42). The residue at  $z = 0$  reproduces the original amplitude  $\mathcal{M}(0)$  which we are interested in, while the residues at the remaining

poles evaluate to

$$\begin{aligned} \text{Res}_{\substack{z=z_A \\ +\frac{1}{2q \cdot k_2} \frac{2\pi im}{\log p}}} \left( \frac{\mathcal{M}(z)}{z} \right) &= -\frac{V_{\Delta_{12A}}, V_{\Delta_{A5B}}, V_{\Delta_{34B}}, \beta_p(s_B - \Delta_B - s_A + \Delta_A, n - \Delta_{345A},)}{(s_A - \Delta_A) \log p + 2\pi im} \\ \text{Res}_{\substack{z=z_B \\ -\frac{1}{2q \cdot k_2} \frac{2\pi im}{\log p}}} \left( \frac{\mathcal{M}(z)}{z} \right) &= -\frac{V_{\Delta_{12A}}, V_{\Delta_{A5B}}, V_{\Delta_{34B}}, \beta_p(s_A - \Delta_A - s_B + \Delta_B, n - \Delta_{125B},)}{(s_B - \Delta_B) \log p + 2\pi im}, \end{aligned} \quad (\text{D.44})$$

for all  $m \in \mathbb{Z}$ , where we made important use of the identity  $q \cdot k_2 = -q \cdot k_3$  which follows from (D.36)-(D.37). Using (D.21) to sum up the residues, we obtain

$$\begin{aligned} &\mathcal{M}(0) \\ &= -\mathcal{M}(k_1(z), k_2, -k_1(z) - k_2) \Big|_{z=z_A} \left( \zeta_p(s_A - \Delta_A) - \frac{1}{2} \right) \mathcal{M}_{\Delta_B}(k_1(z) + k_2, k_5, k_3, k_4(z)) \Big|_{z=z_A} \\ &\quad - \mathcal{M}_{\Delta_A}(k_1(z), k_2, k_5, k_3 + k_4(z)) \Big|_{z=z_B} \left( \zeta_p(s_B - \Delta_B) - \frac{1}{2} \right) \mathcal{M}(-k_3 - k_4(z), k_3, k_4(z)) \Big|_{z=z_B} \\ &\quad + I, \end{aligned} \quad (\text{D.45})$$

where we have used (D.23) and have defined the (off-shell) sub-amplitude

$$\begin{aligned} \mathcal{M}_{\Delta}(k_a, k_b, k_c, k_d) &\equiv -V_{-k_a^2, -k_b^2, \Delta} V_{-k_c^2, -k_d^2, \Delta} \\ &\quad \times \beta_p \left( -(k_a + k_b)^2 - \Delta, n + k_a^2 + k_b^2 + k_c^2 + k_d^2 \right) \end{aligned} \quad (\text{D.46})$$

with  $k_a + k_b + k_c + k_d = 0$ . The sub-amplitude

$$\mathcal{M}(k_1(z), k_2, -k_1(z) - k_2) = V_{\Delta_1, \Delta_2, s_A(z)} \quad (\text{D.47})$$

in (D.45) is on-shell at  $z = z_A$ , i.e. all external momenta go on-shell at  $z = z_A$ . Moreover, at this value of  $z$ , it precisely takes the form of an (on-shell) three-point contact Mellin amplitude. Similarly, the sub-amplitude,

$$\begin{aligned} \mathcal{M}_{\Delta_B}(k_1(z) + k_2, k_5, k_3, k_4(z)) &= -V_{s_A(z), \Delta_5, \Delta_B} V_{\Delta_3, \Delta_4, \Delta_B} \\ &\quad \times \beta_p \left( s_B(z) - \Delta_B, n - \Delta_3 - \Delta_4 - \Delta_5 - s_A(z) \right) \end{aligned} \quad (\text{D.48})$$

is on-shell at  $z = z_A$ , whence  $s_A(z_A) = \Delta_A$ ,  $s_B(z_A) = -(k_3 + k_4(z_A))^2 = s_B - s_A + \Delta_A$ , and we recognize from the previous subsection that (D.48) takes precisely the form of an

(on-shell) four-point exchange diagram (see, e.g. (D.6)):

$$\begin{aligned}
\mathcal{M}_{\Delta_B}(k_1(z_A) + k_2, k_5, k_3, k_4(z_A)) &= \text{Diagram} \\
&= \mathcal{M}_{-k_5^2 - (k_1(z_A) + k_2)^2; -k_3^2 - k_4(z_A)^2}^{1-\text{int}} \left( -(k_3 + k_4(z_A))^2, \Delta_B \right) \\
&= \mathcal{M}_{\Delta_5 + \Delta_A; \Delta_3 + \Delta_4}^{1-\text{int}} (s_B - s_A + \Delta_A, \Delta_B).
\end{aligned} \tag{D.49}$$

A similar interpretation can be given to the sub-amplitudes in the second term on the r.h.s. of (D.45), which are to be evaluated at  $z = z_B$ .

We still need to take into account the boundary contribution in (D.45), denoted by  $I$ . Just like in the previous subsection, such a contribution is non-vanishing and can be directly computed by evaluating the contour integral at infinity in (D.42). We omit the details of the computation, but point out that just like in the previous subsection, the boundary contribution combines with the sum of residues at all (non-zero) poles to give

$$\begin{aligned}
&\mathcal{M}(0) \\
&= -\mathcal{M}(k_1(z), k_2, -k_1(z) - k_2) \Big|_{z=z_A} \beta_p(s_A - \Delta_A, n - \Delta_\Sigma) \mathcal{M}_{\Delta_B}(k_1(z) + k_2, k_5, k_3, k_4(z)) \Big|_{z=z_A} \\
&\quad - \mathcal{M}_{\Delta_A}(k_1(z), k_2, k_5, k_3 + k_4(z)) \Big|_{z=z_B} \beta_p(s_B - \Delta_B, n - \Delta_\Sigma) \mathcal{M}(-k_3 - k_4(z), k_3, k_4(z)) \Big|_{z=z_B}.
\end{aligned} \tag{D.50}$$

We may write this diagrammatically as

$$\begin{aligned}
& \text{Diagram with external momenta } k_1, k_2, k_3, k_4 \text{ and internal momenta } k_1+k_2, k_3+k_4, k_5 \\
& = - \text{Diagram with external momenta } k_1(z_A), k_2, -k_1(z_A)-k_2 \text{ multiplied by } \beta_p(s_A - \Delta_A, n - \Delta_\Sigma) \\
& \quad - \text{Diagram with external momenta } k_5, k_4(z_A), k_3, k_1(z_A)+k_2 \text{ multiplied by } \beta_p(s_B - \Delta_B, n - \Delta_\Sigma) \\
& \quad - \text{Diagram with external momenta } k_1(z_B), k_2, k_3+k_4(z_B) \text{ multiplied by } \beta_p(s_B - \Delta_B, n - \Delta_\Sigma) \\
& \quad - \text{Diagram with external momenta } k_3, k_4(z_B), -k_3-k_4(z_B) \text{ multiplied by } \beta_p(s_B - \Delta_B, n - \Delta_\Sigma)
\end{aligned} \tag{D.51}$$

Equivalently, the result (D.50) may also be recast in the form of (5.11) as

$$\begin{aligned}
& \text{Diagram with external legs } 1, 2, 3, 4 \text{ and internal legs } s_A, s_B, \Delta_A, \Delta_B \\
& = - \text{Diagram with external legs } 1, 2, 5 \text{ and internal leg } A \text{ multiplied by } \beta_p(s_A - \Delta_A, n - \Delta_\Sigma) \\
& \quad - \text{Diagram with external legs } 5, 4, 3, 1 \text{ and internal leg } \Delta_B \text{ multiplied by } \beta_p(s_B - \Delta_B, n - \Delta_\Sigma) \\
& \quad - \text{Diagram with external legs } 1, 2, 5 \text{ and internal leg } B \text{ multiplied by } \beta_p(s_B - \Delta_B, n - \Delta_\Sigma) \\
& \quad - \text{Diagram with external legs } 4, 3, 1, 5 \text{ and internal leg } B \text{ multiplied by } \beta_p(s_B - \Delta_B, n - \Delta_\Sigma)
\end{aligned} \tag{D.52}$$

which avoids any reference to momentum variables. Further, we may use the decomposition (D.29)-(D.30) from the previous subsection to further reduce (D.51)-(D.52) in such a way that the r.h.s. is given entirely in terms of the three-point (contact) Mellin amplitudes.

The proof presented in section 5 (for the on-shell recursive prescription IV) sheds light on

the appearance of non-vanishing boundary terms in the examples considered in this appendix, where we apply Cauchy’s theorem in the complexified auxiliary momentum space to obtain an on-shell recursion relation: Had we chosen instead the complex-cylindrical manifold for the complex variable  $z$  like we do in section 5, the boundary terms would not have made an appearance in the intermediate steps.

## References

- [1] J. Penedones, “Writing CFT correlation functions as AdS scattering amplitudes,” *JHEP* **03** (2011) 025, [10.1007/JHEP03\(2011\)025](https://arxiv.org/abs/10.1007/JHEP03(2011)025), [1011.1485](https://arxiv.org/abs/1011.1485).
- [2] S. S. Gubser, J. Knaute, S. Parikh, A. Samberg, and P. Witaszczyk, “ $p$ -adic AdS/CFT,” *Commun. Math. Phys.* **352** (2017), no. 3 1019–1059, [10.1007/s00220-016-2813-6](https://arxiv.org/abs/10.1007/s00220-016-2813-6), [1605.01061](https://arxiv.org/abs/1605.01061).
- [3] M. Heydeman, M. Marcolli, I. Saberi, and B. Stoica, “Tensor networks,  $p$ -adic fields, and algebraic curves: arithmetic and the AdS<sub>3</sub>/CFT<sub>2</sub> correspondence,” *Adv. Theor. Math. Phys.* **22** (2018) 93–176, [10.4310/ATMP.2018.v22.n1.a4](https://arxiv.org/abs/10.4310/ATMP.2018.v22.n1.a4), [1605.07639](https://arxiv.org/abs/1605.07639).
- [4] C. B. Jepsen and S. Parikh, “ $p$ -adic Mellin Amplitudes,” [1808.08333](https://arxiv.org/abs/1808.08333).
- [5] E. Melzer, “Nonarchimedean Conformal Field Theories,” *Int. J. Mod. Phys. A* **4** (1989) 4877, [10.1142/S0217751X89002065](https://arxiv.org/abs/10.1142/S0217751X89002065).
- [6] A. L. Fitzpatrick, J. Kaplan, J. Penedones, S. Raju, and B. C. van Rees, “A Natural Language for AdS/CFT Correlators,” *JHEP* **11** (2011) 095, [10.1007/JHEP11\(2011\)095](https://arxiv.org/abs/10.1007/JHEP11(2011)095), [1107.1499](https://arxiv.org/abs/1107.1499).
- [7] M. F. Paulos, “Towards Feynman rules for Mellin amplitudes,” *JHEP* **10** (2011) 074, [10.1007/JHEP10\(2011\)074](https://arxiv.org/abs/10.1007/JHEP10(2011)074), [1107.1504](https://arxiv.org/abs/1107.1504).
- [8] D. Nandan, A. Volovich, and C. Wen, “On Feynman Rules for Mellin Amplitudes in AdS/CFT,” *JHEP* **05** (2012) 129, [10.1007/JHEP05\(2012\)129](https://arxiv.org/abs/10.1007/JHEP05(2012)129), [1112.0305](https://arxiv.org/abs/1112.0305).
- [9] V. Goncalves, J. Penedones, and E. Trevisani, “Factorization of Mellin amplitudes,” *JHEP* **10** (2015) 040, [10.1007/JHEP10\(2015\)040](https://arxiv.org/abs/10.1007/JHEP10(2015)040), [1410.4185](https://arxiv.org/abs/1410.4185).
- [10] E. Y. Yuan, “Loops in the Bulk,” [1710.01361](https://arxiv.org/abs/1710.01361).

- [11] E. Y. Yuan, “Simplicity in AdS Perturbative Dynamics,” [1801.07283](#).
- [12] C. Cardona, “Mellin-(Schwinger) representation of One-loop Witten diagrams in AdS,” [1708.06339](#).
- [13] I. Bertan and I. Sachs, “Loops in Anti-de Sitter Space,” [1804.01880](#).
- [14] R. Britto, F. Cachazo, B. Feng, and E. Witten, “Direct proof of tree-level recursion relation in Yang-Mills theory,” *Phys. Rev. Lett.* **94** (2005) 181602, [10.1103/PhysRevLett.94.181602](#), [hep-th/0501052](#).
- [15] R. Rattazzi, V. S. Rychkov, E. Tonni, and A. Vichi, “Bounding scalar operator dimensions in 4D CFT,” *JHEP* **12** (2008) 031, [10.1088/1126-6708/2008/12/031](#), [0807.0004](#).
- [16] D. Poland, D. Simmons-Duffin, and A. Vichi, “Carving Out the Space of 4D CFTs,” *JHEP* **05** (2012) 110, [10.1007/JHEP05\(2012\)110](#), [1109.5176](#).
- [17] F. Kos, D. Poland, and D. Simmons-Duffin, “Bootstrapping the  $O(N)$  vector models,” *JHEP* **06** (2014) 091, [10.1007/JHEP06\(2014\)091](#), [1307.6856](#).
- [18] F. Kos, D. Poland, and D. Simmons-Duffin, “Bootstrapping Mixed Correlators in the 3D Ising Model,” *JHEP* **11** (2014) 109, [10.1007/JHEP11\(2014\)109](#), [1406.4858](#).
- [19] S. El-Showk, M. F. Paulos, D. Poland, S. Rychkov, D. Simmons-Duffin, and A. Vichi, “Solving the 3d Ising Model with the Conformal Bootstrap II. c-Minimization and Precise Critical Exponents,” *J. Stat. Phys.* **157** (2014) 869, [10.1007/s10955-014-1042-7](#), [1403.4545](#).
- [20] M. F. Paulos, “JuliBootS: a hands-on guide to the conformal bootstrap,” [1412.4127](#).
- [21] D. Simmons-Duffin, “A Semidefinite Program Solver for the Conformal Bootstrap,” *JHEP* **06** (2015) 174, [10.1007/JHEP06\(2015\)174](#), [1502.02033](#).
- [22] R. Gopakumar, A. Kaviraj, K. Sen, and A. Sinha, “A Mellin space approach to the conformal bootstrap,” *JHEP* **05** (2017) 027, [10.1007/JHEP05\(2017\)027](#), [1611.08407](#).
- [23] O. Aharony, L. F. Alday, A. Bissi, and E. Perlmutter, “Loops in AdS from Conformal Field Theory,” *JHEP* **07** (2017) 036, [10.1007/JHEP07\(2017\)036](#), [1612.03891](#).

- [24] L. F. Alday, A. Bissi, and E. Perlmutter, “Holographic Reconstruction of AdS Exchanges from Crossing Symmetry,” *JHEP* **08** (2017) 147, [10.1007/JHEP08\(2017\)147](https://arxiv.org/abs/1705.02318), [1705.02318](https://arxiv.org/abs/1705.02318).
- [25] L. F. Alday and A. Bissi, “Loop Corrections to Supergravity on  $AdS_5 \times S^5$ ,” *Phys. Rev. Lett.* **119** (2017), no. 17 171601, [10.1103/PhysRevLett.119.171601](https://arxiv.org/abs/10.1103/PhysRevLett.119.171601), [1706.02388](https://arxiv.org/abs/1706.02388).
- [26] L. Rastelli and X. Zhou, “Mellin amplitudes for  $AdS_5 \times S^5$ ,” *Phys. Rev. Lett.* **118** (2017), no. 9 091602, [10.1103/PhysRevLett.118.091602](https://arxiv.org/abs/10.1103/PhysRevLett.118.091602), [1608.06624](https://arxiv.org/abs/1608.06624).
- [27] L. Rastelli and X. Zhou, “How to Succeed at Holographic Correlators Without Really Trying,” *JHEP* **04** (2018) 014, [10.1007/JHEP04\(2018\)014](https://arxiv.org/abs/10.1007/JHEP04(2018)014), [1710.05923](https://arxiv.org/abs/1710.05923).
- [28] S. Raju, “BCFW for Witten Diagrams,” *Phys. Rev. Lett.* **106** (2011) 091601, [10.1103/PhysRevLett.106.091601](https://arxiv.org/abs/10.1103/PhysRevLett.106.091601), [1011.0780](https://arxiv.org/abs/1011.0780).
- [29] S. Raju, “Recursion Relations for AdS/CFT Correlators,” *Phys. Rev.* **D83** (2011) 126002, [10.1103/PhysRevD.83.126002](https://arxiv.org/abs/10.1103/PhysRevD.83.126002), [1102.4724](https://arxiv.org/abs/1102.4724).
- [30] S. S. Gubser and S. Parikh, “Geodesic bulk diagrams on the Bruhat–Tits tree,” *Phys. Rev.* **D96** (2017), no. 6 066024, [10.1103/PhysRevD.96.066024](https://arxiv.org/abs/10.1103/PhysRevD.96.066024), [1704.01149](https://arxiv.org/abs/1704.01149).
- [31] S. S. Gubser, M. Heydeman, C. Jepsen, M. Marcolli, S. Parikh, I. Saberi, B. Stoica, and B. Trundy, “Edge length dynamics on graphs with applications to  $p$ -adic AdS/CFT,” *JHEP* **06** (2017) 157, [10.1007/JHEP06\(2017\)157](https://arxiv.org/abs/10.1007/JHEP06(2017)157), [1612.09580](https://arxiv.org/abs/1612.09580).
- [32] S. S. Gubser, C. Jepsen, S. Parikh, and B. Trundy, “ $O(N)$  and  $O(N)$  and  $O(N)$ ,” *JHEP* **11** (2017) 107, [10.1007/JHEP11\(2017\)107](https://arxiv.org/abs/10.1007/JHEP11(2017)107), [1703.04202](https://arxiv.org/abs/1703.04202).
- [33] S. S. Gubser, M. Heydeman, C. Jepsen, S. Parikh, I. Saberi, B. Stoica, and B. Trundy, “Signs of the time: Melonic theories over diverse number systems,” *Phys. Rev.* **D98** (2018), no. 12 126007, [10.1103/PhysRevD.98.126007](https://arxiv.org/abs/10.1103/PhysRevD.98.126007), [1707.01087](https://arxiv.org/abs/1707.01087).
- [34] A. Bhattacharyya, L.-Y. Hung, Y. Lei, and W. Li, “Tensor network and ( $p$ -adic) AdS/CFT,” *JHEP* **01** (2018) 139, [10.1007/JHEP01\(2018\)139](https://arxiv.org/abs/10.1007/JHEP01(2018)139), [1703.05445](https://arxiv.org/abs/1703.05445).
- [35] M. Marcolli, “Holographic Codes on Bruhat–Tits buildings and Drinfeld Symmetric Spaces,” [1801.09623](https://arxiv.org/abs/1801.09623).
- [36] P. Dutta, D. Ghoshal, and A. Lala, “Enhanced Symmetry of the  $p$ -adic Wavelets,” *Phys. Lett.* **B783** (2018) 421–427, [10.1016/j.physletb.2018.07.007](https://arxiv.org/abs/10.1016/j.physletb.2018.07.007), [1804.00958](https://arxiv.org/abs/1804.00958).

- [37] S. Bhowmick and K. Ray, “Holography on local fields via Radon Transform,” *JHEP* **09** (2018) 126, [10.1007/JHEP09\(2018\)126](https://arxiv.org/abs/1805.07189), [1805.07189](https://arxiv.org/abs/1805.07189).
- [38] F. Qu and Y.-h. Gao, “Scalar fields on  $p$ AdS,” *Phys. Lett.* **B786** (2018) 165–170, [10.1016/j.physletb.2018.09.043](https://arxiv.org/abs/1806.07035), [1806.07035](https://arxiv.org/abs/1806.07035).
- [39] S. S. Gubser, C. Jepsen, and B. Trundy, “Spin in  $p$ -adic AdS/CFT,” [1811.02538](https://arxiv.org/abs/1811.02538).
- [40] B. Stoica, “Building Archimedean Space,” [1809.01165](https://arxiv.org/abs/1809.01165).
- [41] M. Heydeman, M. Marcolli, S. Parikh, and I. Saberi, “Nonarchimedean Holographic Entropy from Networks of Perfect Tensors,” [1812.04057](https://arxiv.org/abs/1812.04057).
- [42] L.-Y. Hung, W. Li, and C. M. Melby-Thompson, “Wilson line networks in  $p$ -adic AdS/CFT,” [1812.06059](https://arxiv.org/abs/1812.06059).
- [43] G. Lauricella, “Sulle funzioni ipergeometriche a piu variabili,” *Rendiconti del Circolo Matematico di Palermo* **7** (Dec, 1893) 111–158, [10.1007/BF03012437](https://arxiv.org/abs/10.1007/BF03012437).
- [44] H. M. Srivastava and P. W. Karlsson, *Multiple Gaussian hypergeometric series*. Ellis Horwood, 1985.
- [45] R. M. Aarts, “Lauricella Functions.” From MathWorld—A Wolfram Web Resource, created by Eric W. Weisstein.  
<http://mathworld.wolfram.com/LauricellaFunctions.html>.
- [46] P. G. O. Freund, “ $p$ -adic Strings Then and Now,” [1711.00523](https://arxiv.org/abs/1711.00523).